Transient Simulation of a Lithium Bromide-Water Vapour Absorption Refrigeration System

by

Dawood Jeggels

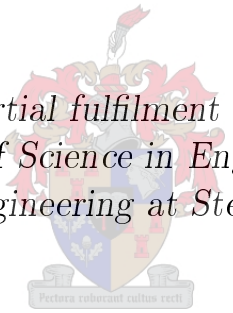

Thesis presented in partial fulfilment of the requirements for the degree of Master of Science in Engineering (Mechanical) in the Faculty of Engineering at Stellenbosch University

Supervisor: Mr. R.T. Dobson

December 2015

Declaration

By submitting this thesis electronically, I declare that the entirety of the work contained therein is my own, original work, that I am the sole author thereof (save to the extent explicitly otherwise stated), that reproduction and publication thereof by Stellenbosch University will not infringe any third party rights and that I have not previously in its entirety or in part submitted it for obtaining any qualification.

Date: .....

Abstract

Transient Simulation of a Lithium Bromide-Water Vapour Absorption Refrigeration System

D. Jeggels

Thesis: MScEng (Mech)

December 2015

Vapour absorption is a thermally activated heat pump process that can be used to produce refrigeration. The attraction of this technology is that it can harness low temperature sources of thermal energy to produce a useful output. This is of relevance when considering the possible implementation of this technology as a source of renewable energy as well as a mechanism for waste heat recovery and utilization.

In order to work towards a better understanding of this technology this project set the goal to theoretically simulate a vapour absorption system. After evaluation of the possible implementations of this technology the decision was made to investigate a water/lithium-bromide variant of vapour absorption cycles. Through the application of the fundamental principles of conservation a transient simulation was developed for a single effect water/lithium-bromide vapour absorption system.

The resulting simulation was used to describe the start up and refrigeration effect of a theoretical vapour absorption system. In particular no transient absorption system simulation work was found in the available published literature. For verification of the developed simulation model, hence, an experimental apparatus was constructed to obtain experimental results for comparison and validation of the developed simulation. When comparing the results obtained from the simulation and the experimental work the difference in temperature values was at most 23%.

Uittreksel

Oorgangs Simulasie van 'n Litiumbromied-Water Dampabsorpsie Verkoeling Siklus

("Transient Simulation of a Lithium Bromide-Water Vapour Absorption Refrigeration System")

D. Jeggels

Tesis: MScIng (Mech)

Desember 2015

Dampabsorpsie is 'n termies geaktiveerde hittepompproses wat gebruik kan word om verkoeling te produseer. Die aantreklikheid van hierdie tegnologie is dat dit 'n lae temperatuur bron van hitteenergie kan benut om 'n nuttige uitset te produseer. Veral, kan dit gebruik word as 'n manier vir die herwinning van hernubare energie asook as afvalhitte.

Ten einde om 'n beter begrip van hierdie tegnologie te bewerkstellig is die doel van hierdie tesis projek om 'n teoretise simulasie model saam te stel. Na evaluering van die moontlike implementering van hierdie tegnologie is die besluit geneem om 'n water-litiumbromied variant van dampabsorpsie te ondersoek. Deur die toepassing van die fundamentele beginsels van die behoud van massa en energie is 'n oorgangssimulasie model vir 'n enkeleffek water-litiumbromied dampabsorpsie stelsel ontwikkel.

Die resulteerende simulasie is gebruik om die aktivering en verkoelingseffek van 'n teoretiese damp absorpsie stelsel te beskryf. Soortgelyke werk kon nie in die gepubliseerde literatuur gevind word nie. Dus is 'n eksperimentele apparaat gebou om resultate te verkry vir 'n vergelyking met die teoretise simulasie. 'n Vergelyking tussen die temperatuur waardes van die simulasie en die eksperimentele werk wys dat die verskil in temperatuur op die meeste 23% was.

Acknowledgements

I would like to express my sincere gratitude to my family, friends and supervisor for their enduring support.

Contents

List of Figures

List of Tables

Nomenclature

Constants

$\pi =$	3.141 592
$R =$	8.314 462 [kJ/(kmol·K)]

Variables

A	Area	$[\,m^2\,]$
C	Concentration	$[\,kg/kg\,]$
c	Specific heat	$[\,J/(kg \cdot K)\,]$
d	Diameter	$[\,m\,]$
E	Energy	$[\,J\,]$
h	Enthalpy	$[\,J/kg\,]$
h	Heat transfer coefficient	$[\,W/(m^2 \cdot K)\,]$
h	Height	$[\,m\,]$
k	Thermal conductivity	$[\,W/(m \cdot K)\,]$
L	Length	$[\,m\,]$
m	Mass	$[\,kg\,]$
$\dot{m}$	Mass flow rate	$[\,kg/s\,]$
P	Pressure	$[\,Pa\,]$
$\dot{Q}$	Rate of heat transfer	$[\,W\,]$
R	Thermal resistance	$[\,K/W\,]$
T	Temperature	$[\,K\,]$
t	Time	$[\,s\,]$
UA	Overall heat transfer coefficient	$[\,W/K\,]$
V	Volume	$[\,m^3\,]$
$\dot{W}$	Work rate	$[\,W\,]$
x	Molar concentration	$[\,mol/mol\,]$
ρ	Density	$[\,kg/m^3\,]$

Abbreviations

COP	Coefficient of Performance
H_2O	Water
LiBr	Lithium Bromide

NH_3	Ammonia
SHX	Solution Heat Exchanger

Component Subscripts

A	Absorber
E	Evaporator
EA	Evaporator-Absorber
C	Condenser
f	Film
G	Generator
GC	Generator-Condenser
L	Evaporator Load
P	Vapour Purification
p	Pool
$pump$	Pump
R	Recuperator
S	Solution Heat Exchanger
w	Wall

Fluid Subscripts

f	Liquid
g	Vapour (Gas)
sat	Saturated
sol	Solution
v	Vapour

Stream Subscripts

cw	Cooling water
$cond$	Condensation
hw	Heating water
i	Flow into a pipe or control volume
j	Cell
o	Flow exiting a pipe or control volume

1 Introduction

An increasing amount of attention has been focused on renewable, sustainable and environmentally friendly practices in industry as well as in the methods employed in the production of energy. This can be attributed to the concerns relating to the rate at which green house gasses are produced and the effect that this may have on the climate. In addition to this, the dependence on fossil fuels, with respect to cost and availability, is another concern that helps to motivate efforts towards developing new technologies as well as improving existing technologies.

There are also concerns in South Africa relating to the production of power. Firstly, that the generating capacity cannot meet the demands placed upon the infrastructure. Secondly, while it is advantageous in economical terms that the overwhelming majority of energy production is obtained from coal fired power plants the environmental and health risks associated with this practice cannot be overlooked (McDaid, 2014; McCarthy, 2011).

Many renewable sources of energy can be harnessed through the implementation of applicable technologies in order to obtain environmentally friendly sources of energy. These energy sources can be utilized through the use of wave energy converters, hydroelectric power generation, wind turbines, geothermal steam generation, concentrated solar power generation and photovoltaic technology. An extension on the environmental sources of energy that have been mentioned is the recovery and utilization of thermal energy from process streams that would ordinarily be discarded. This type of process heat is referred to as waste heat and if utilized in an appropriate manner can be used to improve the overall efficiency of industrial installations by converting a resource that was considered to be a by-product into a useful commodity.

A technology that can be powered by a number of these sources of renewable energy such as solar, geothermal and waste heat is vapour absorption. Vapour absorption is a thermally activated process and the principle of vapour absorption can be applied in a few different manners, where the most widely used application is in the refrigeration industry.

Due to the nature of the vapour absorption technology and the current drive for environmentally sound practice, the decision was made to investigate vapour technology with the intent of obtaining a better understanding of its principles and operation for the future goal of improving the operation of the technology. This introductory chapter will continue by briefly discussing refrigeration in order to highlight the differences between vapour compression and vapour absorption. The interest in vapour absorption is related to the possibilities in which the technology can be fuelled and this is the next topic

that is discussed. Thereafter, the basic principles that are used in a simple vapour absorption cycle will be discussed in order to explain the operation of a vapour absorption cycle. This chapter will then conclude with a discussion concerning the goals for this project.

1.1 Refrigeration and Vapour Absorption

The purpose of refrigeration is to provide for a cooling or chilling effect. This cooling effect is realised through the introduction of an energy sink that is at a temperature that is lower than the stream, object or space that is to be cooled. However, a low temperature energy sink is not always available due to the geographical limitations, seasonal variation or daily fluctuation in temperature. This limitation with respect to the availability of a low temperature energy can be overcome through the introduction of an artificial means of producing a low temperature energy sink and this can be achieved through refrigeration process.

The methods used to provide for or produce refrigeration has changed drastically over the last two centuries. With the process evolving from the harvesting and transportation of natural ice to mechanical means of producing ice and this was in turn surpassed by various sophisticated mechanical refrigeration systems. The place that vapour absorption has in the field of refrigeration is that it is one of the principle methods through which a cooling effect can be produced. The differences between refrigeration by vapour compression and vapour absorption are briefly discussed in Appendix E.

Vapour absorption systems require both thermal and electrical sources of energy that are supplied to the vapour generation and electrical components respectively. It is however important to note that the electrical energy requirements of a vapour absorption system are dwarfed by the thermal energy requirements. Due to this large discrepancy between the thermal and electrical requirements it is not uncommon for the coefficient of performance (COP) of a vapour absorption system to be calculated without the inclusion of the electrical power for pumping requirements and control related components.

With respect to the heating stream, the viable temperature range for this stream that is fed to the vapour absorption system can, dependant on system configuration, be between 70 ℃ and 250 ℃. This entire temperature range is not feasible for use in any single type of vapour absorption system, but is viable for a number of different physical configurations. Three of these configurations are referred to as the single, double and triple effect vapour absorption cycles and the typical temperature of the heating stream as well as the associated COP values for these system configurations can be seen in Table 1.1, (Srikhirin *et al.*, 2001; Labus *et al.*, 2013).

Looking beyond environmental sources of energy for a vapour absorption system opens the door into the utilization of a wide array of possible sources

Table 1.1: Comparison of vapour absorption performance values

Configuration	Heating Stream Temperature Range (℃)	COP
Single Effect	70 – 150	0.5 – 0.75
Double Effect	120 – 170	0.8 – 1.2
Triple Effect	200 – 250	1.4 – 1.7

of waste heat that can be harnessed and converted into a useful end product. Waste heat is energy that is released by mechanical, electrical or chemical processes that is considered to be a disposable by-product of a process or system. There are numerous sources of waste heat that originate in a wide variety of industrial fields and processes. These waste heat streams are typically classified into three different categories; high, medium and low, according to the temperature of the waste heat streams. Depending on the literature that is referenced, the values which determine the boundaries of these groupings can vary, but for the purposes of this project the temperature range of the three different classes of waste heat will be defined as:

- High Temperature Waste Heat: above 650 ℃
- Medium Temperature Waste Heat: from 200 to 650 ℃
- Low Temperature Waste Heat: below 200 ℃

In a 2008 report evaluating waste heat recovery opportunities in the United States it was found that between 20 and 50 % of the energy that is used in industrial processes is lost as waste heat (BCS Incorporated, 2008). It was also estimated that roughly 60 % of all waste heat is at a low temperature. This gives an indication that there is a large source of low temperature thermal energy that is being discarded. An example of this would be the implementation of a vapour absorption system as the means through which to recover waste heat from an existing vapour compression system. The end result of this hybrid system would be that the combined efficiency would be better than the original vapour compression system. However, in practice the implementation of waste heat recovery is an endeavour that faces many practical and economical concerns.

1.2 Project Objectives

The desired outcomes for this project was the furthering of the knowledge base of the University of Stellenbosch with regard to vapour absorption refrigeration and its possible applications. A decision was made during the early stages of the project to achieve this goal through the development of a theoretical

simulation. This theoretical simulation would provide the means by which to investigate and model the behaviour of a vapour absorption cycle.

Prior to any work regarding the development of a theoretical simulation additional information was required regarding vapour absorption in general and the currently available solutions for theoretically simulating a vapour absorption cycle. Validation of the theoretical simulation is to be achieved through the comparison of results with those found in literature and/or experimentation.

The next chapter discusses the literature survey that was performed in order to further familiarize the author with vapour absorption terminology and technology. This survey was used as a basis upon which the decisions were made with regard to the nature of the theoretical and experimental work that was performed.

2 Background Literature and Theory

The goal for this section of the report is to introduce and discuss vapour absorption as well as topics related to it in a manner that is accessible and informative. A number of topics will be discussed in this section which include the history of vapour absorption, the possible working fluids, the operation of a vapour absorption cycle and research that is related to this project.

2.1 The History of Vapour Absorption

The earliest reference to the principle of vapour absorption can be traced to the 1750s when William Cullen used diethyl ether to produce a small quantity of ice (Labus *et al.*, 2013). In 1810 Sir John Leslie made use of the manner in which sulphuric acid absorbs water vapour in order to produce ice (Gosney, 1982). Machines making use of Leslie's method were implemented in order to chill wine, but required periodic recharging of the sulphuric acid. In 1824 Michael Faraday made use of a combination of silver chloride and ammonia to produce a chilling effect (Marsh and Olivo, 1979). In Leslie's method, sulphuric acid was the absorbent and water was the refrigerant while in Faraday's apparatus silver chloride was the absorbent and ammonia the refrigerant. Although both of these methods successfully implemented the principle of vapour absorption, more significant developments in vapour absorption were still to come in decades to follow.

In 1859 Ferdinand Carré developed an absorption system that made use of a combination of ammonia and water, where ammonia was the refrigerant and water was the absorbent (Gosney, 1982). A significant advantage that this system had at the time of its development is that it could operate continuously to produce refrigeration at low temperatures. The ammonia/water system developed by Carré was used for many years and formed the foundation for future progress in the field of refrigeration (Gosney, 1982).

In the early 1920s, Baltzar von Platen and Carl Munters invented what is referred to as the Platen-Munters absorption system that makes use of water, ammonia and hydrogen. The purpose behind the inclusion of an additional substance, in this case hydrogen, was to operate the system at a single pressure and by operating at a single pressure level, notwithstanding slight pressure differences due to changes in height, the electrical pump and pressure reducing components were no longer necessary for the operation of the system. Two

attractive aspects of a Platen-Munters system are that it operates silently and does not require an electrical input for a pump. These systems were manufactured by a company called AB Arctic and in 1925 Electrolux purchased this company (Electrolux, 2011). By 1936 Electrolux had manufactured its one millionth absorption refrigerator (Grant, 2003). The silent operation has made this type of refrigeration system attractive for use as a hotel room refrigerator. Caravans, motor-homes and recreational vehicles typically have no access to electricity, making the use of a Platen-Munters system attractive. Another single pressure absorption system is the Einstein Cycle, invented by Einstein and Szilard in the 1920s and patented in 1930 (Einstein and Szilard, 1930). This system made use of butane, water and ammonia in order to operate at a single pressure. This type of single pressure vapour absorption system is at times referred to as a diffusion absorption system.

An absorption system that made use of a solution of water and lithium-bromide was introduced in the 1930s (Srikhirin *et al.*, 2001). In this type of system water is used as the refrigerant and lithium-bromide as the absorbent. Like the ammonia/water system, the water/lithium-bromide system can operate continuously. One disadvantage of a water/lithium-bromide system in comparison with the ammonia/water system is that due to water being the refrigerant, the system can only supply refrigeration at temperatures above 0 °C.

While absorption refrigeration gained popularity in the early 1900s, the technology was overshadowed by the successes and subsequent popularity of vapour compression cycles. Due to this, absorption technologies were neglected in the west until the 1930s (Jordan and Priester, 1949), when large scale absorption refrigeration plants were implemented. However, the portion of global sales that originated in the United States (US) decreased significantly from the 1970s to 1990. This decline in interest in vapour absorption resulted in the US vapour absorption industry falling behind with respect to the technological developments made by the Japanese vapour absorption manufacturers (Garland *et al.*, 1998).

Srikhirin *et al.* (2001) discusses a number of the improvements that have been made in the field of vapour absorption. A few of these improvements include the addition of heat exchangers to the ammonia/water system in order to improve the performance, the introduction of various refrigeration cycle stages that operate at multiple pressures and the replacement of hydrogen with helium for safety in the Platen-Munters system. Developments concerning working fluids are discussed in Section 2.3.5 and research that has been performed on developing new and innovative absorption configurations is discussed in Section 2.4

2.2 The Fundamentals of a Vapour Absorption Cycle

This section gives the background literature relating to the operating principles upon which a vapour absorption refrigeration cycle works. It is essentially a summary of the known information (King, 1971; Marsh and Olivo, 1979; Srikhirin *et al.*, 2001), and is given to add coherency to the point of departure upon which the transient models were developed.

Vapour absorption is a process by which a solution can attract and absorb the vapour in its vicinity. Specific solution compositions are required in vapour absorption applications where the two part solution is composed of a refrigerant and absorbent. This refrigerant/absorbent solution can be manipulated through the application of a cooling or heating effect in order to absorb or release refrigerant respectively. While the principle of vapour absorption can be applied in a number of applications, as discussed by Ziegler (1999), the functionality of vapour absorption that is of interest to this project is with relevance to refrigeration.

Two examples will be used in order to explain the principle of vapour absorption. These examples will in turn be used to explain the operation of a basic vapour absorption refrigeration cycle.

For the first example consider a pair of vessels that are linked together, but initially separated, where the first vessel contains refrigerant and the second vessel contains a refrigerant/absorbent solution. Once the vapour space becomes common between the two vessels and provided that the conditions are appropriate the refrigerant vapour that is exposed to the liquid solution will be absorbed by it, as seen in Figure 2.1.

The resulting effect of this absorption on the solution is that the temperature of the solution will increase, due to the nature of the process, and the mass fraction of absorbent present in the solution will decrease as the solution contains additional refrigerant. These changes are important to note as they both contribute to the conditions in the solution being viable for the absorption of vapour. In order to promote a continued vapour absorption process the solution needs to be cooled. However, for the purposes of this example this cooling of the solution will only briefly extend the absorption of vapour until the mass fraction of absorbent in the solution leads to the vapour absorption process stopping.

The liquid refrigerant is also affected, albeit in a different manner, by the absorption of vapour. Evaporation of liquid refrigerant takes place in order to compensate for the "removal" of vapour through the vapour absorption process. In doing so it can be interpreted that the refrigerant/absorbent solution is indirectly "pulling" the liquid refrigerant from the first vessel into the solution of the second vessel.

Without the interaction of an external interface the evaporation of the

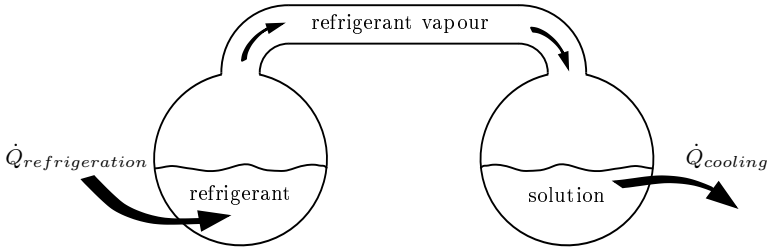

Figure 2.1: Absorption principle, part one – absorption of vapour

liquid refrigerant would cool the remaining liquid. However, the evaporation that the liquid refrigerant undergoes can be used to cool an external medium, stream or space through the inclusion of a heat transfer mechanism. Thereby allowing the liquid refrigerant to draw the latent heat of vaporization from an external source which in turn will lead to a cooling or chilling effect. This example has shown how cooling a solution of refrigerant/absorbent can be used to indirectly cool an external stream.

For the second example consider once again a situation where two vessels are linked together. As in the previous example one vessel contains refrigerant, in liquid and vapour form, and the other holds a two part refrigerant/absorbent solution. However, the difference is that for this example the liquid in the solution vessel is heated and the vapour in the refrigerant vessel is cooled. This configuration can be seen in Figure 2.2.

Heating the solution will promote the separation of refrigerant vapour from the solution. While this is taking place, the cooling of the vapour in the refrigerant vessel will, provided that the conditions are conducive, cause the refrigerant vapour to condense and drip into the refrigerant liquid pool. This process taking place can be seen as the inverse of the process taking place in the first example. The mass fraction of absorbent in the solution increases as the total mass of the solution decreases due to the loss of refrigerant from the solution.

These two examples used separately have limited practical applications as each process operates in an intermittent manner. Where the configuration used in the first example would provide for refrigeration until either the supply of liquid refrigerant has been exhausted or the state of the liquid solution

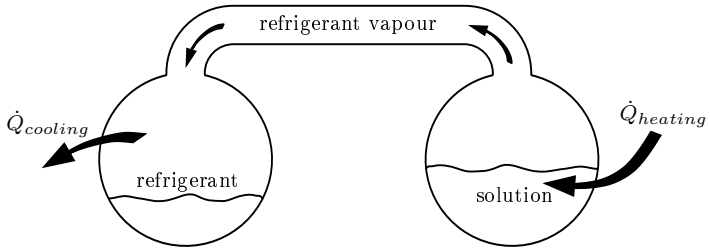

Figure 2.2: Absorption principle, part two – generation of vapour

is no longer conducive to vapour absorption. The generation and subsequent condensation of the refrigerant vapour would also eventually cease to occur. However, combining these two processes into a single process makes it possible to obtain a configuration of components that would allow for the continuous absorption and generation of vapour refrigeration, which in turn makes it feasible to continuously produce a cooling effect through evaporation.

Figure 2.3 shows a component configuration that combines, with the addition of a pump and two throttling devices, the two previously discussed examples. This component configuration forms the basic continuous vapour absorption cycle. While this configuration will function, as it contains the essential components that form a vapour absorption system, there are typically many additional components that are included in a commercial vapour absorption cycle. In this configuration the previously discussed examples for the absorption of vapour and the generation of vapour are operated at two different pressures levels. The high pressure components will be referred to as the condenser and the generator while the low pressure components will be referred to as the evaporator and the absorber. Operating the condenser and generator at a higher pressure than the evaporator and absorber makes it possible to cool the refrigerant vapour in the condenser with a medium at ambient conditions, or at another temperature that is higher than the evaporator temperature, while still making it possible to provide for low temperatures for cooling in the evaporator.

Starting from the absorber, the solution is pumped to the generator where

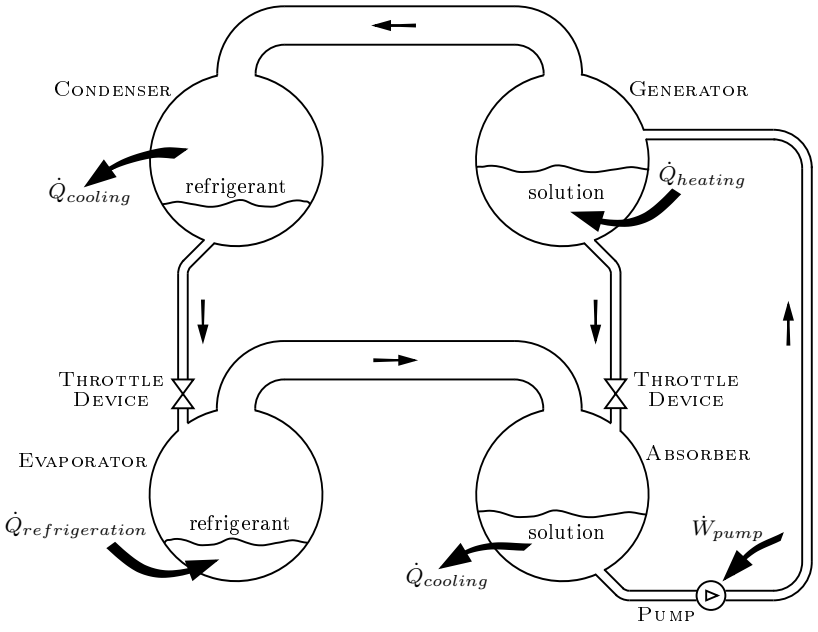

Figure 2.3: Absorption principle, part three – absorption and generation of vapour combined for a complete cycle

it is heated and a portion of the refrigerant is separated from the solution. Two streams leave the generator the first of which is the refrigerant vapour going to the condenser and the second is the solution, now with a higher concentration of absorbent, that returns to absorber. The refrigerant vapour entering the condenser is cooled and condensed, this condensate then passes through a throttling device before entering the evaporator as a stream of low temperature refrigerant liquid that contains a very small percentage of vapour. The liquid portion of this refrigerant entering the evaporator is used to provide for a refrigeration effect on an external space or stream. The solution leaving the generator also passes through a throttling device before entering the absorber. Once in the absorber, the solution has to be cooled in order to help facilitate the absorption of the vapour leaving the evaporator and maintain a low temperature. Once the refrigerant has been absorbed into the solution, thereby decreasing the concentration of absorbent, it can once again be pumped up to the generator which will complete the cycle.

This configuration of components constitutes the basic single effect vapour absorption cycle. Additional components are included in commercial cycles for a number of purposes such as cycle measurement and diagnosis, cycle control, increased efficiency and refrigerant specific requirements. Additional components that are required to accommodate for specific requirements of working fluids as well as components that are used to improve the performance of the cycle as a whole are discussed in the following sections. In addition to this, various component configurations and their applications will also be discussed.

2.3 Working Fluid of a Vapour Absorption Cycle

In order for the absorption process to be realised a working pair of two substances is required, a refrigerant and an absorbent. This combination of refrigerant and absorbent has to fulfil a number of requirements in order to be viable for use in a vapour absorption application. Jordan and Priester (1949) and Owen (2009) discuss the characteristics that are desired in substances for a refrigerant/absorber pair and these properties are listed below:

- No Solid Phase – There must not be a solid phase present in the working pair. If conditions exist where there is a possibility of solidification, the vapour absorption cycle must be controlled in order to ensure that these conditions are avoided
- Relative Volatility – If the refrigerant is not sufficiently volatile in comparison to the absorbent, the amount of energy required to separate the refrigerant from the absorbent will increase

- Affinity – A strong affinity for the refrigerant is desired of the absorbent, as this will reduce the amount of absorbent circulation necessary for a similar refrigeration effect
- Pressure – The operating pressure under which a combination of refrigerant and absorbent would operate has to be taken into account for the possible equipment requirements
- Stability – A high chemical stability is desired as this will prevent the formation of gases, solids and corrosive substance during the many years of operation
- Corrosion – Any possibility of corrosion has to be negated by proper material selection as well as where necessary, the use of corrosion inhibitors
- Safety – If the working pair or its separate substances should pose any serious toxic, flammable or pressure issues hazards safety precautions will have to be implemented
- Fluid Properties – A number of fluid properties are also of importance when evaluating a working pair, these are viscosity for heat transfer and pumping requirements, surface tension for heat transfer and absorption, thermal diffusivity, mass diffusivity and latent heat.
- Environmental Soundness – The global warming potential and the ozone depletion potential are the parameters that are of significance

Taking these criteria into account, the selection process in finding a working pair is a matter of weighing the strengths and weaknesses associated with the properties of possible refrigerant and absorbent substances in addition to the properties of the combined refrigerant/absorbent working pair in order to evaluate whether the implementation of a substance pair is viable. Marcriss *et al.* (1988) and Marcriss and Zawacki (1989) performed an extensive study into collecting the known properties of more than 40 refrigerant and 200 absorbent substances. Although the possible substance combinations for use in vapour absorption are numerous only a few working pairs have been widely implemented. These working pairs are ammonia/water, water/lithium-bromide and a specialized combination of ammonia/water/hydrogen or helium. The properties of water, ammonia and lithium-bromide as well the two working pairs of ammonia/water and water/lithium-bromide and the extent to which these working pairs meet the above criteria will now be discussed further. This will be followed by a brief overview of alternate working fluid pairs.

2.3.1 Water

The relevance of water to vapour absorption processes is that water can be used to fulfil the role of refrigerant or absorbent in vapour absorption appli-

cations. There are numerous sources in literature available for the properties of water and steam. The main source that was used for this project is from "International Association for the Properties of Steam and Water" (Wagner *et al.*, 2000). This was supplemented by the information available in two heat transfer textbooks (Mills, 1999; Çengel, 2003).

2.3.2 Ammonia and Ammonia/Water

At atmospheric conditions ammonia is a pungent colourless gas that is composed of nitrogen and hydrogen in the form of NH_3. It has a number of applications in various fields, with some examples being: refrigerant, fertilizer, cleaning agent and as an ingredient for explosives. While the odour of ammonia is unpleasant, the hazards and risks associated with exposure to ammonia make it beneficial that ammonia can be detected by smell at very low concentrations (James, 1973).

At atmospheric pressure ammonia boils at -33 ℃ and due to this, larger quantities of ammonia are typically stored and transported in a liquid phase. In order to achieve this, the ammonia gas is compressed and cooled. The complications and risks associated with the storage of ammonia is an entirely separate field of study and will not be discussed further.

Ammonia reacts with a wide range of substances, but the combination that will be discussed is the solution of ammonia and water. This combination of ammonia/water can be referred to as aqua ammonia, hydrous ammonia or aqueous ammonia. Anhydrous ammonia is toxic to people and is corrosive to a number of metals. Exposure to anhydrous ammonia can drain the skin of moisture and in effect "burns" a person's skin. Appendix A.4 discusses some of the risks associated with ammonia as well as ammonia/water in further detail. Anhydrous ammonia will corrode copper, zinc, silver and related alloys such as brass. This makes the use of copper in an ammonia/water system impossible. The materials of choice for use in ammonia/water system are steel and stainless steel, although corrosion inhibitors are required with steel.

For the purposes of an absorption system the ammonia assumes the role of refrigerant and water is the absorbent. A distinct advantage of the ammonia/water working pair is that, due to the properties of ammonia, it can provide for refrigeration at temperatures below 0℃.

One complication in a ammonia/water vapour absorption cycle is that the relative volatility between ammonia and water leads to small amounts of water leaving the ammonia/water solution with the ammonia. If this water that leaves the generator with the ammonia is not removed from the refrigerant stream it will have a detrimental effect on the performance and reliability of an ammonia/water vapour absorption cycle (Fernández-Seara and Sieres, 2006). Therefore, the ammonia vapour being generated is always purified. This purification of the refrigerant leaving the generator can be achieved by passing the stream through a purification process like a rectifier or a distillation

column. In addition to the need for vapour purification, an ammonia/water vapour absorption cycle operates at pressure well above atmospheric pressure and therefore requires pressure vessels.

The various properties of ammonia/water are readily available in literature as graphs, tables as well as equations that can be incorporated in a computer program in order to calculate the required properties of the solution. Examples of relevant literature to refer to for properties of ammonia/water can be found in the following works: Ziegler and Trepp (1984), Pátek and Klomfar (1995), Mejbri and Bellagi (2006) and Owen (2009).

2.3.3 Lithium-Bromide and Water/Lithium-Bromide

Lithium-bromide (LiBr) is a white salt and is known for its excellent ability to attract and absorb water. This characteristic is referred to as a hygroscopic property and is highly desirable in a desiccant. The salt has also been used as a sedative, component in the manufacture of chemicals and as a braze and weld flux. However, the use of lithium-bromide that is relevant to this project is that the salt can be used as an absorbent in the working solution of water/lithium-bromide where it is mixed with water at a mass ratio of roughly 50 % (Appendix A.3).

Water is the refrigerant in the working pair of water/lithium-bromide and due to this, the working pair of water/lithium/bromide cannot produce cooling at temperatures below 0 ℃ as the refrigerant will freeze. While this limits the operational range of this working pair to a temperature typically above 5 ℃, the volatility of lithium-bromide, or the lack thereof, ensures that the refrigerant leaving the generator portion of a water/lithium-bromide cycle is for all practical purposes pure water. The properties and operating conditions of water/lithium-bromide systems lead to the operating pressure of a water/lithium-bromide often being at a pressure below atmospheric pressure. When operating an apparatus, such as a water/lithium-bromide system, at vacuum conditions the presence of non-condensible gasses can have a detrimental effect on the operation performance and operation of said apparatus. This issue is exacerbated by the quality of the vacuum and the chemical stability of the working fluid. In a situation where the presence of any non-condensible gasses becomes an issue the system's vacuum pump will have to be activated periodically.

In comparison to ammonia and the solution of ammonia/water, there are significantly less safety concerns to be mindful of when handling and working with lithium-bromide. Lithium-bromide is not flammable, toxic or explosive, but is considered to be detrimental to a person's well being to the extent where when handling lithium-bromide care must be taken not to ingest the salt as this is hazardous. While less hazardous, exposure on the skin or eyes should also be avoided. The safety concerns related to absorption working fluids are discussed further in Appendix A.4.

A complication concerning the use of an aqueous solution of lithium-bromide is that it can solidify or crystallize under certain conditions, which are referred to as the solubility limit of the solution. Boryta (1970) as well as Pátek and Klomfar (2006*b*) describe the characteristics of the solubility limit in addition to the composition and temperature at which a phase change will occur. This phenomenon has to be taken into account when designing and operating a water/lithium-bromide vapour absorption cycle as if it should occur that the solution crystallizes the operation of the vapour absorption cycle will deteriorate until the function is compromised. Wang *et al.* (2011) provides a lengthy discussion surrounding scenarios that can lead to crystallization as well as the chemical, physical and control methods that can be implemented in order to prevent the occurrence of crystallization as well as the recovery of a system from a condition where crystallization has taken place.

If oxygen is present in a water/lithium-bromide vapour absorption cycle, the solution will be corrosive to carbon steel and copper. Corrosion is reduced when the vacuum and vessels that compose the system are of a high quality as this will ensure that very little oxygen is present in the system. The rate of corrosion can be reduced with the addition of corrosion inhibitors, where these inhibitors are added to the vapour absorption cycle in small mass fraction quantities, typically less than 1%. Additives for vapour absorption are discussed further in Section 2.3.4.

Applications that require a high temperature solution of water/lithium-bromide eliminate the possibility of using copper or stainless steel as copper becomes more susceptible to corrosion at high temperature and stainless steel is likely to exhibit pitting and cracking. Copper-nickel alloys, while being more expensive than copper, are a viable option to implement when operating at high temperatures or when the external cooling or heating streams are corrosive (Herold *et al.*, 1996). Additionally, the difference in heat transfer characteristics is not significant and can easily be taken into consideration. However, galvanic corrosion is a problematic design issue that has to be taken into when two or more metals are in contact or in close proximity to one another in the presence of an electrolyte.

The properties of water/lithium-bromide in the form of graphs, equations and tables are also readily available in literature. Examples of literature sources for the properties of water/lithium-bromide include Owen (2009), Teja *et al.* (1991), Chua *et al.* (2000) and Pátek and Klomfar (2006*a*).

2.3.4 Additives for Enhancing an Absorption System

The operation of an absorption system can be improved through the inclusion of small quantities of supplementary chemicals, or additives. Various additives can be included in both water/lithium-bromide and ammonia/water systems for the purpose of corrosion mitigation as well as the improvement of the heat and mass transfer characteristics. In addition to this, there are also additives

that can be included in water/lithium-bromide systems in order to reduce the likelihood of encountering crystallization of the solution.

The decision was made to not use any additives in this project. However, it was deemed necessary to briefly discuss a number of pertinent sources from literature with regards to possible additives.

Herold *et al.* (1996) discusses the reduction of corrosion rates in water/lithium-bromide cycles through the inclusion of a number of possible lithium salts such as lithium chromate, lithium molybdate, lithium nitrate and lithium hydroxide. Agrawal and Hindin (1994) and Mansfeld and Sun (2003) discuss the uses of a number of possible additives for corrosion mitigation in ammonia/water vapour absorption cycles including sodium silicate, sodium chromate, sodium dichromate and cerium chloride.

Kulankara and Herold (2000) presented a paper on the manner in which additives can reduce the surface tension of water/lithium-bromide solutions. This reduction in surface tension improves the vapour absorption process and is referred to as the vapour surfactant theory. Möller and Knoche (1996) investigated the effect that the inclusion of a surfactant has on surface tension and mass transfer of ammonia/water.

The likelihood of crystallization can be reduced through the inclusion of heat and mass transfer additives as these additives will improve system performance thereby avoiding undesired operating conditions. Even so, a substantial amount of research has been performed in an effort to identify chemical additives as well as chemical mixtures for use as absorbent that will have more robust characteristics with regard to crystallization. Wang and Chua (2009) discusses the use of caesium chloride as a means through which the crystallization characteristics can be improved. Wang *et al.* (2011) discusses the research and development of chemical additives, such as pyrophosphoric acid, as well as absorbent combinations such as lithium bromide and potassium formate.

2.3.5 Fluid Working Pairs of Interest

Numerous working fluid pairs have been considered for use in vapour absorption applications including water/sodium hydroxide, water/sulphuric acid and ammonia/sodium-thiocyanate (Herold *et al.*, 1996). Srikhirin *et al.* (2001) and Labus *et al.* (2013) both make reference to the use of various salt mixtures in vapour absorption applications where combinations of two to four salts were used in order to obtain an improvement in fluid characteristics over the more standard single salt implementation of LiBr. The use of Freon 21 and 22 in combination with organic solvents such as dimethyl ether of tetraethylene and dimethyl formamide has also been investigated (Srikhirin *et al.*, 2001). However, the only working pair combinations that have been considered and applied into practical applications is ammonia/lithium-nitrate (NH_3-$LiNO_3$) and water/lithium-chloride (H_2O-LiCl) (Labus *et al.*, 2013).

2.4 Vapour Absorption System Configurations

The focus of this section will be to discuss a few of the various vapour absorption cycle configurations referenced in literature. However, before this topic is approached a number of questions can be asked in order to assist in making a distinction between various vapour absorption installations:

- What is the function that the installation must achieve?
- What is the capacity that the installation must deliver?
- Working fluid that is to be implemented?
- Nature of the external interfaces?
- Component configuration of installation?

Vapour absorption installations can be used to fulfil the function of obtaining only a cooling or chilling effect, only a heating effect, heat transformation or the possibility of cooling and heating. Furthermore, in a situation where a vapour absorption system is used to obtain cooling, the extent of the cooling effect can provide further categories within which to classify various chillers. An example of these categories would be the temperature ranges of <0 ℃ for freezing and ice-making, 0 to 7 ℃ for food storage and 7 to 18 ℃ for air-conditioning purposes (Labus *et al.*, 2013).

The desired capacity of a vapour absorption installation affects the design of the absorption components and the space required by the installation. In addition to this, the desired capacity of an installation can play a role in determining which working fluid must be implemented (Srikhirin *et al.*, 2001).

Options are currently limited with regards to mature vapour absorption technologies in terms of the working fluid that is used. The two current choices for working fluid pairs is ammonia/water and water/lithium-bromide, both of which have their respective benefits and drawbacks (Section 2.3).

The manner in which the vapour absorption installation interacts with the external interfaces has a significant impact on the design of said installation. These external interfaces are the heating of the generator and the cooling of the condenser. In the case of the generator heating, the use of a direct or indirect source of heating is a decision that has to be taken into consideration. With regard to cooling mechanism used for the system, the implementation of water cooling or air cooling in the condenser and absorber has a significant impact on the design and dimensions of the vapour absorption installation. In addition to this, the use of air cooled technology can lead to complications with regard to the possible crystallization in water/lithium-bromide systems (Wang and Chua, 2009).

There are many configurations in which the components that apply the principle of vapour absorption can be implemented. The configuration through

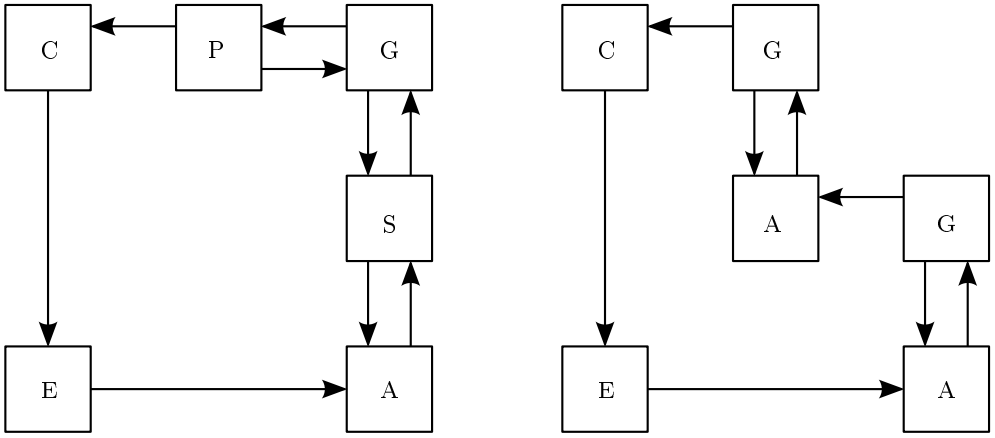

(a) Single effect (b) Double lift

Figure 2.4: Component configurations for the single effect and double lift vapour absorption cycles

which this report has introduced vapour absorption is the "single effect" configuration comprising four core components: a generator (G), a condenser (C), an absorber (A) and an evaporator (E) as seen in Figure 2.4a. Internal energy recovery can also be included in vapour absorption systems through the use of internal fluid heat exchangers, the most common of which is the inclusion of a solution heat exchanger (S) between the generator and the absorber. A vapour purification process (P) is required in vapour absorption systems where the volatility of the absorbent can lead to the "contamination" of the vapour leaving the generator (Section 2.3.2). This is the basic vapour absorption configuration and was used as the foundation upon which to make further developments with regards to vapour absorption technologies. These developments and expansion upon the single effect configuration become necessary when it is desired to utilize sources of thermal energy that fall outside of the feasible operating temperature of the single effect configuration. The discussion surrounding further configurations will exclude energy recovery components as well as vapour purifications processes in order to highlight the differences in fundamental component interaction.

The "half effect" or "double lift" configuration makes use of an additional generator and absorber that is located at an intermediate pressure level, as seen in Figure 2.4b. This configuration performs half as well as a single effect configuration, but can be operated with a lower supply temperature (Srikhirin *et al.*, 2001).

Wang and Chua (2009) discusses the "single effect double lift" configuration. This configuration expands the single effect cycle with the inclusion of two additional generators and an additional absorber, as shown in the double lift cycle (Figure 2.4b, resulting in the configuration shown in Figure 2.5a. In

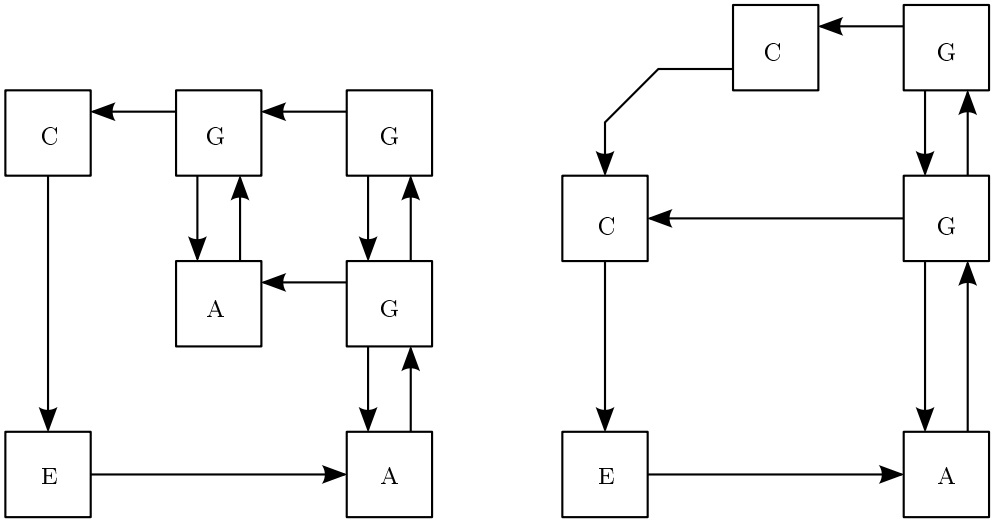

(a) Single effect-double lift (b) Double effect

Figure 2.5: Component composition for the single effect and double lift vapour absorption cycles

doing so this configuration makes it possible to fuel the cycle with a heating stream at temperatures as low as 55 ℃ and at a COP of between 0.35 and 0.7.

The "double effect" vapour absorption configuration makes it possible to utilize higher temperature heating streams in a manner that results in a higher COP than a single effect cycle. This is achieved through the inclusion of an additional generator-condenser pair at a higher pressure level than found in a single effect cycle, as seen in Figure 2.5b. A higher temperature source of heat is used to fire the higher pressure generator and what would be the standard single effect high pressure generator is now heated by the energy of condensation in the higher pressure condenser. This type of vapour absorption cycle was patented and commercialized in 1970 (Wang and Chua, 2009). Many variations in component configuration and flow control are possible in a double effect cycle with an example being that the solution leaving the absorber can flow to the generators in a series or parallel manner (Srikhirin *et al.*, 2001).

The "one and a half effect" vapour absorption cycle seeks to improve on the COP achievable in a single effect cycle while operating below the temperature requirements of a double effect cycle. This is achieved through the inclusion of two solution circuits with a total of three generators. The physical characteristics of this type of system make it possible to implement two different absorbent substances in the solution circuits (Wang and Chua, 2009).

Herold *et al.* (1996, chap. 11) discusses the "generator-absorber heat exchange" (GAX) vapour absorption configuration at length. In this type of system the effect of the solution heat exchanger is replaced by the energy recuperation through the transfer of energy from the high temperature portion

of the absorber to the generator. This type of system can achieve a COP of 0.9 when operated as a chiller and 1.8 when operated as a heat pump (Labus *et al.*, 2013).

The first commercial "triple effect" vapour absorption cycle using water/lithium-bromide, with a COP of roughly 1.7, was made available on the market in 2005 (Labus *et al.*, 2013). This type of system expands on the double effect system in a similar manner as the double effect is an extension of the single effect cycle. A source of concern for triple effect cycles is the question of material selection and corrosion which becomes more prevalent at the operating temperatures of the cycle (above 200 ℃).

This concludes the discussion surrounding a selection of vapour absorption configurations. Should the reader wish to access more in depth information with regards to the configurations that were discussed as well as configurations that were excluded please refer to the referenced literature.

2.5 Absorption System Studies

A vast amount of research has been performed towards the goal of understanding and improving the operation of vapour absorption technologies. This section discusses a selection of research from the field of vapour absorption that is of relevance to the project at hand.

2.5.1 Simulation Focused Studies

The simulation of vapour absorption systems has been approached through steady state solutions, transient solutions as well as dynamic responses. These various approaches for simulations can provide insight into different aspects of a vapour absorption system. In the case of a steady state simulation the resulting effect of altering operating conditions can be assessed. Transient simulations can be used to investigate the start up behaviour and control of a vapour absorption system. Lastly, dynamic simulations can be used to examine the response that the simulation would have to an external disturbance. In addition to the different types of simulations, the literature that was found regarding the simulation of a vapour absorption system showed that a number of different software packages could be used for the steady state simulations. This section will continue with a short discussion regarding a number of articles that document the simulation of vapour absorption systems.

Herold *et al.* (1996) shows how the Engineering Equation Solver (EES) can be used to simultaneously solve the heat transfer rates, heat transfer surface areas and cycle temperatures from supplied external cycle temperature in combination with the values for the overall heat transfer coefficient values in a steady state scenario. EES is also used in an extension of this example

to maximize the refrigeration potential that can be obtained from the cycle specifications.

Grossman and Zaltash (2001) discusses the development and usage of the ABsorption SIMulation program (ABSIM). This simulation program was made for the sole purpose of steady state simulation of vapour absorption cycles and makes use of a graphical user interface that allows a user to configure the cycle components that are to be simulated. ABSIM is capable of simulating expansive vapour absorption cycles and includes the property functions for a number of vapour absorption working pairs.

Somers *et al.* (2011) made use of ASPEN Plus, a chemical process package, to simulate both a single effect and a double effect vapour absorption cycle. The results of this simulation compared well with the results obtained from a similar simulation that was performed with EES.

Bakhtiari *et al.* (2011) developed a model to assess the steady state behaviour of a single effect water/lithium-bromide cycle. The external streams were used as the user specifications for this steady state simulation. Results from an experimental apparatus were used for verification of the model and the results were favourable.

Kohlenbach and Ziegler (2008) combined the use of a steady state solution with a transient model in order to examine the dynamic response of a water/lithium-bromide cycle. A finite difference Jacobian method was used to solve the equations via MATLAB®.

Kim and Park (2007) implemented differential equations in order to describe the transient behaviour and dynamic response of a single effect ammonia/water absorption chiller. A Runge-Kutta-Merson technique was used to simultaneously solve the equations. The behaviour of the simulated cycle during transient start-up as well as during a dynamic response to a change in the fuel supply of the cycle was discussed.

2.5.2 Experimental Investigations

The majority of articles that were found during the literature survey that referred to experimental investigations regarding the operation of a vapour absorption system made use of commercially available vapour absorption units as part of a larger installation. A further distinction could be made in order to categorize these articles according to similar directions of investigation. Two popular research avenues were encountered, namely the investigation of the steady state performance of a vapour absorption system when the operating conditions were altered and the performance of a solar-driven absorption system. In addition to this, there were a number of articles located that investigated the use of vapour absorption technology in various industrial applications where the heat source for the system was geothermal or from any of a number of sources of process energy.

Three articles were chosen to be discussed with regards to experimental vapour absorption installations. The first of which makes use of a commercial vapour absorption system to examine the effect that variations in operating conditions have on the system. Many applications of vapour absorption were found in literature with reference to the source of the thermal energy. However, the decision was made to include a study that examined the operation of a solar activated vapour absorption system. The last article that is included covers the design and construction of a small capacity vapour absorption cycle.

Asdrubali and Grignaffini (2005) made use of a Yazaki water/lithium-bromide absorption chiller as part of an experimental plant. This experimental plant was used to assess the steady state performance of the absorption chiller at various operating conditions.

Agyenim *et al.* (2010) discusses the use of a small capacity commercial absorption system as the cooling apparatus for a solar powered refrigeration installation. This installation made use of a solar collector to indirectly fuel the absorption chiller. A cold water tank was used as a buffer between the chiller outlet stream and the fan coil unit that was used for the space cooling. The operation and performance of the installation is further discussed with the conclusion being made that as far as electrical consumption is concerned the system as a whole compares well with mechanical air conditioning systems.

Kalogirou *et al.* (2001) discusses the design and construction of a 1 kW water/lithium-bromide vapour absorption chiller. The desired cycle output was used as the design point around which the heat exchangers of the apparatus were sized according to the heat exchanger requirements and the available theory for the heat transfer coefficients. Heat exchangers for the generator, absorber and evaporator were submerged in their respective liquid sections. In addition to this, the length of the generator heat exchanger was varied in order to determine viable lengths of piping for different inlet temperatures.

2.5.3 Heat and Mass Transfer

The specialized nature of vapour absorption working fluids in combination with the absorption process itself make it necessary to look beyond standard heat transfer text books for relevant information regarding the heat and mass transfer characteristics active in vapour absorption technology.

Charters *et al.* (1982) discusses the development of an equation that describes pool boiling of water in addition to the evaporation of water from aqueous solutions like water/lithium-bromide. The findings of this study were only considered to be valid for use with smooth surfaces of platinum, copper and brass.

Varma *et al.* (1994) reported on the results of an experimental investigation into the heat transfer coefficients during the pool boiling of water/lithium-bromide solution. Stainless steel tubes of three different diameters were orientated horizontally in the solution. A finding of this study was that the

solution concentration has a noticeable effect on the value of the heat transfer coefficients.

Táboas *et al.* (2007) compared the results obtained from the boiling correlations for pure and mixed liquids with experimental data for the pooling boiling of ammonia/water. The article presents a new correlation for use with the pool boiling of ammonia/water. This proposed correlation combines the calculation process used in two of the correlations for mixtures.

Fujita and Hihara (2005) presented a model and calculation process for the numerical solution for the heat and mass transfer coefficients in an absorption process. This article compares a few different approaches that can be implemented for the analysis of a falling film absorber and suggests a solution method.

2.6 Planning Towards the Project Goals

A significant decision that had to be made for the project was the choice of working fluid for the absorption cycle that was to be investigated as this would play a critical role in the subsequent work. Only two options were considered for the working pair of this project and these options are ammonia/water and water/lithium-bromide. The deciding factor that pushed the project in favour of making use of water/lithium-bromide was the safety concerns that are associated with the use ammonia, as discussed in Appendix A.4.

Once it was established that the working fluid that would be used in the project was a combination of water and lithium-bromide the project could continue with the work regarding the theoretical simulation. The decision was made that the theoretical simulation would be a transient simulation. This simulation would have to implement user specifications concerning the internal and external characteristics of the simulated vapour absorption cycle. With regard to the software that was used to construct and operate the simulation the decision had to be made between making use of a readily available software package and a custom made solution. The desire to examine a transient simulation made it necessary to develop a custom solution as the existing software packages are focused on the simulation of the inter-vessel streams of a vapour absorption cycle with respect to a steady state solution.

When the question regarding the validation of the theoretical results was revisited, an issue arose with regards to the sources of literature available for theoretical simulations. None of the available theoretical investigations into water/lithium-bromide were of a similar nature to the simulation that was being constructed. This made it necessary to acquire transient results from an experimental apparatus.

A choice had to be made between the purchase and installation of a commercial vapour absorption chiller and the design, fabrication and operation of a vapour absorption chiller. The decision was made that a small capacity vapour

absorption cycle would be constructed on site. A custom built vapour absorption chiller presents a number of advantages as well as disadvantages. It would be beneficial with regard to the physical construction of the vessels and the heat exchangers that the exact dimensions are all known and the interaction of these heat exchangers with the various system fluids can be seen through the assistance of windows. The drawback of constructing a water/lithium-bromide vapour absorption chiller is that there are many physical characteristics and limitations to take into account. These include the operation of the system at vacuum conditions as well as the possibility of crystallization and corrosion.

3 Theoretical Simulation

Simulating a vapour absorption system was a significant goal of this project and this section will discuss the manner in which the theoretical simulation was developed and the results that were obtained. The objective of the work surrounding the theoretical simulation was to develop and construct a simulation capable of modelling the characteristics and behaviour of a vapour absorption system.

It was decided that a transient simulation would be developed using the principles describing the conservation of mass and the conservation of energy. The physical dimensions of the system, the material and fluid properties as well as the parameters of the external streams were supplied to the simulation. Working from known initial conditions an explicit numerical solution method was implemented to realise the transient aspect of the simulation.

The simulation was programmed with the C programming language in a text editor. This code was compiled using Cygwin (Red Hat, 2015) and the results of the simulation were written to a "comma separated values" file (.csv). A number of Python™ scripts were used in Spyder (Raybaut, 2015) to plot the results of the various simulations.

This section will continue with discussing the general equations that were formulated from the conservation principles and how these general equations will be applied to the simulation. The model of the simulation will then be discussed, followed by the manner in which the model was de-constructed and simulated. The section will conclude with a discussion of the results obtained from a test case.

3.1 General Equations

The three properties of a control volume that can be described by a principle of conservation are the mass, energy and momentum. While there are three principles of conservation, it was decided to exclude the conservation of momentum and only make use of the conservation of mass and the conservation of energy. This was feasible because the conservation principles can be formulated in a number of manners to describe different simulation characteristics. However, simplifications and assumptions can be made in order to remove aspects of the governing conservation equations that are considered to be unnecessary for a specific application. In the process of establishing the general equations for this simulation a number of simplifications were made, which include: the

exclusion of kinetic energy and work done, constant fluid density, constant control volume size and one dimensional flow.

A topic that will be discussed before continuing to the development of the general equations is the manner in which the transient aspect of the general equations will be dealt with. At any time step t where the values of all the independent variables of the system are known, it becomes possible to use the conservation equations in conjunction with the equations of state, to make a small "step" forward in time and determine the system condition at an unknown state at time $t+\Delta t$. Once the values of the independent variables have been determined for the previously unknown time $t+\Delta t$, the process can be repeated. This process of using a known state to determine the subsequent unknown state will continue until either the simulation reaches its predetermined end time or any of the simulation failure criterion is triggering.

3.1.1 The Conservation of Mass

The conservation of mass requires that the rate at which the internal mass of the control volume changes, is equal to the combined rate at which mass is introduced to and removed from the control volume. This principle can be described mathematically with the formulation seen in Equation 3.1.1. The principle of the conservation of mass was used to formulate two different general equations for this project, with the first equation considering the total mass present in and affecting a control volume while the second equation only took the mass of absorbent into consideration.

$$\frac{\Delta m}{\Delta t} = \sum \dot{m}_i - \sum \dot{m}_o \tag{3.1.1}$$

While Equation 3.1.1 describes the relationship between the rate of change of the internal mass and the accumulative effect of the external streams, determining the internal mass after a certain amount of time has elapsed is desired. This can be achieved through rewriting the previous equation by changing the subject of the formula. This can be seen in the following equations:

$$\begin{aligned} \frac{m^{t+\Delta t} - m^t}{\Delta t} &= \sum \dot{m}_i - \sum \dot{m}_o \\ m^{t+\Delta t} &= m^t + \Delta t \left(\sum \dot{m}_i - \sum \dot{m}_o \right) \end{aligned} \tag{3.1.2}$$

Working with a two component solution makes it necessary to include the concentration of any solutions present in order to completely describe the condition of the system. The concentration C of a solution was defined as the ratio between the mass of absorbent and the total mass of absorbent and refrigerant, as seen in the following equation:

$$C = m_{absorbent}/(m_{absorbent} + m_{refrigerant}) \tag{3.1.3}$$

Building on what was discussed and applying the conservation of mass to a two part solution makes it possible to determine an updated value for the concentration. The mass of the solution in a control volume is multiplied by its concentration in order to limit the calculations to the mass of absorbent. In addition to this, any solution inlet and outlet stream(s) are multiplied by their respective concentrations in order to determine the rate at which absorbent mass is being introduced to or removed from a control volume. This process is shown mathematically by the following equations:

$$\begin{aligned}
\frac{\Delta m}{\Delta t} &= \sum \dot{m}_i - \sum \dot{m}_o \\
\frac{\Delta mC}{\Delta t} &= \sum \dot{m}_i C_i - \sum \dot{m}_o C_o \\
m^{t+\Delta t} C^{t+\Delta t} - m^t C^t &= \Delta t \left(\sum \dot{m}_i C_i - \sum \dot{m}_o C_o \right) \\
C^{t+\Delta t} &= \frac{m^t C^t + \Delta t \left(\sum \dot{m}_i C_i - \sum \dot{m}_o C_o \right)}{m^{t+\Delta t}}
\end{aligned} \tag{3.1.4}$$

This concludes the discussion surrounding the conservation of mass. Two general equations have been discussed that were used in the transient simulation to describe the change in mass and concentration.

3.1.2 The Conservation of Energy

The principle of energy conservation requires that the rate at which the internal energy of a control volume changes is equal to the accumulative rate at which all internal or external mechanisms add or remove energy from the control volume. Mechanical work, heat transfer and mass transfer are examples of external mechanism that transfer energy across the control volume boundaries. The generation or consumption of energy through a exothermic or endothermic reaction are examples of internal mechanisms through which the internal energy of a control volume can be altered.

This relationship can be represented mathematically by the following equations:

$$\begin{aligned}
\frac{\Delta E}{\Delta t} &= \sum \dot{E}_i - \sum \dot{E}_o \\
\frac{\Delta E}{\Delta t} &= \sum \dot{m}_i h_i + \sum \dot{Q}_i + \sum \dot{W}_i + \sum \dot{Q}_{gen} \\
&\quad - \sum \dot{m}_o h_o - \sum \dot{Q}_o - \sum \dot{W}_o
\end{aligned}$$

An assumption that was made that the fluids used in the simulation to be considered to be incompressible. This assumption simplified the simulation by making it possible to perform the conservation of energy calculations using

enthalpy values instead of internal energy. This is shown below:

$$\frac{\Delta E}{\Delta t} = \frac{\Delta(mcT)}{\Delta t}$$
$$\frac{\Delta E}{\Delta t} = \frac{\Delta(mh)}{\Delta t}$$

This change makes it possible to write the general conservation of energy, ignoring work and energy generation, in the following manner:

$$\begin{aligned}
\frac{\Delta(mh)}{\Delta t} &= \sum \dot{m}_i h_i + \sum \dot{Q}_i - \sum \dot{m}_o h_o - \sum \dot{Q}_o \\
\frac{m^{t+\Delta t}h^{t+\Delta t} - m^t h^t}{\Delta t} &= \sum (\dot{m}_i h_i) + \sum \dot{Q}_i - \sum (\dot{m}_o h_o) - \sum \dot{Q}_o \\
m^{t+\Delta t}h^{t+\Delta t} &= m^t h^t + \Delta t \left(\sum \dot{m}_i h_i + \sum \dot{Q}_i - \sum \dot{m}_o h_o - \sum \dot{Q}_o \right) \\
h^{t+\Delta t} &= \frac{m^t h^t + \Delta t \left(\sum \dot{m}_i h_i + \sum \dot{Q}_i - \sum \dot{m}_o h_o - \sum \dot{Q}_o \right)}{m^{t+\Delta t}}
\end{aligned} \tag{3.1.5}$$

Should the assumption be made that a substance has a constant specific heat it is possible to rewrite the energy balance equation in order to make the new temperature the subject of the formula:

$$T^{t+\Delta t} = \frac{m^t c T^t + \Delta t \left(\sum \dot{m}_i h_i + \sum \dot{Q}_i - \sum \dot{m}_o h_o - \sum \dot{Q}_o \right)}{m^{t+\Delta t} c} \tag{3.1.6}$$

This section has shown how two equations for use in the simulation have been derived from the conservation of energy. Equation 3.1.6 can be used, when applicable, to directly calculate a new temperature while Equation 3.1.5 can be used to determine an updated temperature in an indirect manner.

3.2 Constructing the Simulation

The process that was followed for constructing the simulation simulation began with development of a theoretical model that would adequately describe the properties, features and behaviour of the vapour absorption system and its processes. This theoretical model would be described by the application of the principles of conservation.

Figure 3.1 shows the model that was chosen for implementation in the theoretical simulation. This theoretical model contains all of the major components necessary for the operation of a single effect vapour absorption cycle. A number of simplifications were made in the development of this model, the most significant of which was the decision to combine a liquid and vapour control volume in both the generator and the evaporator into single control

volumes. This made it possible to assess the change to the combined control volume for the generator solution and vapour as well as the evaporator liquid and vapour in a manner that eliminated the need to examine the interactions across these two vapour-liquid boundaries.

The generator solution is in direct contact with a heating stream and the shared generator-condenser vapour space is exposed to a source of cooling. Valves and a pump are included for the purpose of separating the simulation into two distinct pressure levels. In a similar manner to the generator and condenser combination, the evaporator liquid is exposed to an external load that it has to cool and the shared absorber-evaporator vapour space is exposed to liquid solution upon which absorption can take place. Furthermore, the absorber liquid solution is exposed to an external source of cooling.

The decision was made to construct the absorption portion of the simulation in a flexible manner by including two possible surfaces that could interact with the common vapour space.

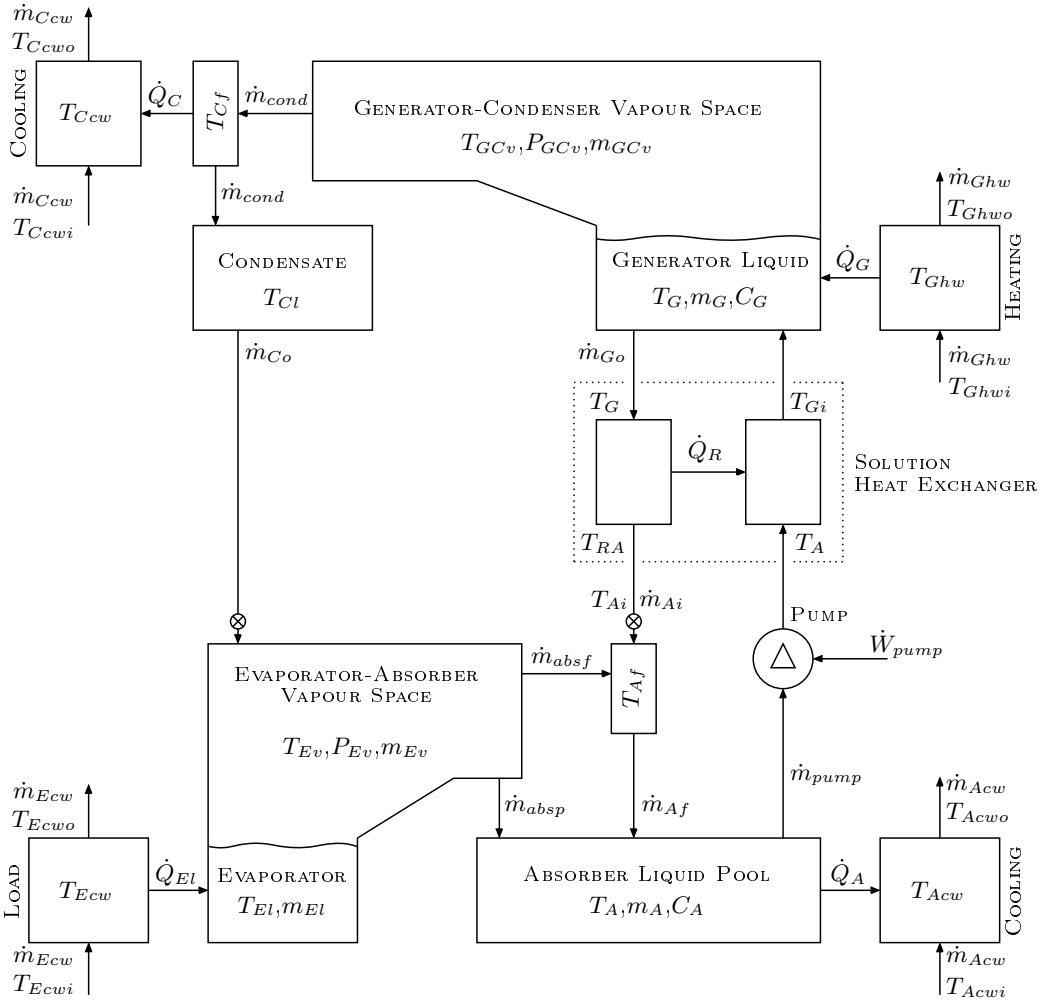

Figure 3.1: Theoretical model of a vapour absorption system

In addition to the assumption made with regard to the combination of vapour and liquid control volumes the following general assumptions and simplifications were made when developing the model and equations that were used to describe the control volumes of the simulation:

- No heat transfer to or from the surroundings
- No conduction heat transfer between control volumes
- External streams are supplied at a constant temperature and mass flow rate
- The pressure in the generator is the same as in the condenser
- The pressure in the absorber is the same as in the evaporator
- Refrigerant is pure water
- Refrigerant leaving the condenser is saturated water
- Pressure loss in the interconnecting pipework is ignored

It was decided to break the complete simulation up into more manageable sections. These sections would be modelled and simulated separately until they functioned in a satisfactory manner. While some of the sections did not serve any significant purpose by themselves, they were all used as building blocks for the complete simulation. Once it was established that the separate sections were operational, the sections would be combined to form the complete simulation.

This section will continue with discussing the manner in which the heat exchangers were dealt with. Thereafter, the various component configurations and their control volumes that were analysed and tested will be discussed. Each component configuration will be discussed in a fixed format. Starting with a very brief introduction for the configuration and a schematic representation of the configuration. Thereafter, the control volumes and variables will be discussed. The process in which the theory was developed will be covered for each configuration. The results that were obtained from the computer simulations will also be shown and discussed. Source code for the simulation computer code will not be discussed. However, the operation of the completed vapour absorption cycle simulation is discussed through the use of a simulation flow diagram in Appendix B.

3.3 Heat Exchanger Modelling

There are five heat exchangers included in this simulation. Four of which are represented by a bank of parallel tubes. These parallel tube heat exchangers

facilitate the transfer of energy between external streams and the vapour absorption cycle. The decision was made that in the simulation the generator, absorber and evaporator heat exchangers would be located in their respective liquid pools. The last of the four parallel tube heat exchangers facilitates the interaction between an external cooling stream and the common generator-condenser vapour space. The fifth heat exchanger included in the simulation is located between the generator and absorber and will be referred to as the solution heat exchanger (SHX). This heat exchanger will be represented by a tube-in-tube heat exchanger and will be discussed separately in Appendix C.3.

The rate at which energy is transferred from the high temperature side of the heat exchanger to the low temperature side is determined by the magnitude of the temperature difference and the nature of the path through which the energy must flow. Two methods were used in this simulation to represent the heat transfer modes and physical characteristics of the heat exchangers. The heat transfer rates for the generator, absorber, evaporator and the SHX were represented through the use of an overall heat transfer coefficient while the condenser calculation was approached through the use of thermal resistances. These two methods are interchangeable, but were both used in different locations for a matter of convenience. Equation 3.3.1 shows these two methods of representing heat transfer:

$$\dot{Q} = \begin{cases} \Delta T/R \\ UA\Delta T \end{cases} \tag{3.3.1}$$

During the initial development of the simulation a simple approach was taken with regard to the heat exchanger calculations. One part of this simplification was the assumption that the temperature of the internal fluid of each heat exchanger remained constant throughout the length of the heat exchanger. This assumption was used in conjunction with a user defined value for the product of the overall heat transfer coefficient and area of each heat exchanger. These simplifications made it possible to begin development of the simulation under the condition that the manner in which the heat transfer characteristics and temperatures were dealt with would be improved at a later date.

These improvements came later through the implementation of a generalized process by which the internal heat exchangers of the simulation would be modelled and calculated. This was achieved by the use of multiple control volumes that would divide each heat exchanger into smaller cells along the length of the various heat exchangers.

3.3.1 Control Volumes

The heat exchangers were all divided up into cells along their length with each cell being assigned variables for mass and temperature. The assumption

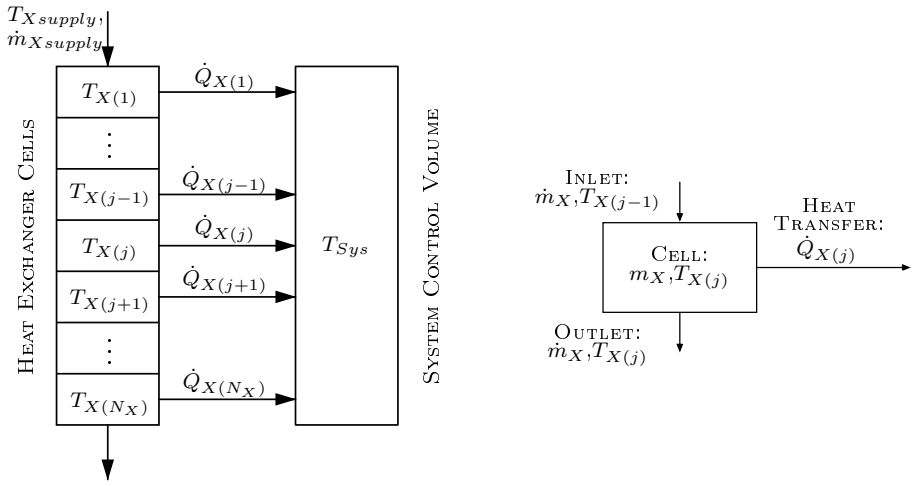

(a) Complete heat exchanger (b) Cell

Figure 3.2: General heat exchanger

was made that the mass in each heat exchanger cell would remain constant throughout the simulation. In addition to this, the decision was made that the vapour absorption system control volumes that interacted with the various heat exchangers would always be well mixed. The implication of this is that the temperature and, when relevant, concentration of a system control volume would be homogeneous. This is illustrated in Figure 3.2a where, for this example, the assumption is made that the temperature in the heat exchanger cells are higher than the temperature in the system control volume. Figure 3.2b shows a single cell from this heat exchanger "X" that is assigned mass and temperature values $m_{X(j)}$ and $T_{X(j)}$ respectively.

At each time step calculations are performed in order to determine the heat transfer rates to or from each cell of each heat exchanger. Once the heat transfer rates for the various cells are determined the conditions in each heat exchanger cell will be determined for the next time step. In addition to this, the accumulative effect of all the cells in a heat exchanger is taken into account for use in the conservation of energy calculation for the respective system control volumes. Appendix C.2 discusses the manner in which the boundary conditions of the cell are dealt with in addition to a more detailed explanation concerning the calculation process through the use of a flow diagram.

The heat transfer rate calculations for the generator, absorber and evaporator cells were all achieved by dividing the total UA value of the respective heat exchangers in a manner where each cell is assigned a value. In the case of the condenser the calculation is dealt with slightly differently due to the use of thermal resistances and this is discussed further in Appendix C.4.

3.3.2 Derivation of Equations

This section will discuss how the general equations for the conservation of mass and energy were applied to the heat exchanger control volumes in order to establish a process through which the behaviour of all the tube bank heat exchangers could be determined. The application of the general conservation equations was done in a manner that ensured that the resulting equations would remain valid irrespective of the approach that was used to obtain the heat transfer rate between a heat exchanger cell and a system control volume.

The general equation for the conservation of energy is the only equation that was applied to the heat exchangers in order to determine their conditions at consecutive time steps. This is because of the assumption that was made that the mass in each cell of each heat exchanger was constant, making it unnecessary to update the mass variables for each cell at each time step. In addition to this, the external streams are assumed to be single component fluids.

Applying the conservation of energy to the general heat exchanger cell results in the following equation:

$$T_{X(j)}^{t+\Delta t} = T_{X(j)}^{t} + \Delta t/(m_{X(j)}^{t} c)(\dot{m}_X c T_{X(j-1)} - \dot{m}_X c T_{X(j)} - \dot{Q}_{X(j)}) \qquad (3.3.2)$$

3.4 Generator and Condenser

The component combination of generator and condenser form the high pressure side of a vapour absorption system. These components are used to separate vapour refrigerant from the liquid solution that is present in the generator, while simultaneously condensing vapour refrigerant. Figure 3.3 illustrates a representation of these components where the generator heat exchanger is submerged in the liquid solution and the condenser heat exchanger can interact with the vapour refrigerant.

Simulating the generator or condenser components separately was deemed unnecessary due to the manner in which additional features would have had to be added in order to construct a useful transient simulation. Due to this, it

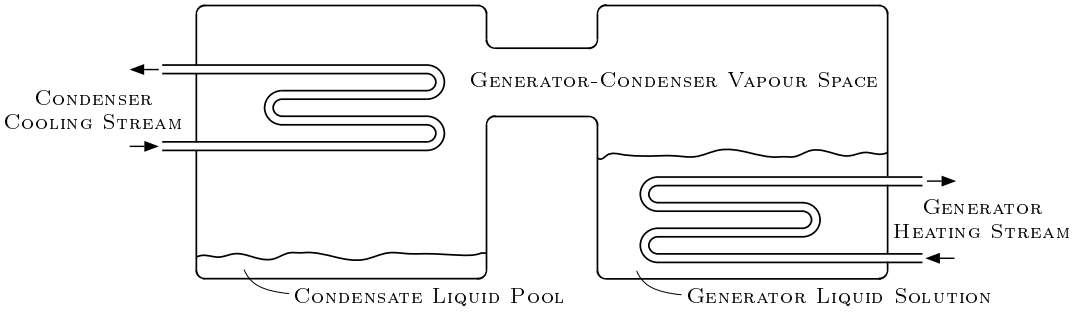

Figure 3.3: Generator and condenser schematic

was decided to work towards a configuration that combined a generator and condenser in a single shared vessel.

3.4.1 Control Volumes and Variables

The control volumes that were used for the generator-condenser combination can be seen in Figure 3.4. It should be noted that in order to keep the figure legible, a number of the variables were not included in the figure. The condition and behaviour of the generator liquid and vapour is now dependent on the interaction between the vapour and the condenser. Should no condensation take place the results of this simulation will be uneventful. However, when conditions are appropriate condensation will take place and the behaviour of configuration alters significantly.

3.4.2 Derivation of Equations

This section discusses the application of the general equations for the conservation of mass and energy to the generator and condenser component configuration. While a number of general assumptions were discussed in Section 3.2 the generator and condenser combination has specific assumptions with regard to the condition of the vapour. The initial assumption that was made is that the vapour in the shared vapour space is at the same temperature as the generator solution. This assumption was made in order to reduce the number of independent variables in the simulation. The implication of this assumption is that the vapour is assumed to be superheated. In addition to this, it was assumed that the volume of the vapour space would not change to such an extent that it was feasible to let the vapour space volume lag behind by one time step in order to simplify the calculations. These two assumptions made it possible to use the known conditions of the combined solution and vapour

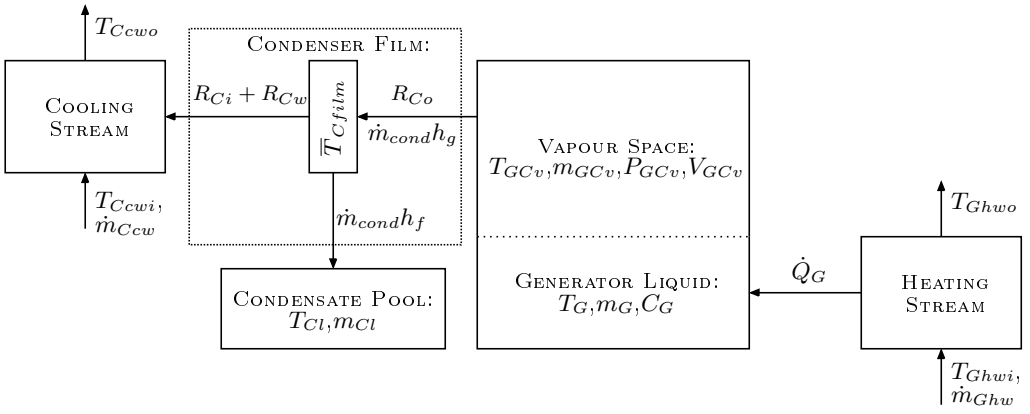

Figure 3.4: Control volumes for generator, condenser and external streams

space in conjunction with the external interfaces to determine the condition of this control volume at a small interval in the "future".

The mass of the vapour was defined as the product of the volume and the density, where the density is a function of temperature and pressure:

$$m_{GCv} = V_{GCv}\rho_g\{T_G, P_G\} \tag{3.4.1}$$

This relationship can then be used in combination with the rate of condensation, that is determined separately from these calculations, in order to complete the conservation of mass for this control volume:

$$\begin{aligned}
\frac{\Delta m}{\Delta t} &= \sum \dot{m}_i - \sum \dot{m}_o \\
\frac{\Delta m_G}{\Delta t} + \frac{\Delta m_{GCv}}{\Delta t} &= 0 - \dot{m}_{cond} \\
m_G^{t+\Delta t} - m_G^t + m_{GCv}^{t+\Delta t} - m_{GCv}^t &= \Delta t(-\dot{m}_{cond}) \\
m_G^{t+\Delta t} &= m_G^t + m_{GCv}^t - m_{GCv}^{t+\Delta t} + \Delta t(-\dot{m}_{cond}) \\
m_G^{t+\Delta t} &= m_G^t + m_{GCv}^t - V_{GCv}\rho_g\{T_G^{t+\Delta t}, P_G^{t+\Delta t}\} + \Delta t(-\dot{m}_{cond})
\end{aligned} \tag{3.4.2}$$

where $P_G^{t+\Delta t}$ can be written as a function of $T_G^{t+\Delta t}$ and $C_G^{t+\Delta t}$.

The next application of the conservation of mass is the calculation of the solution concentration for the next time step. In a similar manner to the derivation seen for Equation 3.1.4 the solution concentration can be recalculated:

$$\begin{aligned}
\frac{\Delta mC}{\Delta t} &= \sum \dot{m}_i C_i - \sum \dot{m}_o C_o \\
\frac{\Delta(m_G C_G)}{\Delta t} &= 0 - 0 \\
\frac{m_G^{t+\Delta t} C_G^{t+\Delta t} - m_G^t C_G^t}{\Delta t} &= 0 \\
C_G^{t+\Delta t} &= \frac{m_G^t C_G^t}{m_G^{t+\Delta t}}
\end{aligned} \tag{3.4.3}$$

The conservation of energy can be applied to the shared control volume in

the following manner:

$$\begin{aligned}
\frac{\Delta E}{\Delta t} &= \sum \dot{E}_i - \sum \dot{E}_o \\
\frac{\Delta(mh)}{\Delta t} &= \sum \dot{m}_i h_i + \sum \dot{Q}_i - \sum \dot{m}_o h_o - \sum \dot{Q}_o \\
\frac{\Delta(m_G h_G)}{\Delta t} + \frac{\Delta(m_{GCv} h_{GCv})}{\Delta t} &= 0 + \dot{Q}_G - \dot{m}_{cond} h_{GCv} - 0 \\
\frac{m_G^{t+\Delta t} h_G^{t+\Delta t} - m_G^t h_G^t}{\Delta t} + \frac{m_{GCv}^{t+\Delta t} h_{GCv}^{t+\Delta t} - m_{GCv}^t h_{GCv}^t}{\Delta t} &= \dot{Q}_G - \dot{m}_{cond} h_{GCv} \\
m_G^{t+\Delta t} h_G^{t+\Delta t} + m_{GCv}^{t+\Delta t} h_{GCv}^{t+\Delta t} &= \Delta t(\dot{Q}_G - \dot{m}_{cond} h_{GCv}) + m_G^t h_G^t + m_{GCv}^t h_{GCv}^t
\end{aligned} \tag{3.4.4}$$

where the entirety of the right hand side of this equations is known and the left hand side can be rewritten, through the inclusion of Equations 3.4.2 and 3.4.3 as well as the property equations, in a manner where the only unknown is $T_G^{t+\Delta t}$. This makes it possible to iteratively calculate the new generator solution temperature and once this has been determined the dependent variables can be calculated.

The last portion of this configuration that must be defined is the liquid pool of the condenser. It is assumed that the liquid entering the condenser is saturated water at the film temperature. This assumption forms the basis for the conservation of energy, but the conservation of mass has to be tackled first:

$$\begin{aligned}
\frac{\Delta m}{\Delta t} &= \sum \dot{m}_i - \sum \dot{m}_o \\
\frac{\Delta m_{Cl}}{\Delta t} &= \dot{m}_{cond} - 0 \\
m_{Cl}^{t+\Delta t} &= m_{Cl}^t + \Delta t \dot{m}_{cond}
\end{aligned}$$

Thereafter the conservation of energy can be applied:

$$\begin{aligned}
\frac{\Delta E}{\Delta t} &= \sum \dot{m}_i h_i + \sum \dot{Q}_i - \sum \dot{m}_o h_o - \sum \dot{Q}_o \\
\frac{\Delta m_{Cl} c_p T_{Cl}}{\Delta t} &= \dot{m}_{cond} h_{cond} + 0 - 0 - 0 \\
m_{Cl}^{t+\Delta t} c_f T_{Cl}^{t+\Delta t} - m_{Cl}^t c_f T_{Cl}^t &= \Delta t \dot{m}_{cond} c_f T_{Cfilm} \\
T_{Cl}^{t+\Delta t} &= \frac{\Delta t \dot{m}_{cond} c_f T_{Cfilm} + m_{Cl}^t c_f T_{Cl}^t}{m_{Cl}^{t+\Delta t} c_f}
\end{aligned}$$

where it can be seen that choosing to calculate the enthalpy of the liquid pool as the product of the specific heat and temperature makes it possible to find an explicit solution for the "new" temperature of the liquid in the pool.

3.4.3 Results

The results obtained from the computer code for the combination of generator and condenser will now be discussed. Table 3.1 shows the variables that were specified as initial conditions, constants as well as external streams.

Table 3.1: Initial conditions and constants for the generator-condenser pair

Generator Liquid Pool	
T_G	25 °C
C_G	0.5 kg/kg
m_G	12 kg
Generator Vapour Space	
T_{GCv}	20 °C
V_{GCv}	1.1 m^3

Heating Stream	
T_{Ghwi}	80 °C
$\dot{m}_{Ghw}$	0.5 kg/s
UA_G	500 W/°C
Condenser Liquid Pool	
T_{Cl}	25 °C
m_{Cl}	5 kg

Cooling Stream	
T_{Ccwi}	20 °C
$\dot{m}_{Ccw}$	0.5 kg/s
k	18
Simulation Parameters	
t_{end}	1 hour
Δt	0.001 second

A selection of variables were plotted in order to show the manner in which this configuration, with the chosen conditions, approaches equilibrium. These plots can be seen in Figure 3.5 and include the temperatures, masses, heat transfer rates, concentration, pressure and rate of condensation.

The temperature in the generator liquid solution increases, but slows down once condensation begins to occur. It can be seen how as the mass in the generator solution pool decreases, the mass of condensate increases. While

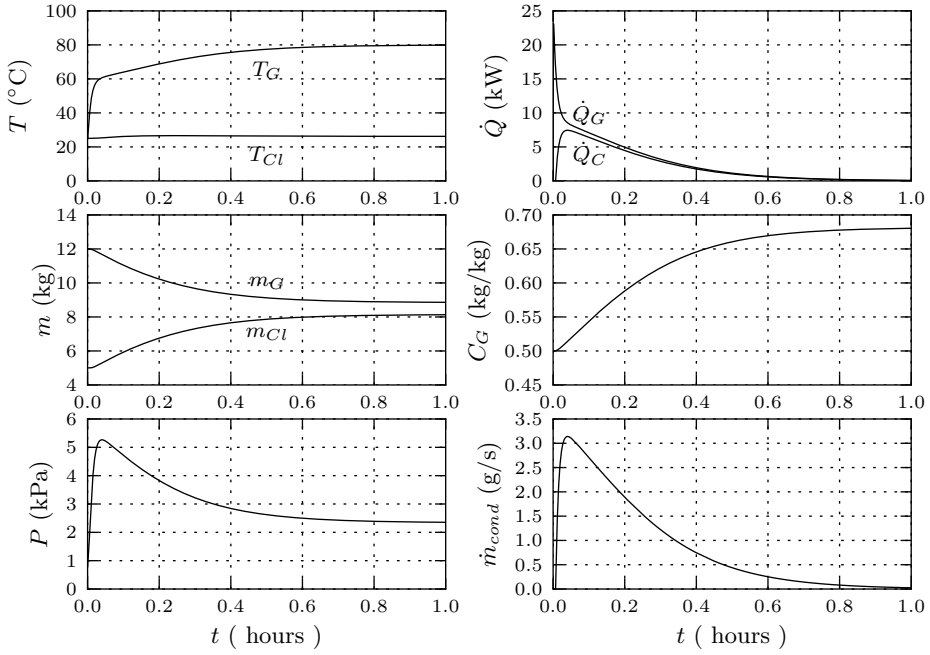

Figure 3.5: Generator-Condenser simulation results assuming no renewal of generator's solution

not shown, there are changes in the mass of vapour in the configuration, but these changes are of a significantly smaller nature than those in the liquid variables. It can be seen how the heat transfer rate to the generator decreases as the temperature of the liquid approaches that of the heating stream. The energy being removed from the vapour decreases as the rate of condensation decreases.

The rate of condensation is related to a number of conditions in the simulation. It can be seen that when the pressure in the vessel is higher, the rate of condensation is at its highest. However, the rate of condensation decreases as the pressure decreases. The decrease in pressure in the vessel is due to the manner in which the saturation pressure of the solution is a function of both temperature and concentration. As the concentration increases, due to the loss of water to the condenser, the saturation pressure of the solution decreases. Therefore, if one wanted to maintain a more constant rate of condensation, the concentration of the solution in the generator would have to be reduced. This would be possible with the introduction of a stream of lower concentration solution being fed into the generator.

3.5 Generator and Condenser with External Streams

It is shown in the previous section that the production of condensate gradually diminishes until it stops entirely. This can be attributed to the manner in which the condition of the liquid solution is altered over the course of the simulation through the application of heat in conjunction to the condensation of refrigerant.

In order to produce condensate in a continuous manner the temperature and more importantly the concentration of the generator solution need to be decreased and this can only be achieved through the introduction of an external mass stream that will interact with the liquid solution. The inclusion of two more external mass streams is required for the purposes of this configuration to ensure that the size of the liquid pools does not become excessive. However, in the context of the complete vapour absorption cycle these two return streams would be used to feed a supply of refrigerant to the evaporator and return a stream heated solution at a high concentration to the absorber.

Figure 3.6 shows the addition of these three mass streams to the generator-condenser configuration.

3.5.1 Control Volumes and Variables

The alterations made to the control volumes that were previously used in Section 3.4.1 did not justify the inclusion of another control volume diagram. The newly introduced inlet and outlet streams that are shown in Figure 3.6 can

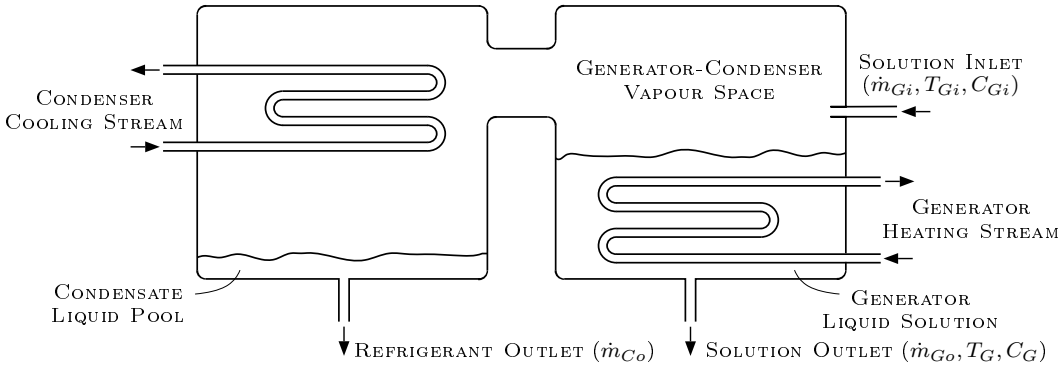

Figure 3.6: Schematic for the generator and condenser pair with mass streams

be described in the following manner: a stream of solution enters the generator solution control volume at a rate of $\dot{m}_{Gi}$ a temperature T_{Gi} and concentration C_{Gi}. The generator solution outlet stream leaves the generator solution pool at T_G and C_G and flows at a rate of $\dot{m}_{Go}$. Lastly, the condenser outlet is at the same state as the condensate pool and has a flow rate of $\dot{m}_{Co}$.

3.5.2 Derivation of Equations

This section will not discuss the entire derivation of the principle equations that describe the behaviour of the control volumes. Only the changes to the final form of the four main equations that characterise the configuration will be covered.

This starts with the application of the conservation of mass to the theoretical configuration. After applying the conservation of mass to the combination of generator solution and the common vapour space the following updated equation is obtained:

$$m_G^{t+\Delta t} + m_{GCv}^{t+\Delta t} = m_G^t + m_{GCv}^t + \Delta t(\dot{m}_{Gi} - \dot{m}_{cond} - \dot{m}_{Go}) \tag{3.5.1}$$

It can be seen that the only difference between this equation and Equation 3.4.2 from the previous configuration is that the solution inlet and outlet stream is included in the calculations. In a similar manner, the updated concentration calculation changes through the inclusion of the inlet and outlet streams. This can be seen in the following equation:

$$C_G^{t+\Delta t} = (m_G^t C_G^t + \Delta t(\dot{m}_{Gi} C_{Gi} - \dot{m}_{Go} C_{Go}))/m_G^{t+\Delta t} \tag{3.5.2}$$

The conservation of energy when applied to the generator solution and the common vapour space yields the following equation:

$$\begin{aligned} m_G^{t+\Delta t} h_G^{t+\Delta t} + m_{GCv}^{t+\Delta t} h_{GCv}^{t+\Delta t} = {} & m_G^t h_G^t + m_{GCv}^t h_{GCv}^t \\ & + \Delta t(\dot{Q}_G + \dot{m}_{Gi} h_{Gi} - \dot{m}_{cond} h_g - \dot{m}_{Go} h_{Go}) \end{aligned} \tag{3.5.3}$$

The refrigerant outlet that is connected to the condensate liquid pool changes the calculation for the updated temperature of the liquid pool in the following manner:

$$T_{Cl}^{t+\Delta t} = (m_{Cl}^{t} c_p^{t} T_{Cl}^{t} + \Delta t(\dot{m}_{cond} c_p T_{Cfilm} - \dot{m}_{Co} c_p T_{Cl}))/(m_{Cl}^{t+\Delta t}) \qquad (3.5.4)$$

3.5.3 Results

Table 3.2 shows the variables that were used for this simulation. The inlet and outlet streams were assigned static values for their respective mass flow rates. Only the solution inlet stream was assigned values for the condition of the stream as conditions of the two outlet streams would be at the condition of the liquid pool that the stream originates from.

The results that were obtained from the theoretical simulation of the generator-condenser configuration are shown in Figure 3.7. Here it can be seen that the inclusion of the external mass streams has altered the operation of the configuration in a manner that makes it possible to continually produce and remove a stream of liquid refrigerant from the condenser section of the configuration.

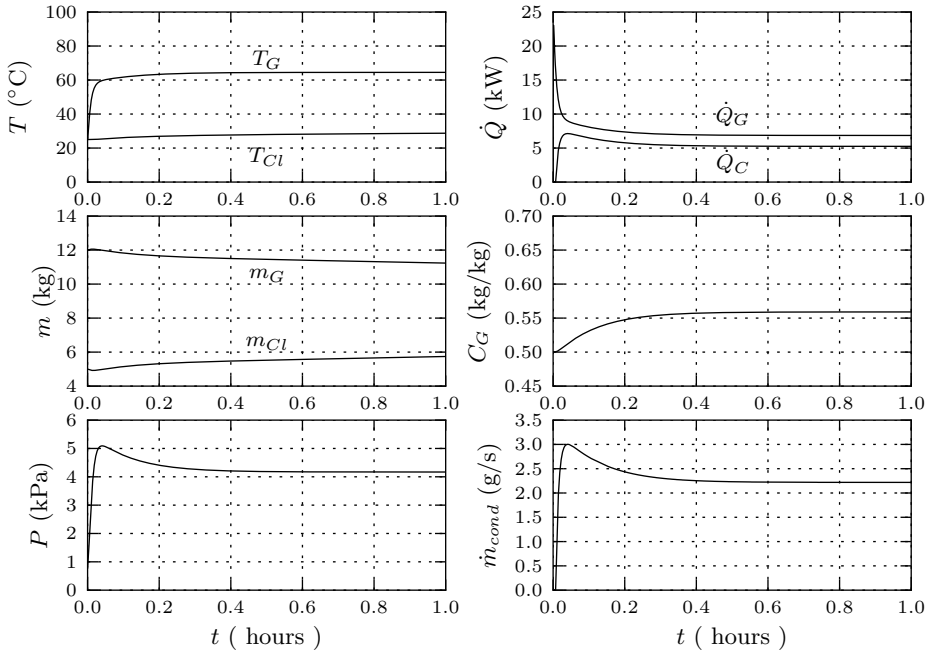

Figure 3.7: Generator-Condenser simulation results assuming continuous renewal of generator's solution

Table 3.2: Initial conditions and constants for the generator-condenser pair with external mass streams

Heating Stream	
T_{Ghwi}	80 °C
$\dot{m}_{Ghw}$	0.5 kg/s
UA_G	500 W/°C
Solution Inlet	
$\dot{m}_{Gi}$	0.012 kg/s
T_{Gi}	40 °C
C_{Gi}	0.50 kg/kg
Solution Outlet	
$\dot{m}_{Go}$	0.0189 kg/s

Simulation Parameters	
t_{end}	1 hour
Δt	0.01 second
Common Vapour Space	
T_{GCv}	20 °C
V_{GCv}	1.1 m^3
Generator Liquid Pool	
T_G	25 °C
C_G	0.5 kg/kg
m_G	10 kg

Cooling Stream	
T_{Ccwi}	20 °C
$\dot{m}_{Ccw}$	0.25 kg/s
k	18 W/(m °C)
l	10.5 m
d_o	0.0127 m
t	0.0012 m
Condenser Liquid Pool	
m_{Cl}	5 kg
Refrigerant Outlet	
$\dot{m}_{Co}$	0.0007 kg/s

3.6 Evaporator and Absorber

The purpose of a typical vapour absorption system is to provide for refrigeration. If no vapour is absorbed in the absorber, no evaporation will take place and the system will be unable to provide a refrigeration effect. This is why the absorption process can be considered to be the most important process in a vapour absorption system, because if the absorption process should fail to occur in a continuous and reliable manner the system as a whole will not serve any useful purpose.

Investigating the manner in which the absorber interacts with a pool of refrigerant and the associated vapour space was the next step taken in creating a simulation of a vapour absorption system. Similarly to the work concerning the condenser, it was decided that investigating the absorber and the evaporator separately would not be a beneficial endeavour. The reason for this is that in the case of the absorber-evaporator pair, each separate component will do nothing on its own and can only function while combined with a single vapour space.

When the evaporator and absorber share the same vapour space there is no direct contact between the liquid refrigerant in the evaporator and the liquid solution in the absorber. The entirety of the interaction between absorber and evaporator takes place through the shared vapour space. Naturally if the conditions are appropriate and equilibrium has been achieved the absorber-evaporator combination will also cease to function, but scenarios will only be investigating where the conditions are conducive to the possibility of absorption taking place. The contents of the absorber-evaporator vessel will always be trying to reach an equilibrium condition. To this end, the manner in which the absorber facilitates progress towards equilibrium is that it will pull (absorb) vapour refrigerant into the liquid solution. As this vapour is pulled into the solution, the condition of the refrigerant liquid and vapour is disrupted and liquid refrigerant will need to vaporize in order to adjust to the new condition. This is the process through which the liquid solution present in the absorber section can indirectly lead to cooling through evaporation.

There are a number of ways in which the absorber can be configured and these configurations are dependent on the vapour-liquid interface that is implemented. Possibilities for the vapour-liquid interface include a film, a liquid pool or combination of both. In addition to this, it is possible to include cooling for the liquid pool and/or the film.

The decision was made to approach the absorption process, or more specifically, the rate of mass absorption as a mass transfer calculation where the rate of mass absorption is driven by the difference in the absorber-evaporator vapour pressure and the saturation pressure of the solution that the vapour is exposed to in the absorber. The rate of mass absorption was then formulated in the following manner:

$$\dot{m}_{abs} = h_{abs} A_{abs} (P_{EAv} - P_A) \tag{3.6.1}$$

where the rate of mass absorption is the product of an absorption coefficient or factor h_{abs}, the surface area of the solution that is exposed to the vapour A_{abs} and the difference in pressure between the vapour space P_{EAv} and the absorber solution P_A. It was decided to make use of an assumed value and thereafter improve on that with experimental results. Furthermore, this equation is only considered to be valid when the vapour pressure is greater than the saturation pressure of the solution film. Should it occur that the vapour pressure becomes less than or equal to the film saturation pressure, the rate of mass absorption is assumed to be zero. The calculation or development of robust theory concerning the absorption factor with respect to Equation 3.6.1 would be an entire study in itself. Killion and Garimella (2001) presented an extensive survey investigating different approaches to characterize the heat and mass transfer present in absorption systems. However, from the literature it appears that a reasonable value for the mass transfer coefficient is in the order of 0.001 and 0.01.

While the difference in concentration between the vapour and solution was not used directly in the calculation of the rate of absorption, the saturation pressure of the solution is dependent on the concentration of the solution. Therefore, it can be argued that the difference in concentration between the vapour and solution is still used in the calculation for the rate of absorption, but in a indirect manner.

This section will continue with a discussion of a number of absorber-evaporator configurations that were tested during the process of constructing the evaporator-absorber portion of the simulation. All of the configurations as well as results related to the absorber-evaporator section could not be included in this section of the report and if additional information is desired upon the conclusion of this section, it can be found in Appendix D.

3.6.1 Pool Absorber with Cooling

The first configuration that was investigated was a configuration where a pool of liquid refrigerant was exposed to a pool of liquid solution. In this first configuration only one external interface was included. This interface is a heat exchanger through which a stream was circulated for the purpose of cooling the liquid solution in the absorber section. A representation of this configuration can be seen in Figure 3.8.

A variation of this configuration was also examined where the liquid solution in the absorber was not cooled. While the results obtained from this scenario are interesting, it was decided that the results of the cooled configuration were of more importance than the results of the configuration without cooling. Therefore, this scenario was excluded from the main body of the report and if additional information is desired with regards to the non-cooled absorber configuration, it can be found in Appendix D.5.

3.6.1.1 Control Volumes and Variables

The manner in which the absorber-evaporator configuration was separated into control volumes can be seen in Figure 3.9. It can be seen that the liquid in the evaporator is assumed to be pure refrigerant as there is no variable assigned for concentration. This is however not the case for the liquid solution present in the absorber portion of the configuration as the solution present requires an additional variable in order to thoroughly describe the condition of the liquid.

The approach used for the vapour-liquid interaction in the absorption section of the absorber-evaporator section made it attractive to combine the common vapour space and the evaporator liquid into a single control volume, at least for the purpose of the conservation of mass and energy.

The heat transfer process is described completely through the associated temperatures and the heat transfer coefficient and area through which energy is to pass.

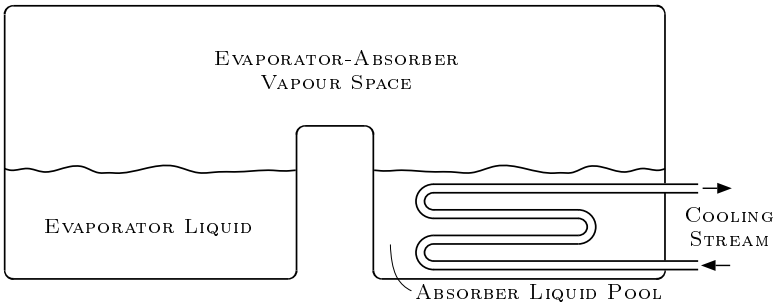

Figure 3.8: Representation of the physical configuration for the evaporator-absorber combination including cooling for the evaporator liquid section

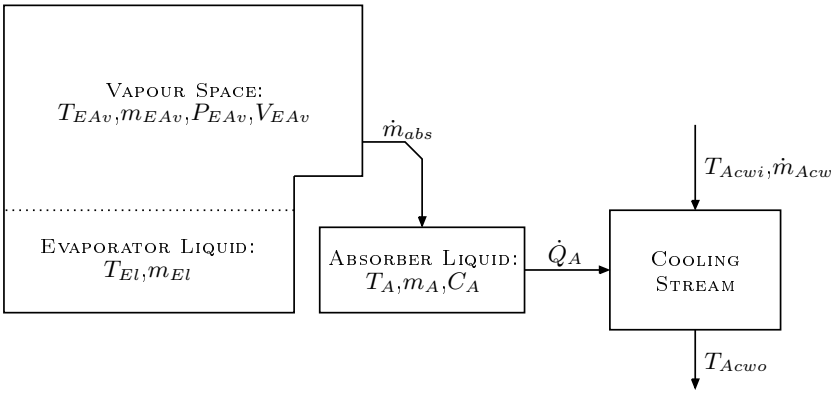

Figure 3.9: Control volumes and variables for the pool evaporator-absorber combination with a cooled absorber pool

3.6.1.2 Derivation of Equations

The equations for the conservation of mass and the conservation of energy were each used for the two internal control volumes. Firstly for the liquid solution in the absorber section of the configuration. Secondly for the combination of the common vapour space and the liquid in the evaporator section.

The process of determining the updated state for the absorber solution starts with the calculation of the new mass of solution. Applying the conservation of mass to the control volumes gives the following equation:

$$\begin{aligned} \Delta m &= \Delta t \left(\sum \dot{m}_i - \sum \dot{m}_o \right) \\ m_A^{t+\Delta t} - m_A^t &= \Delta t(\dot{m}_{abs} - 0) \\ m_A^{t+\Delta t} &= m_A^t + \Delta t \dot{m}_{abs} \end{aligned} \tag{3.6.2}$$

Application of the conservation of mass to the same solution control volume, but with respect to the mass of absorbent makes it possible to determine the new concentration of the solution in the following manner:

$$\begin{aligned} \Delta m &= \Delta t \left(\sum \dot{m}_i - \sum \dot{m}_o \right) \\ C_A^{t+\Delta t} m_A^{t+\Delta t} - C_{Al}^t m_{Al}^t &= \Delta t(0 - 0) \\ C_A^{t+\Delta t} &= C_A^t m_A^t / m_A^{t+\Delta t} \end{aligned} \tag{3.6.3}$$

Once the updated mass and concentration are known it is possible to make use of the conservation of energy in order to determine the energy state of the liquid solution. This is shown below:

$$\begin{aligned} \Delta E &= \Delta t \left(\sum \dot{Q}_i + \sum \dot{m} h_i - \sum \dot{Q}_o - \sum \dot{m} h_o \right) \\ m_A^{t+\Delta t} h_A^{t+\Delta t} - m_A^t h_A^t &= \Delta t(0 + \dot{m}_{abs} h_{gsat}\{T_{EAv}\} - \dot{Q}_A - 0) \\ h_A^{t+\Delta t} &= (m_A^t h_A^t + \Delta t(\dot{m}_{abs} h_{gsat}\{T_{EAv}\} - \dot{Q}_A))/m_A^{t+\Delta t} \end{aligned} \tag{3.6.4}$$

where the updated temperature can be determined through the use of the equations of state and the updated values for enthalpy and concentration. All of the updated values for the independent variables for the liquid solution have now been defined and the calculations can continue with the combined common vapour space and evaporator liquid.

In the case of the combination of common vapour space and evaporator liquid, the assumption was made that the evaporator liquid and the vapour in contact with it would be in equilibrium with one another. This made it possible to make use of the vapour space volume and the fluid properties of the evaporator liquid and the absorber liquid solution in order to determine the mass of vapour present. While this approach is attractive in the sense that the liquid-vapour interaction between the evaporator liquid and the vapour space no longer has to be determined it does make it necessary to follow an iterative process in order to determine the updated condition of the evaporator liquid in combination with the shared vapour space.

Applying the conservation of mass in conjunction with the assumption regarding the combined condition of the vapour and liquid make it possible to derive the updated value for the mass of liquid in the evaporator section. This process is shown below:

$$\begin{aligned} \Delta m =& \Delta t \left(\sum \dot{m}_i - \sum \dot{m}_o \right) \\ m_{El}^{t+\Delta t} - m_{El}^{t} + m_{EAv}^{t+\Delta t} - m_{EAv}^{t} =& \Delta t (0 - \dot{m}_{abs}) \\ m_{El}^{t+\Delta t} + m_{EAv}^{t+\Delta t} =& m_{El}^{t} + m_{EAv} - \Delta t \dot{m}_{abs} \end{aligned} \tag{3.6.5}$$

This reduces the equation to two unknown values which are the updated values for the mass of vapour and liquid. However, it is possible to replace the unknown value for the updated mass of vapour with a calculation that makes use of the updated temperature of the combined vapour and liquid condition:

$$m_{EAv}^{t+\Delta t} = V_{EAv} \rho_{gsat} \{ T_{El}^{t+\Delta t} \} \tag{3.6.6}$$

It is now possible to rewrite Equation 3.6.5 by replacing the updated vapour mass term with the contents of Equation 3.6.6. The resulting equation has been manipulated to such an extent that the updated value for the mass of liquid is now the subject of the equation, as shown below in Equation 3.6.7:

$$m_{El}^{t+\Delta t} = m_{El}^{t} + m_{EAv} - \Delta t \dot{m}_{abs} - V_{EAv} \rho_{gsat} \{ T_{El}^{t+\Delta t} \} \tag{3.6.7}$$

resulting in an equation where the two unknowns are the updated mass of the liquid and the updated temperature of the liquid. However, the conservation of energy can still be applied to the control volume in question in the following manner:

$$\begin{aligned} \Delta E =& \Delta t \left(\sum \dot{Q}_i + \sum \dot{m} h_i - \sum \dot{Q}_o - \sum \dot{m} h_o \right) \\ \Delta(m_{El} h_{El}) + \Delta(m_{EAv} h_{EAv}) =& \Delta t (0 + 0 - 0 - \dot{m}_{abs} h_{EAv}) \\ m_{El}^{t+\Delta t} h_{El}^{t+\Delta t} + m_{EAv}^{t+\Delta t} h_{EAv}^{t+\Delta t} =& m_{El}^{t} h_{El}^{t} + m_{EAv}^{t} h_{EAv}^{t} - \Delta t \dot{m}_{abs} h_{EAv} \end{aligned} \tag{3.6.8}$$

making it possible to solve these two unknowns in an iterative manner. All of the terms on the left hand side of the equation are unknown, but they can all be written as a function of the updated value for the liquid in the evaporator. Substituting Equations 3.6.6 and 3.6.7 makes it possible to rewrite the left hand side of Equation 3.6.8 in the following manner:

$$\begin{aligned} m_{El}^{t+\Delta t}h_{El}^{t+\Delta t} + m_{EAv}^{t+\Delta t}h_{EAv}^{t+\Delta t} = \\ (m_{El}^{t} + m_{EAv} - \Delta t\dot{m}_{abs} - V_{EAv}\rho_{gsat}\{T_{El}^{t+\Delta t}\})c_p\{T_{El}^{t+\Delta t}\}T_{El}^{t+\Delta t} \\ + V_{EAv}\rho_{gsat}\{T_{El}^{t+\Delta t}\}h_{gsat}\{T_{El}^{t+\Delta t}\} \end{aligned} \tag{3.6.9}$$

The manipulation of the conservation of energy leaves Equation 3.6.8 in a form where the right hand side of the equation is entirely known and the left and side of the equation is dependent on the unknown $T_{El}^{t+\Delta t}$. This makes it possible to iteratively solve for the unknown temperature until the value that is obtained from Equation 3.6.9 is equal to the right hand side of Equation 3.6.8.

3.6.1.3 Results

The initial conditions and simulation specifications that were chosen to be used for this configuration of absorber-evaporator can be seen below in Table 3.3. The liquid internal volumes were specified by temperature and mass and in the case of the solution the concentration was specified. The vapour space was specified by choosing a temperature in combination with the total internal volume of the configuration. Working from the total volume and subtracting the volume of the liquid sections made it possible to determine the volume that was occupied by vapour.

The simulation data that was obtained was processed into six plots. These plots can be found in Figure 3.10, where it can be seen that the temperatures in the absorber and evaporator liquid sections initially change rapidly from their original values before gradually approaching an equilibrium condition. The reduction of and eventually cessation of vapour absorption can be attributed to both the concentration and temperature of the solution, these two properties determine the saturation pressure of the liquid solution. Firstly, if the total

Table 3.3: Initial conditions and constants for absorber-evaporator with absorber pool cooling

Absorber Liquid Pool	
T_A	20 °C
C_A	0.5 kg/kg
m_A	5 kg
Cooling Stream	
T_{Acw}	25 °C
UA_A	250 W/°C

Common Vapour Space	
T_{EAv}	20 °C
V_{EAt}	1.3 m^3
Vapour-Liquid Interface	
h_{abs}	0.0002
A_{abs}	0.25 m^2

Evaporator Liquid Pool	
T_{El}	20 °C
m_{El}	5 kg
Simulation Parameters	
t_{end}	500 seconds
Δt	0.01 second

mass of solution had been higher it would have been possible for the solution to absorb a larger quantity of vapour before the change in concentration became a limiting factor in the absorption process. Secondly, if the solution were cooled even further the manner in which the temperature of the solution limited the absorption would be been delayed. However, both of these scenarios would only delay the manner in which the absorption of vapour would inevitably cease to occur.

The most important occurrence to take place is the manner in which the temperature of the evaporator liquid has decreased. This is the result that was expected to occur and made it possible to continue to the next absorber-evaporator configuration.

Under very specific operating conditions it is possible to force the vapour pressure to decrease to such an extent that there is a possibility for the formation of ice. The conditions surrounding this scenario are discussed further in Appendix D.6.

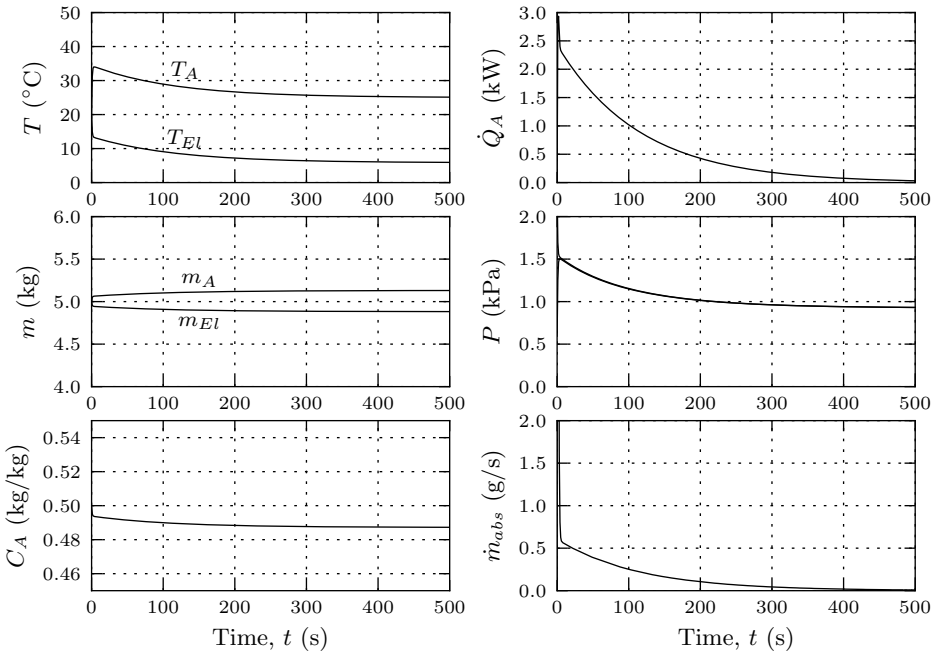

Figure 3.10: Simulation results for the absorber-evaporator pair with absorber cooling assuming no renewal of solution in absorber and no renewal of refrigerant in evaporator

3.6.2 Cooled Pool Absorber with External Evaporator Load

In the first absorber-evaporator configuration it can be seen that the evaporator liquid cools down as vapour is absorbed into the liquid solution. While this is good from a vapour absorption and evaporation point of view, the goal of the absorber-evaporator pair is to provide for cooling to an external load. To this end, the absorber-evaporator configuration was expanded to include a heat exchanger in the liquid section of the evaporator that was connected to an external load, as seen in Figure 3.11.

The decision was made that the external load would be a mass of water. With this configuration it became possible to confirm if the theoretical approach that was implemented would be appropriate to model the indirect manner in which the absorption of vapour in the absorber-evaporator section would cool an external load that was circulated through the evaporator heat exchanger.

3.6.2.1 Control Volumes and Variables

An external load with a mass, temperature and circulation rate was added to the absorber-evaporator configuration. This external load was represented by a fixed mass of water, with known initial temperature and known circulation rate. As for the heat exchanger it was decided to assign an overall heat transfer coefficient and area. Figure 3.12 shows these additions to the previously discussed configuration and it can be seen that the previously used variables and control volumes remain unchanged.

3.6.2.2 Derivation of Equations

There are no significant alterations to be made to the equations from the original absorber-evaporator configuration. With regards to the internal volumes,

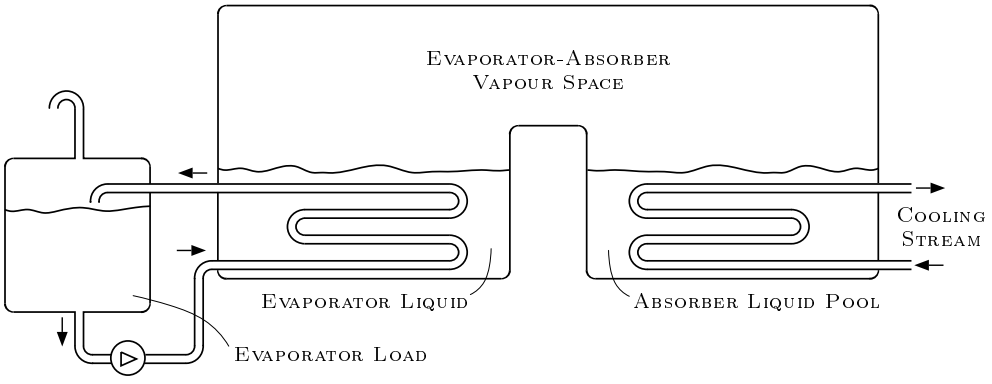

Figure 3.11: Representation of physical configuration for the inclusion of an external evaporator load

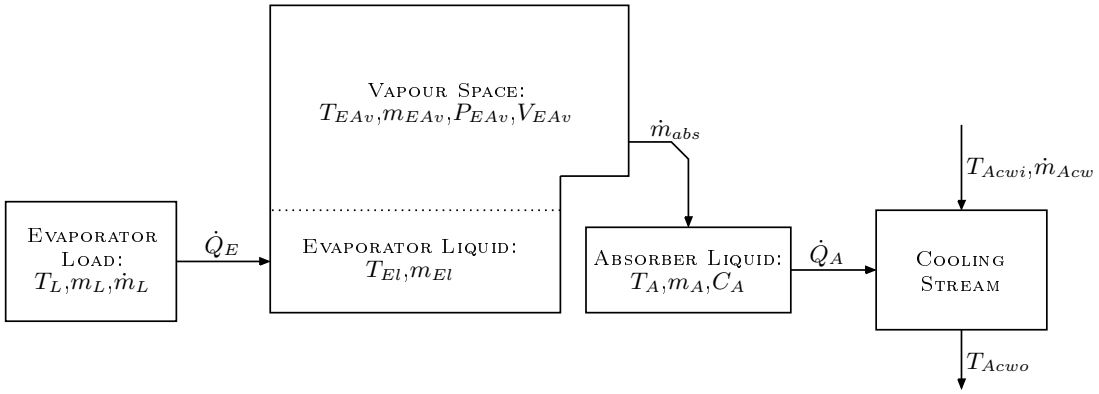

Figure 3.12: Control volumes and variables for the cooled pool evaporator-absorber combination

the calculations concerning the liquid solution in the absorber section are entirely unchanged. The only equation that requires alteration is the conservation of energy for the evaporator liquid-vapour combination. An additional term is required in order to include the effect of the external load on the evaporator. This alteration to Equation 3.6.8 is shown below with the addition of the heat transfer term:

$$m_{El}^{t+\Delta t}h_{El}^{t+\Delta t} + m_{EAv}^{t+\Delta t}h_{EAv}^{t+\Delta t} = m_{El}^{t}h_{El}^{t} + m_{EAv}^{t}h_{EAv}^{t} + \Delta t(-\dot{m}_{abs}h_{EAv}) \quad (3.6.10)$$

The process that was followed in order to determine the updated values for the mass and temperature of the internal volumes remains the same as before. However, the temperature of the external load has to be recalculated for the next time step.

The assumption was made that the mass of liquid in the external load will remain constant. This eliminates any need to update the mass of the external load. However, the temperature of the load will change as energy transfer takes place between the load and the evaporator. Using the conservation of energy with its application to the external load can be seen below:

$$\begin{aligned} \Delta E &= \Delta t(\sum \dot{Q}_i + \sum \dot{m}_i h_i - \sum \dot{Q}_o - \sum \dot{m}_o h_o) \\ m_L c \Delta T_L &= \Delta t(0 + \dot{m}_L c T_{Ecwo} - 0 - \dot{m}_L c T_L) \\ m_L c(T_L^{t+\Delta t} - T_L^t) &= \Delta t(\dot{m}_L c T_{Ecwo} - \dot{m}_L c T_L) \\ T_L^{t+\Delta t} &= T_L^t + \Delta t \dot{m}_L / m_L (T_{Ecwo} - T_L) \end{aligned} \quad (3.6.11)$$

With the derivation of the updated load temperature the discussion can continue to the results that were obtained from this simulation.

3.6.2.3 Results

The only change that was made to the parameters of the simulation was the addition of the external load. This can be seen in Table 3.4 where the evaporator

Table 3.4: Initial conditions and constants for the absorber-evaporator pair with pool cooling and external evaporator load

Absorber Liquid Pool	
T_A	20 °C
C_A	0.5 kg/kg
m_A	5 kg
Absorber Cooling Stream	
T_{Acw}	25 °C
UA_A	300 W/°C

Common Vapour Space	
T_{EAv}	20 °C
V_{EAt}	1.3 m^3
Vapour-Liquid Interface	
h_{abs}	0.0002
A_{abs}	0.25 m^2
Simulation Parameters	
t_{end}	1200 seconds
Δt	0.01 second

Evaporator Liquid Pool	
T_{El}	20 °C
m_{El}	5 kg
Evaporator Load	
UA_E	250 W/°C
$\dot{m}_L$	0.2 kg/s
T_L	20 °C
m_L	10 kg

load was assigned values for the initial temperature and mass in conjunction with values for the mass flow rate and the overall heat transfer coefficient.

The data obtained as an output of the simulation was plotted to the same set of axes, where the only additional plot was the evaporator load temperature. These plots can be seen in Figure 3.13, where it can be seen that the inclusion of the evaporator load has altered the results in a few different ways.

All of the changes in operation that are seen between the current configuration and the configuration sans load can be attributed to the manner in which the inclusion of the external load reduces the rate at which the evaporator liquid temperature decreases. This is caused by the process in which

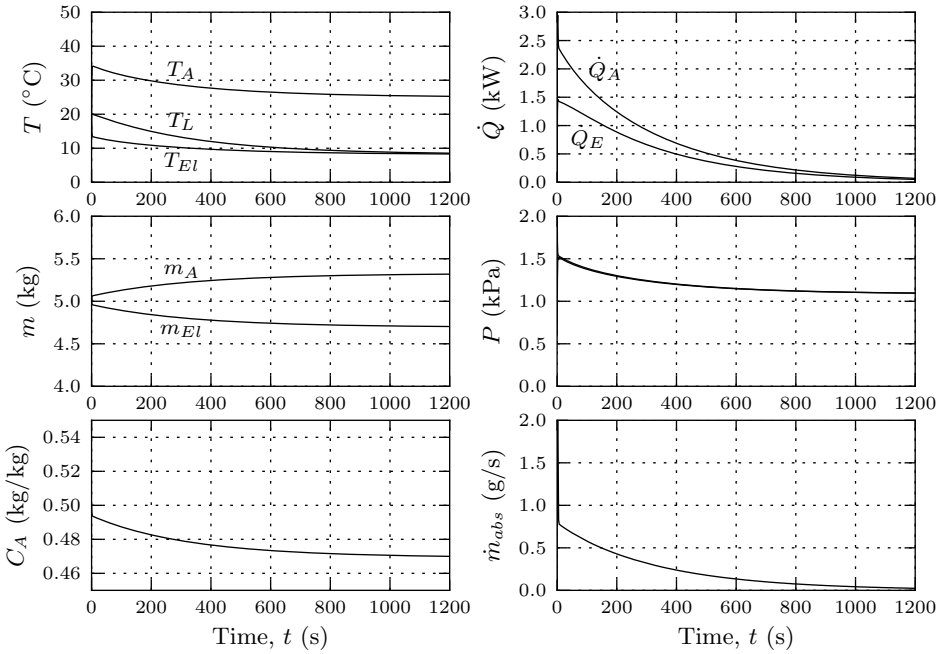

Figure 3.13: Plotted output of the absorber-evaporator configuration with evaporator load and absorber cooling

the energy for vapourization is indirectly supplied from the load instead of the evaporator liquid itself. Due to the chosen formulation for the rate of absorption, the rate of absorption is dependent on the condition of the evaporator liquid. Therefore, the reduced rate of change in the evaporator liquid temperature leads to the absorption process continuing for a longer period of time. Absorbing vapour refrigerant for a longer period of time is what causes the larger reduction in the concentration of the absorber solution in combination with the larger change in total mass for both the evaporator and absorber liquid sections.

It can be seen that this configuration is an improvement on the previously discussed configuration in that it produces a refrigeration effect on the external load. However, the cooling capabilities of the configuration are limited. If the mass of the load is increased sufficiently then the solution in the absorber section cannot absorb a sufficient amount of vapour in order to cool the load sufficiently.

3.6.3 Cooled Pool Absorber with External Evaporator Load and External Mass Streams

A number of scenarios have been discussed where the operation of absorber-evaporator pair will cease to function. A few of these scenarios can however be avoided by the introduction of external liquid streams to the absorber-evaporator configuration.

The configuration would be limited by the temperature of the absorber cooling stream or the changes in the internal masses and concentration. The absorber side of the process is limited through the change in concentration of the liquid solution and for the evaporator it is possible, under appropriate conditions, that the evaporator liquid section can run dry. Both of these situations can be avoided through the introduction of a source of refrigerant into the evaporator in combination with the introduction of a source of solution for the absorber. Including two mass inlet streams without removing an equal amount of mass would eventually lead to the configuration filling to such a point where the liquid section would mix and thereafter fill the entire space. Therefore, an outlet stream was also included in the configuration. It should also be noted that these changes were done partly in an effort to extend the operation of the absorber-evaporator configuration and partly to work towards eventually incorporating the entire configuration into a simulation for a complete vapour absorption cycle.

An additional change that was made to the conceptualized configuration, which can be seen in Figure 3.14, is that the evaporator liquid section was raised slightly with respect to the absorber liquid section. This was done in order to ensure that the mass of refrigerant did not become excessive because any excess liquid refrigerant that would be present due to the refrigerant inlet

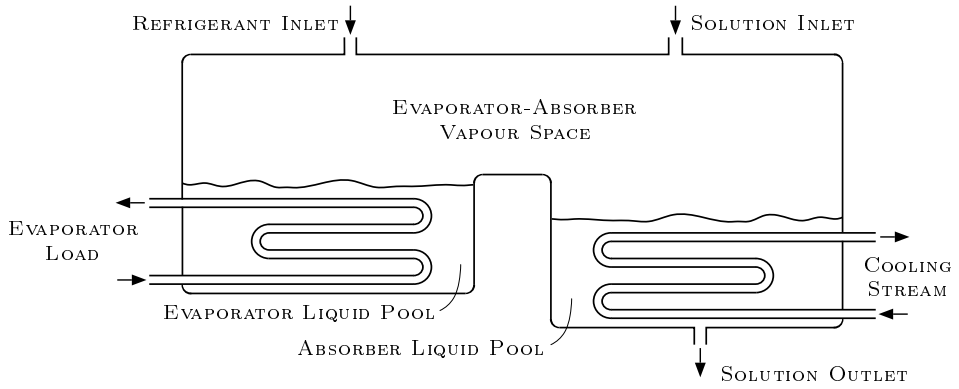

Figure 3.14: Absorber-evaporator configuration with the addition of external mass streams

would flow over into the liquid solution of the absorber section.

3.6.3.1 Control Volumes and Variables

The only change made to the control volumes was the introduction of four new mass streams. These mass streams are the refrigerant inlet into the common vapour space and evaporator combination, the solution inlet into the absorber solution, the solution outlet from the absorber solution and the refrigerant overflow from the evaporator liquid section in the absorber liquid section. All of these changes can be seen in Figure 3.15.

3.6.3.2 Derivation of Equations

All of the equations that were derived from the conservation of mass and energy changed with the inclusion of the inlet and outlet mass streams. However, the

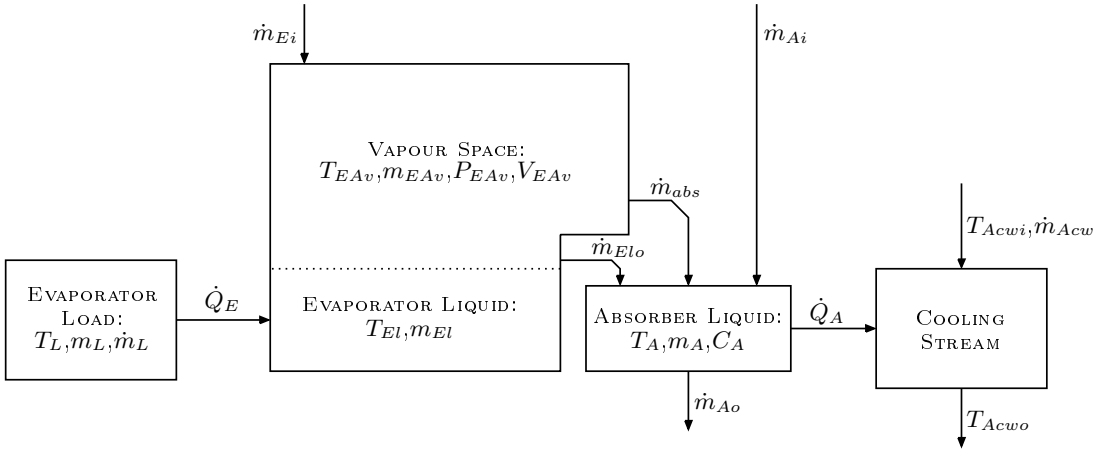

Figure 3.15: Control volumes and variables for the pool evaporator-absorber combination with a cooled absorber pool and heated evaporator pool

same process was followed in order to solve for the unknown values. In order to keep things more concise the entire derivation of each equation will not be discussed, but only the final equations.

The conservation of mass when applied to the total mass in the absorber liquid section becomes:

$$m_A^{t+\Delta t} = m_A^t + \Delta t(\dot{m}_{Ai} + \dot{m}_{abs} + \dot{m}_{Elo} - \dot{m}_{Ao}) \tag{3.6.12}$$

Only taking the mass of absorbent into consideration when applying the conservation of mass gives the following equation:

$$C_A^{t+\Delta t} = (m_A^t C_A^t + \Delta t(\dot{m}_{Ai} C_{Ai} - \dot{m}_{Ao} C_A))/m_A^{t+\Delta t} \tag{3.6.13}$$

Applying the conservation of energy to the absorber solution in order to determine the updated enthalpy and thereafter making use of the equations of state for the liquid solution makes it possible to determine the new temperature in the following manner:

$$\begin{aligned} h_A^{t+\Delta t} =& (m_A^t h_A^t + \Delta t(\dot{m}_{abs} h_{gsat}\{T_{EAv}\} + \dot{m}_{Ai} h_{sol}\{T_{Ai}, C_{Ai}\} \\ &+ \dot{m}_{Elo} c\{T_{El}\} T_{El} - \dot{Q}_A))/m_A^{t+\Delta t} \end{aligned} \tag{3.6.14}$$

$$T_A^{t+\Delta t} = T_{sol}\{h_A^{t+\Delta t}, C_A^{t+\Delta t}\} \tag{3.6.15}$$

The conservation of mass and energy was used in order to determine the updated values for the combination of common vapour and evaporator liquid control volume. The updated conservation of mass equation can be seen below as:

$$m_{El}^{t+\Delta t} = m_{El}^t + m_{EAv}^t + \Delta t(\dot{m}_{Ei} - \dot{m}_{Elo} - \dot{m}_{abs}) - V_{EAv}\rho_{gsat}\{T_{El}^{t+\Delta t}\} \tag{3.6.16}$$

The resulting equation that was obtained from applying the conservation of energy to the combination of common vapour space and evaporator liquid is:

$$\begin{aligned} m_{El}^{t+\Delta t} h_{El}^{t+\Delta t} + m_{EAv}^{t+\Delta t} h_{EAv}^{t+\Delta t} =& m_{El}^t h_{El}^t + m_{EAv}^t h_{EAv}^t \\ &+ \Delta t(\dot{m}_{Ei} h_{Ei} + \dot{Q}_E - \dot{m}_{abs} h_{EAv}^t - \dot{m}_{Elo} h_{El}^t) \end{aligned} \tag{3.6.17}$$

As before, the new state of the evaporator section will be calculated iteratively by determining the new value for T_{El} until it satisfies the constraints of the conservation of mass and energy.

3.6.3.3 Results

Table 3.5 shows the variables that were used to define the simulation for the current configuration. The decision was made to forgo controlled inlet or outlet streams in order to focus on the behaviour of the configuration without varying

Table 3.5: Initial conditions and constants for the absorber-evaporator pair with pool cooling, external evaporator load and external mass streams

Absorber Liquid Pool	
T_A	20 °C
C_A	0.5 kg/kg
m_A	5 kg
Absorber Cooling Stream	
T_{Acw}	20 °C
UA_A	300 W/°C
Solution Inlet	
T_{Ai}	50 °C
C_{Ai}	0.55 kg/kg
$\dot{m}_{Ai}$	0.012 kg/s

Common Vapour Space	
T_{EAv}	20 °C
V_{EAt}	1.3 m^3
Vapour-Liquid Interface	
h_{abs}	0.0002
A_{abs}	0.25 m^2
Simulation Parameters	
t_{end}	4 hours
Δt	0.001 second
Solution Outlet	
$\dot{m}_{Ao}$	0.013 kg/s

Evaporator Liquid Pool	
T_{El}	20 °C
m_{El}	5 kg
Evaporator Load	
UA_E	250 W/°C
$\dot{m}_L$	0.5 kg/s
T_L	20 °C
m_L	100 kg
Refrigeration Inlet	
$\dot{m}_{Ei}$	0.001 kg/s
h_{Ei}	104838 J/kg

the external interfaces. Therefore, the inlet and outlet mass flow rates were kept constant at their respective values. The accumulative effect of the mass overflow from the evaporator with the inlet and outlet mass streams, at their current chosen values, results in preventing any large changes in the internal liquid masses present in the evaporator and absorber.

The added functionality of the external mass streams could not be demonstrated adequately with the same evaporator load that was previously used. This was due to the manner in which the load would be cooled down in a sufficient amount of time to avoid the limitations of the previous configuration.

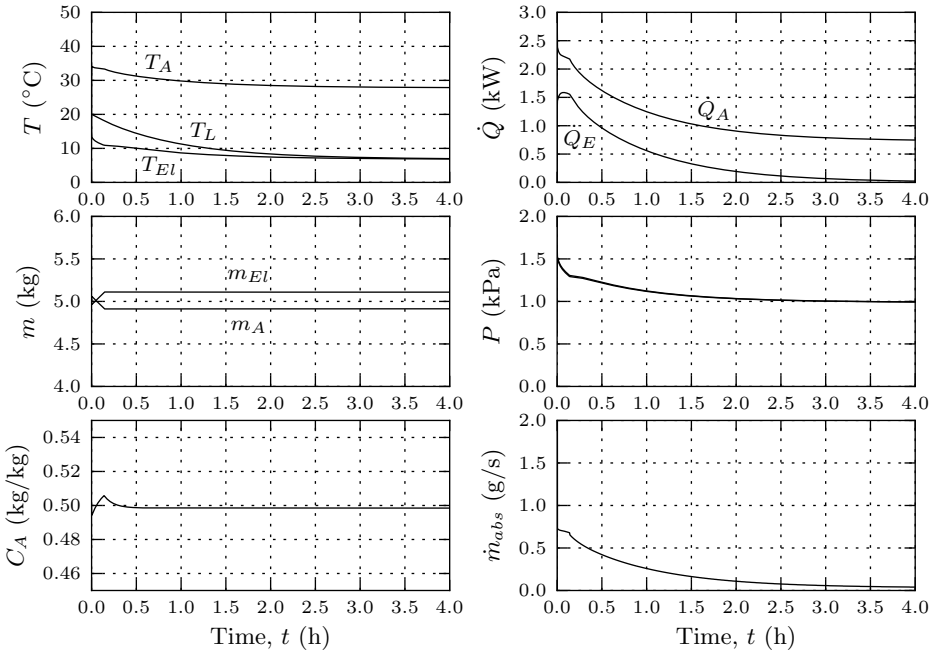

Figure 3.16: Simulation output graphs for absorber-evaporator configuration with external mass streams

Therefore, the mass of the load was increased in order to force the configuration to require additional cooling. This in turn led to the configuration requiring a longer amount of time in order to cool the evaporator load.

The results obtained from the simulation are shown in Figure 3.16. Here it can be seen that while the mass of the load has been increased, this configuration does manage to cool the load down to a reasonable temperature. The combined effect of the constant mass flow rates for the external streams and the overflow from the evaporator to absorber results in the mass of liquid and solution in the evaporator and absorber remaining constant.

3.6.4 Cooled Film and Pool Absorber with External Evaporator Load and External Mass Streams

The decision was made to extend the functionality of the theoretical absorber-evaporator configuration through the inclusion of a surface upon which a film of solution could be used to absorb additional vapour. The presence of the absorber film meant that there would be two surfaces upon which the vapour-solution interaction could take place. This presented a number of possibilities concerning the manner in which the solution film and pool in the absorber section of the configuration could be configured. However, while there may be a number of possible manners in which to configure the absorber, only three of these configurations were deemed useful.

The first of the viable absorber configurations is a configuration where a pool of solution is cooled and the film is excluded; this configuration has already been discussed in Section 3.6.3. Inclusion of the film can be done in two productive manners, the first of which will be covered in this section is where a film and pool of solution are cooled. The last useful configuration is discussed in Appendix D.4, where only the solution film is cooled.

The film was incorporated into the simulation in a manner such that the solution entering the absorber from the generator would first pass through the film, then continue onwards to the pool of solution located at the bottom of the absorber section. This configuration can be seen in Figure 3.17.

3.6.4.1 Control Volumes and Variables

Figure 3.18, as seen on the following page, shows the manner in which the addition of an absorber film changes the control volumes of the absorber-evaporator configuration. It is illustrated that the solution inlet no longer feeds directly into the solution pool, but now has to pass through the absorber film first. In addition to this, the vapour-liquid interaction between the common vapour space and the solution film is included with the option for the cooling of the film.

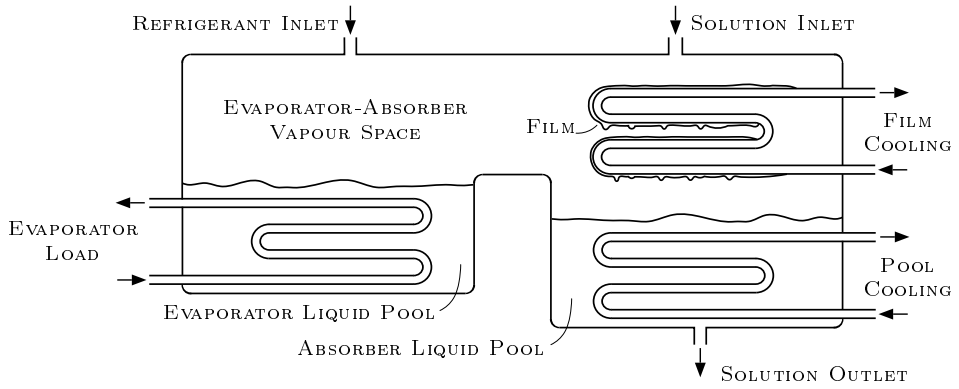

Figure 3.17: Representation of an absorber-evaporator configuration including a solution film

3.6.4.2 Derivation of Equations

The addition of the solution film control volumes changes the previously used control volumes in varying degrees. Only minor changes are required for the absorber liquid section in so far as the names of the variables being used will change from the solution inlet to the solution outlet from the film. The common vapour space and evaporator liquid calculations were updated to include the additional rate of absorption variable.

The method that was used to determine the updated combination of common vapour space and evaporator liquid was not altered. Due to this, only the updated equations will be included after which the discussion will continue with the absorber solution film.

The conservation of mass when applied to the evaporator-common control

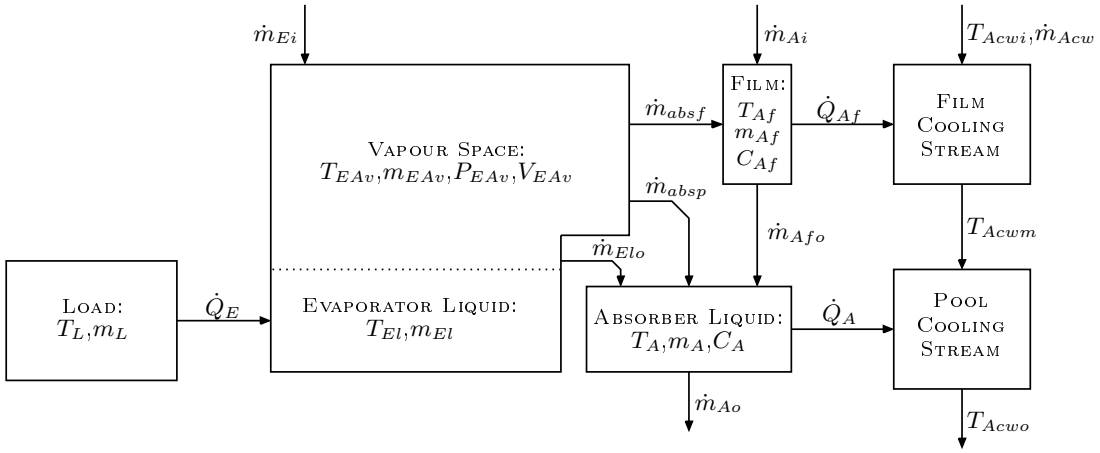

Figure 3.18: Control volumes and variables for the cooled pool evaporator-absorber combination

volume gives the following equation:

$$m_{El}^{t+\Delta t} + m_{EAv}^{t+\Delta t} = m_{El}^{t} + m_{EAv}^{t} + \Delta t(\dot{m}_{Ei} - \dot{m}_{Eo} - \dot{m}_{absp} - \dot{m}_{absf}) \quad (3.6.18)$$

Applying the conservation of energy to the same control volume gives the following result:

$$\begin{aligned} m_{El}^{t+\Delta t}h_{El}^{t+\Delta t} + m_{EAv}^{t+\Delta t}h_{EAv}^{t+\Delta t} &= m_{El}^{t}h_{El}^{t} + m_{EAv}^{t}h_{EAv}^{t} \\ &\quad + \Delta t(\dot{m}_{Ei}h_{Ei} - \dot{m}_{Eo}h_{El} - \dot{m}_{absp}h_{EAv} - \dot{m}_{absf}h_{EAv}) \end{aligned} \quad (3.6.19)$$

The updated absorber film conditions were also determined through the use of the conservation of mass and energy. The conservation of mass when applied to the absorber film can be seen below:

$$\begin{aligned} \Delta m &= \Delta t(\sum \dot{m}_i - \sum \dot{m}_o) \\ m_{Af}^{t+\Delta t} - m_{Af}^{t} &= \Delta t(\dot{m}_{Ai} + \dot{m}_{absf} - \dot{m}_{Afo}) \\ m_{Af}^{t+\Delta t} &= m_{Af}^{t} + \Delta t(\dot{m}_{Ai} + \dot{m}_{absf} - \dot{m}_{Afo}) \end{aligned} \quad (3.6.20)$$

Applying the conservation of mass to the absorber film, but only with respect to the absorbent mass, made it possible to determine the updated value for the concentration present in the film. This process is shown below:

$$\begin{aligned} \Delta m &= \Delta t(\sum \dot{m}_i - \sum \dot{m}_o) \\ m_{Af}^{t+\Delta t}C_{Af}^{t+\Delta t} - m_{Af}^{t}C_{Af}^{t} &= \Delta t(\dot{m}_{Ai}C_{Ai} - \dot{m}_{Afo}C_{Af}^{t}) \\ C_{Af}^{t+\Delta t} &= (m_{Af}^{t}C_{Af}^{t} + \Delta t(\dot{m}_{Ai}C_{Ai} - \dot{m}_{Afo}C_{Af}^{t}))/m_{Af}^{t+\Delta t} \end{aligned} \quad (3.6.21)$$

The updated temperature can be determined through the use of the conservation of energy:

$$\begin{aligned} \Delta E &= \Delta t(\sum \dot{Q}_i + \sum \dot{m}_i h_i - \sum \dot{Q}_o - \sum \dot{m}_o h_o) \\ m_{Af}^{t+\Delta t}h_{Af}^{t+\Delta t} - m_{Af}^{t}h_{Af}^{t} &= \Delta t(\dot{m}_{Ai}h_{Ai} + \dot{m}_{absf}h_{EAv} - \dot{m}_{Afo}h_{Af} - \dot{Q}_{Af}) \\ h_{Af}^{t+\Delta t} &= (m_{Af}^{t}h_{Af}^{t} + \Delta t(\dot{m}_{Ai}h_{Ai} + \dot{m}_{absf}h_{EAv} - \dot{m}_{Afo}h_{Af} - \dot{Q}_{Af}))/m_{Af}^{t+\Delta t} \end{aligned} \quad (3.6.22)$$

The addition of these functions makes it possible to determine all of the updated values.

3.6.4.3 Results

Variables were added to the specifications in order to cater for the absorber film, the absorber film vapour-liquid interface and the absorber film cooling.

These variables and their values can be seen in Table 3.6. The volume of the absorber film was not chosen directly, but was established through the specification of the dimensions for a number of plates upon which a thin film of solution would rest. The subsequent calculations were then performed in a manner that attempted to keep the volume of the film constant. In doing so the mass of the film could be determined for any temperature and concentration through the use of the volume and the density equation for a solution.

The goal of adding the absorber film was to improve the performance of the absorber-evaporator configuration. It would be reasonable to assume that the addition of the absorber film would improve the operation of the component configuration by increasing the speed at which the load is cooled, improving the temperature to which the load could be cooled or a combination of these two scenarios.

The behaviour of this configuration when simulated using the conditions specified in Table 3.6 can be seen in Figure 3.19. Here it can be seen that there are a number of changes to be noted when comparing the behaviour of this configuration to the configuration discussed in Section 3.6.3.

It can be seen that in a similar time period the final temperature that was reached by this configuration, 4.33 ℃, is lower than that which was achieved in the configuration discussed in Section 3.6.3, 6.99 ℃. This can be attributed to the presence of two vapour-liquid interfaces as well as the higher concentration of absorbent that is present in the absorber solution film.

The initial conditions of the simulation allow for absorption to take place across both of the vapour-liquid vapour interfaces. However, with the inclusion of a second vapour-liquid interface comes the complication of encountering a scenario where the conditions of the two absorption interfaces differ. In this scenario the simulation cannot accommodate both interfaces and the condition of the vapour is determined by one of the vapour-liquid interfaces. This can be seen in the plotted results of the rate of absorption to the solution pool and film in Figure 3.19. Absorption occurs with both the solution film and pool

Table 3.6: Initial conditions and constants for the absorber-evaporator pair with pool cooling, external evaporator load and external mass streams

Absorber Liquid Pool	
T_A	20 ℃
C_A	0.5 kg/kg
m_A	5 kg
Absorber Film	
T_{Af}	20 ℃
V_{Af}	0.00127 m^3
C_{Af}	0.5 kg/kg
Absorber Cooling	
T_{Acw}	25 ℃
UA_A	300 W/℃
UA_{Af}	100 W/℃

Common Vapour Space	
T_{EAv}	20 ℃
V_{EAt}	0.2 m^3
Vapour-Liquid Interface	
h_{absp}	0.0002
A_{absp}	0.25 m^2
h_{absf}	0.0005
A_{absf}	0.6 m^2
Solution Inlet	
$\dot{m}_{Ai}$	0.012 kg/s
T_{Ai}	50 ℃
C_{Ai}	0.55 kg/kg
Solution Outlet	
$\dot{m}_{Ao}$	0.013 kg/s

Evaporator Liquid Pool	
T_{El}	20 ℃
m_{El}	5 kg
Evaporator Load	
UA_E	250 W/℃
$\dot{m}_L$	0.5 kg/s
T_L	20 ℃
m_L	100 kg
Refrigeration Inlet	
$\dot{m}_{Ei}$	0.001 kg/s
h_{Ei}	104838 J/kg
Simulation Parameters	
t_{end}	4 hours
Δt	0.001 second

until the condition of the solution pool is no longer viable for absorption with respect to the condition of the vapour. Once this occurs then the absorption of vapour into the solution pool ceases and solution film becomes the only interface through which absorption takes place.

This behaviour is dependent on the operating conditions of the configuration and more importantly the manner in which the vapour–liquid interaction was formulated. Under different operating conditions the absorption by the film could have been the interface that stopped being viable for the absorption of vapour. However, the scenario where a single interface is governing the condition of the vapour would once again come into play. The reason for this is that the interaction between the vapour and the solution film as well as pool was formulated in a manner that makes the rate of absorption dependent on the saturation pressure of the solution in question and the refrigerant vapour pressure, as seen in Equation 3.6.1. Once one of the absorption surfaces is at a saturation pressure that is lower than the other can reach, the more limited surface can no longer interact with the vapour space through absorption.

In a situation where the saturation pressure associated with one of the vapour absorption interfaces is higher than the vapour pressure then liquid refrigerant can evaporate from the solution into the vapour space in an attempt to attain equilibrium. However, the impact of this scenario was not deemed significant enough to justify the inclusion of the necessary code.

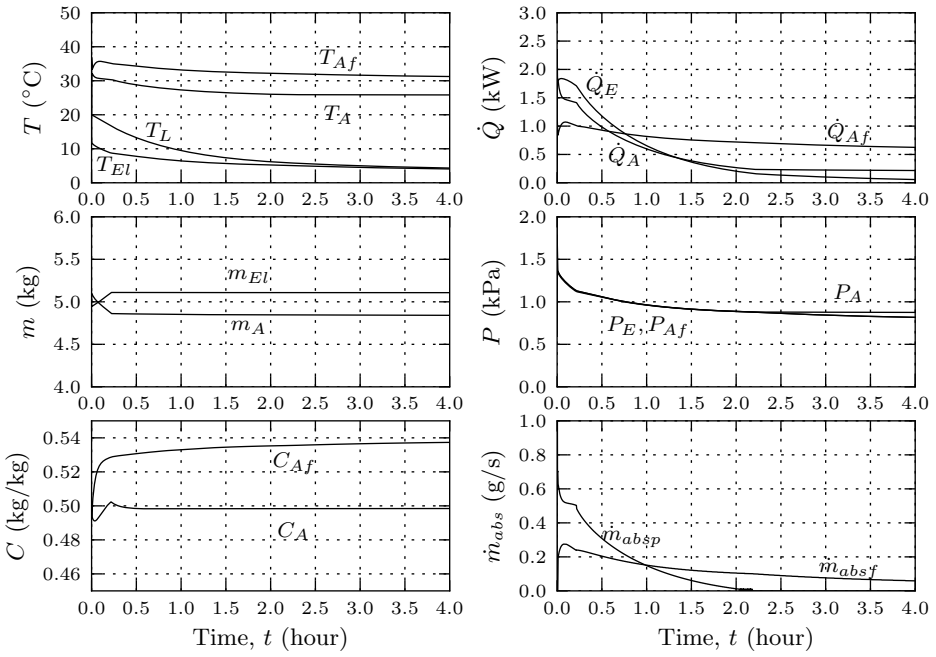

Figure 3.19: Simulation results for the absorber-evaporator configuration that includes external streams and an absorber film

3.7 Complete System

Combining the generator-condenser configuration, as discussed in Section 3.5, with the absorber-evaporator section, as discussed in Section 3.6.4, makes it possible, with the inclusion of additional components, to construct a configuration capable of continuously producing refrigeration through vapour absorption. A representation of this configuration can be seen in Figure 3.20. Here is can be seen that a number of additional components have been included in the transition towards the complete system.

The inclusion of an electrical circulation pump as well as the expansion valves is done in order to maintain a pressure difference between the generator-condenser components and the absorber-evaporator components. These two sets of components have to operate in a manner where the generator-condenser pair is at a higher pressure than the absorber-evaporator pair. The circulation pump has to overcome the pressure difference between the low and high pressure while pumping a specified amount of solution to the generator. A similar function is performed by the valves that are located between the condenser and evaporator as well as the generator and absorber. These valves have to be specified and controlled in a manner that will make it possible for the solution and refrigerant to flow through their respective valves at a specific mass flow

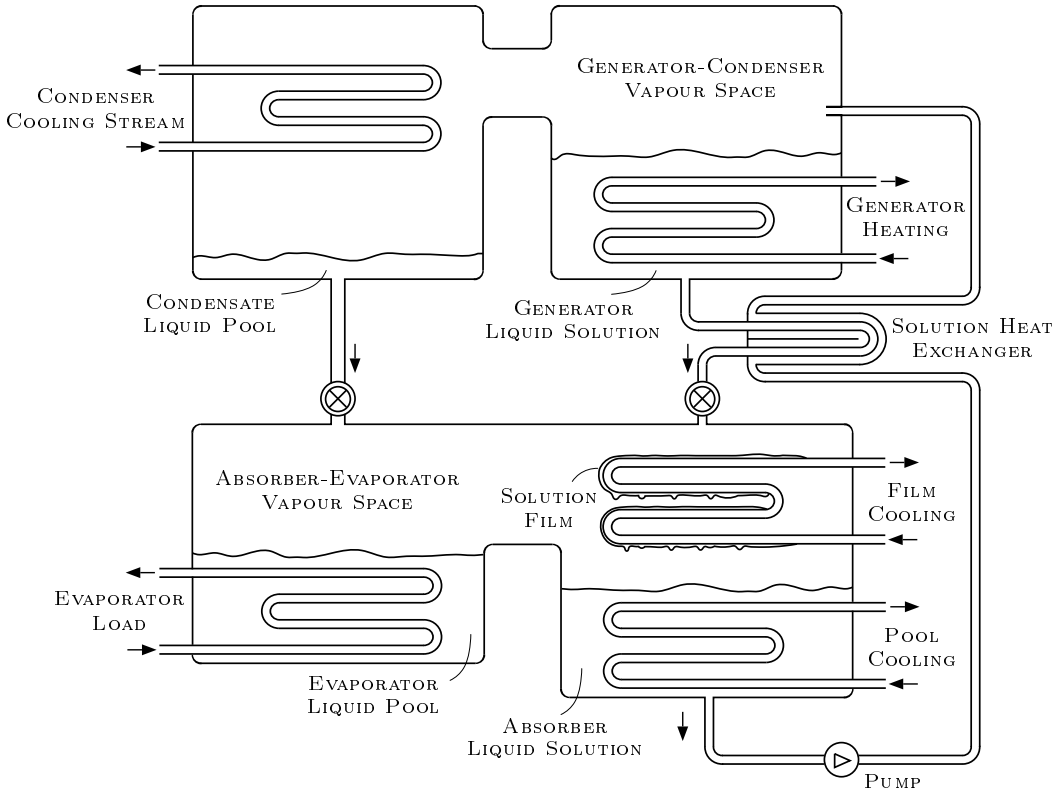

Figure 3.20: Representation of complete vapour absorption system

rate while not affecting the pressure in any of the vessels.

The purpose and simulation of the solution heat exchanger is discussed in Section 2.4 and Appendix C.3 respectively. Therefore, the solution heat exchanger will not be discussed in this portion of the thesis report.

3.7.1 Control Volumes and Variables

The control volume diagram for the complete vapour absorption cycle can be seen in Figure 3.21. This control volume configuration was constructed by combining the control volume diagram for the generator-condenser and the absorber-evaporator configurations as seen in Figures 3.4 and 3.18 respectively. The only addition to 3.21 that was not previously discussed is the solution heat exchanger.

It is important to note that no changes were made whatsoever to the variables and control volumes that were used in the previous sections. A consistent use of variables made it possible to combine the two halves of the vapour absorption cycle without any complications.

The configuration that is shown in combination with the manner in which the simulation was constructed resulted in a highly customizable simulation. A number of the components can each be activated, deactivated or altered by setting a single variable that is tied to each respective component. The relevance of this to the control volume diagram shown in Figure 3.21 is that while all of the indicated components and control volumes are included in the simulation they will not all necessarily be activated.

3.7.2 Derivation of Equations

No significant alterations to the equations were necessary in the progression from the separate simulations, covering the generator-condenser configuration and the absorber-evaporator (Sections 3.5 and 3.6.4 respectively), to the complete cycle. Attention had already been given in the separate simulations to ensure that the variable usage was consistent. Due to this there will not be any new equations derived in the section.

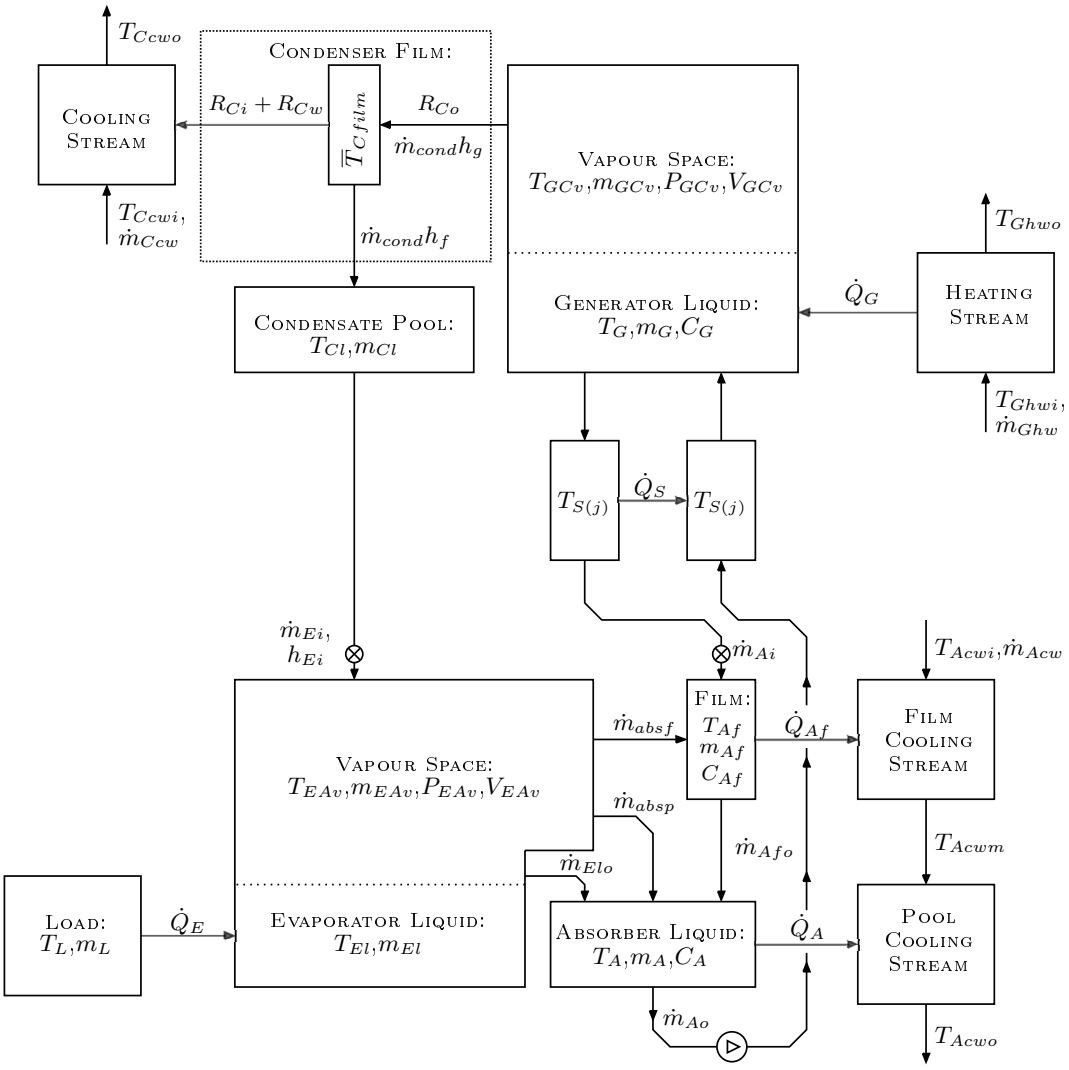

Figure 3.21: Control volume representation of a theoretically simulated lithium-bromide/water vapour absorption cycle

3.7.3 Results

This section will discuss the results of simulating the theoretical vapour absorption cycle as represented in Figure 3.20. An extensive set of variables is required as input for the simulation of the complete vapour absorption cycle. These variables have been listed in tables according to the associated components.

The results obtained from the completed vapour absorption cycle simulation can be seen in Figure 3.22. The simulated cycle successfully cooled the external load of 1000 kg from its initial temperature of 20 ℃ to a final temperature of 10 ℃ over a time span of three hours.

The first selection of variables that will be discussed pertains to the gen-

Table 3.7: Generator and condenser specifications for the complete vapour absorption cycle

Condenser Cooling Stream	
T_{Ccwi}	20 °C
$\dot{m}_{Ccw}$	0.5 kg/s
k	18 W/(m °C)
l	10.5 m
d_o	0.0127 m
t	0.0012 m

Common Vapour Space	
T_{GCv}	20 °C
V_{GCt}	1.1 m^3
Condenser Liquid Pool	
T_{Cl}	20 °C
m_{Cl}	5 kg

Generator Liquid Solution	
T_{Gl}	20 °C
m_G	12 kg
C_G	0.5 kg/kg
Generator Heating Stream	
T_{Ghwi}	80 °C
$\dot{m}_{Ghw}$	0.5 kg/s
UA_G	500 W/°C

erator and condenser section of the cycle. Table 3.7 shows the variables that specify the initial conditions for the internal control volumes in combination with the external streams that interact with the cycle. In a similar manner, Table 3.8 lists the internal and external specifications for the absorber-evaporator section of the complete cycle.

The mass flow rates for the internal streams are shown in Table 3.9. In

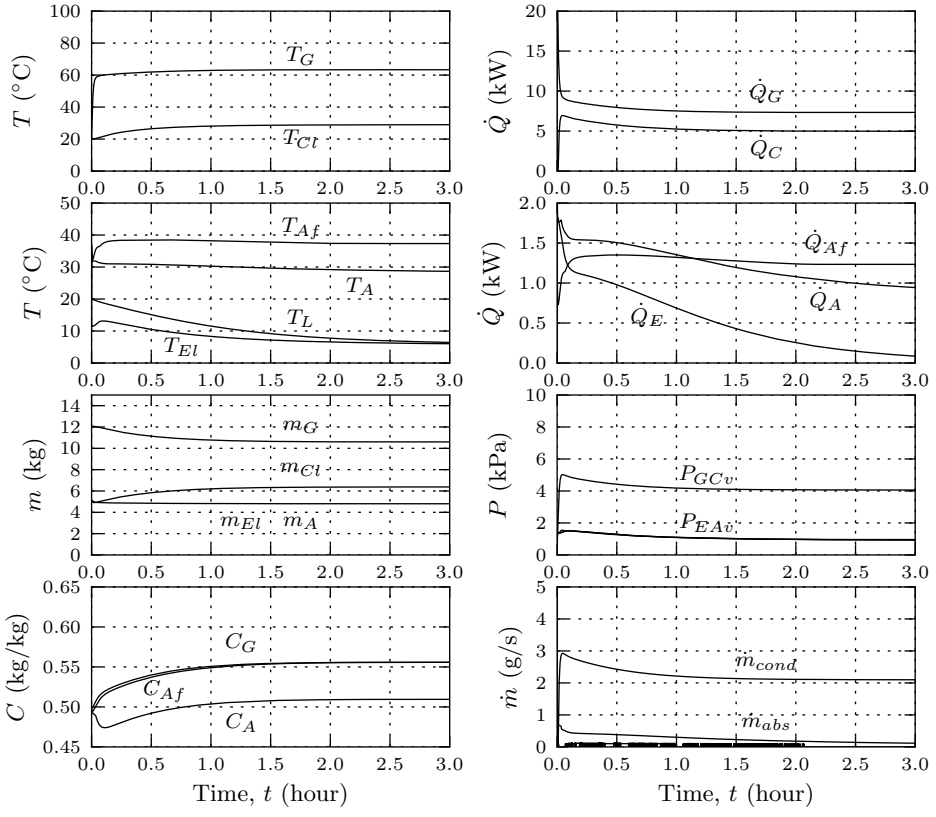

Figure 3.22: Simulation results for the absorber-evaporator configuration that includes external streams and an absorber film

Table 3.8: Absorber and evaporator variables for the simulation of the complete vapour absorption cycle

Evaporator Liquid Pool	
T_{El}	20 ℃
m_{El}	10 kg
Evaporator Load	
T_L	20 ℃
m_L	1000 kg
$\dot{m}_L$	0.5 kg/s
UA_E	250 W/℃

Common Vapour Space	
T_{EAv}	20 ℃
V_{EAv}	1.3m ^{3}
Vapour-Liquid Interfaces	
h_{absf}	0.005
A_{absf}	0.64 m^2
h_{absp}	0.002
A_{absp}	0.25 m^2

Absorber Liquid Solution	
T_A	20 ℃
m_A	20 ℃
C_A	0.5 kg/kg
Absorber Film	
T_{Af}	20 ℃
V_{Af}	0.00127 m^3
C_{Af}	0.5 kg/kg

Table 3.9: Inter-vessel stream, time and component specifications for the simulation of a complete vapour absorption

Condenser to Evaporator	
$\dot{m}_{Co}$	0.0021 kg/s
Time	
t_{end}	3 hours
Δt	0.01 s

Generator to Absorber	
$\dot{m}_{Go}$	0.0231 kg/s
Solution Heat Exchanger	
	active
UA_{SHX}	300 W/℃

Absorber to Generator	
$\dot{m}_{Gi}$	0.0252 kg/s
Absorber Vapour-Liquid Interfaces	
Pool	Cooling @ 25 ℃, 300 W/℃
Film	Active & Cooled @ 25 ℃, 100 W/℃

addition to internal flow rates this table also contains the time related specifications of the simulation.

4 Experimental Apparatus

This section will discuss the experimental vapour absorption cycle that was constructed and tested for this project. The primary goal that motivated the design, fabrication and assembly of the experimental apparatus was the comparison and verification of the results that were obtained from the theoretical simulation. An additional goal that influenced the decisions that were made in the construction of the experimental apparatus was that it be designed and constructed in a manner that would incorporate modular design aspects. The implication of this approach is that the largest components of the experimental apparatus could be adapted, expanded upon or modified in order to facilitate improvements or further experimental testing and research.

Looking beyond the primary goals of the experimental apparatus there were a number of learning opportunities attached to the experimental apparatus. The design and operation of the apparatus gave insight, in terms of the knowledge that the associated staff had, into the decisions that determined the operation of a vapour absorption cycle. In addition to this, the possibility of examining the operation of the vapour absorption components in their operational pairs or as an entire cycle was a desired outcome of the apparatus.

During the process of developing the theoretical simulation the possible physical characteristics and operation of the cycle had to be taken into consideration. A similar relationship had to be considered when designing the experimental apparatus in that there had to be a balance between the physical and the theoretical versions of the vapour absorption cycle. This had to be kept in mind when designing the experimental apparatus. In an effort to realize the goal of including modular aspects in the construction of the apparatus the interconnectivity between components of the cycle had to be taken into consideration. There was also a need to include the possibility of observing the internal behaviour of the cycle and to this end, the inclusion of windows became a requirement of the apparatus.

This chapter will continue discussing the steps that were taken in order to realise the goals of the experimental cycle and the project as a whole. The design, assembly and operation of the experimental apparatus will be discussed followed by the results that were obtained from the apparatus.

4.1 Design and Assembly of the Experimental Apparatus

The factors that played a large role in shaping the design of the experimental apparatus were the material selection and the requirement for windows. Once these concerns were addressed the design would have to accommodate the remainder of the requirements.

Material selection was dictated by the desire to mitigate or entirely negate the possibility of corrosion occurring on the internal and external surfaces of the experimental apparatus. An additional criterion that was taken into consideration was the compatibility with low pressure working environments. The materials that were considered for use in the fabrication of the apparatus were steel and stainless steel. The use of steel would have made it necessary to include additives in the working fluid of the cycle in order to reduce the possibility of corrosion. Another aspect of the apparatus that would affect the possibility of corrosion was that the apparatus would have needed to be under a constant high quality vacuum in order to avoid exposing the wetted surfaces to air. These factors in combination with a desire for the continued use of the experimental apparatus led to the decision being made to fabricate the apparatus from stainless steel.

The desire to observe the internal behaviour of the apparatus made it necessary to investigate the inclusion of windows or viewing panes. An option that was considered was the use of large cylindrical glass or polycarbonate tubes with stainless steel end-plates, but this idea was abandoned after investigating the availability of appropriately sized materials. The decision was then made to make use of large flat polycarbonate windows mounted onto rectangular stainless steel vessels.

The next concern that needed to be addressed was the sizing of the apparatus. This is where the decision was made that instead of sizing the apparatus for a specific capacity, a number of identical heat exchangers would be fabricated and the vessels would have to be designed to accommodate the physical dimensions of these heat exchangers.

4.1.1 Heat Exchangers

The criterion that governed the design of the heat exchanger was that it be fabricated from stainless steel, that the design should incorporate the possibility for alteration or removal and that the vertical space that the heat exchanger occupied be kept to a minimum. After taking these requirements into consideration and working through a number of concepts a design for the heat exchangers was finalized and can be seen in Figure 4.1.

Two layers of parallel stainless steel tubes form the basis for the heat exchanger. These layers of parallel tubing are connected to one another through

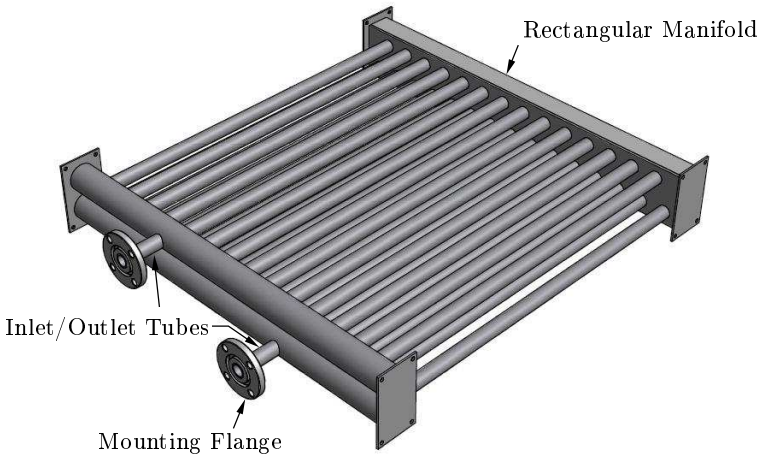

Figure 4.1: Heat exchanger used for the heating and cooling of the generator, condenser, evaporator and absorber

a rectangular manifold. The inlet and outlet tubes each connect to a row of tubes through a tubular manifold. Furthermore, a flange was welded to the inlet and outlet tubes of the heat exchanger in order to make the mounting and removal of the heat exchanger a possibility.

The mounting and associated sealing that was used for each heat exchanger is shown in Figure 4.2 through the use of a vertical section that cuts the wall of the vessel and the heat exchanger. This figure shows the manner in which the heat exchanger flanges are fastened to the internal surface of the vessel and sealed through the use of o-rings. An adaptor piece was mounted and sealed in a similar fashion on the external surface of the vessel. These adaptor pieces served the purpose of providing a connection through which the external heat transfer streams could interface with the heat exchangers and the cycle as a whole.

The soundness of the heat exchangers was tested well in advanced to the assembly of the experimental apparatus. All of the heat exchangers were pressure tested with water to a pressure of three bar absolute.

4.1.2 Vessels

The inclusion of windows in the requirements for the experimental apparatus was not the only aspect of the apparatus that made it beneficial to fabricate the vessels in the shape of rectangular boxes. In addition to the inclusion of windows, a rectangular shaped vessel meant that straight tube heat exchangers could make efficient use of the space that was available. This made it possible to avoid the need for a coil shaped heat exchanger or a heat exchanger that would make inefficient usage of space.

Three rectangular shaped vessels were constructed for the experimental apparatus in a manner that resembled the theoretical simulation. The starting

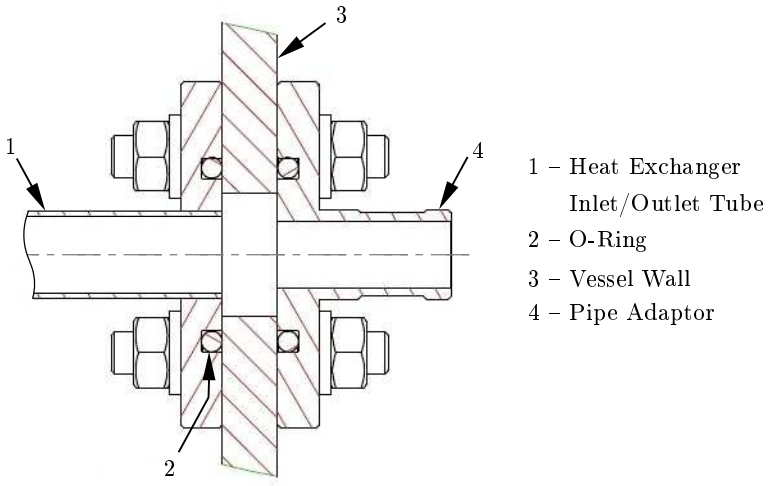

Figure 4.2: Heat exchanger mounting and fastening

point for the manufacture of the vessels was the "box" portion of the vessel that was fabricated from 8 mm stainless steel. Each vessel was constructed out of two parts of laser cut and bent stainless steel. These two parts were welded together to form the main box portion of the vessels.

While a box shaped vessel was convenient with regards to the manufacture, the inclusion of windows and the design of the heat exchangers, the rigidity of the shape is lacking in comparison to a cylindrical vessel. In order to compensate for this the vessels were strengthened by the addition of a frame of stainless steel angles that were welded to the external surface of the vessels. Figure 4.3 shows an example of a typical vessel with the associated internal and external equal angle frames. Where the internal equal angle would provide addition support for the polycarbonate windows. The fastening and sealing of the windows to the vessels was handled through the use of large silicone gas-

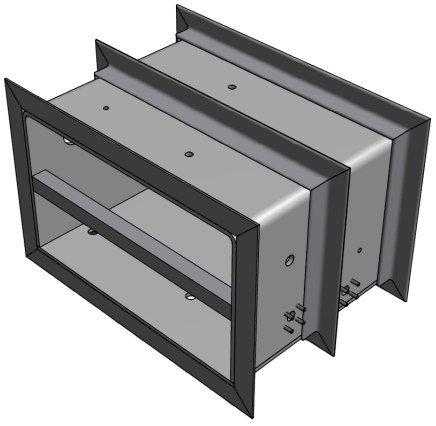

Figure 4.3: Typical vessel

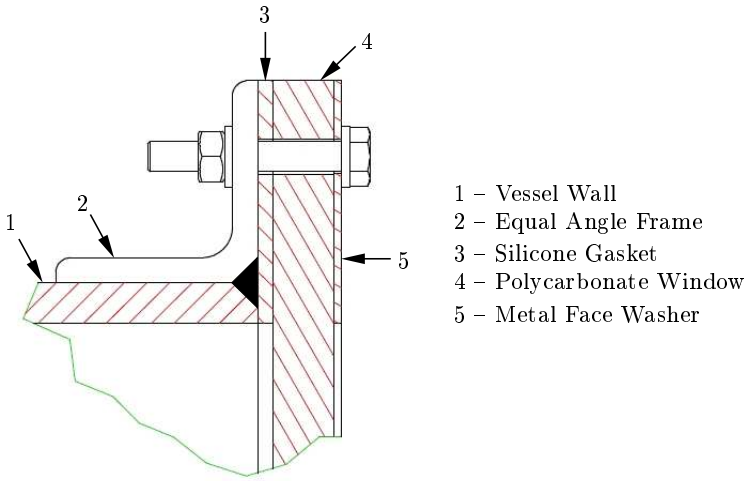

Figure 4.4: Fastening and sealing of windows in the experimental apparatus

kets, polycarbonate windows, large metal washers and a set of bolted fasteners as seen in Figure 4.4.

Interconnectivity between the vessels was taken into consideration through the inclusion of welded sockets for various valves and fittings. However, the connection between the generator and condenser vessels was handled in a different manner. A piece of stainless steel tube in combination with a flange was welded to each of these vessels. This flange configuration was used to link the vapour space of the two vessels together. Furthermore, if it was desired a orifice could be included in the flange configuration in order to measure the flow of vapour from the generator to the condenser.

4.1.3 Assembly

A large frame was fabricated that would house the experimental apparatus. This frame was constructed out of mild steel and was subsequently powder coated.

The assembly of the vessels began with the mounting and fastening of the various heat exchangers, as shown in the previous section. Once this was complete, standard thermocouple probes were inserted and secured into their respective fittings. Calibration of the thermocouples is discussed in Appendix F. The next step in the assembly of the apparatus was the mounting of the windows which started with the silicone gaskets and ended with the fastening of the bolted connections. Figure 4.5a shows the digital version of this stage of the assembly, without the thermocouples.

The interconnectivity between the various vessels was facilitated through the inclusion of valves, fittings and tubing. An exception to this was that the connection between the outlet of the absorber and the inlet of the solution required the inclusion of an electrical pump.

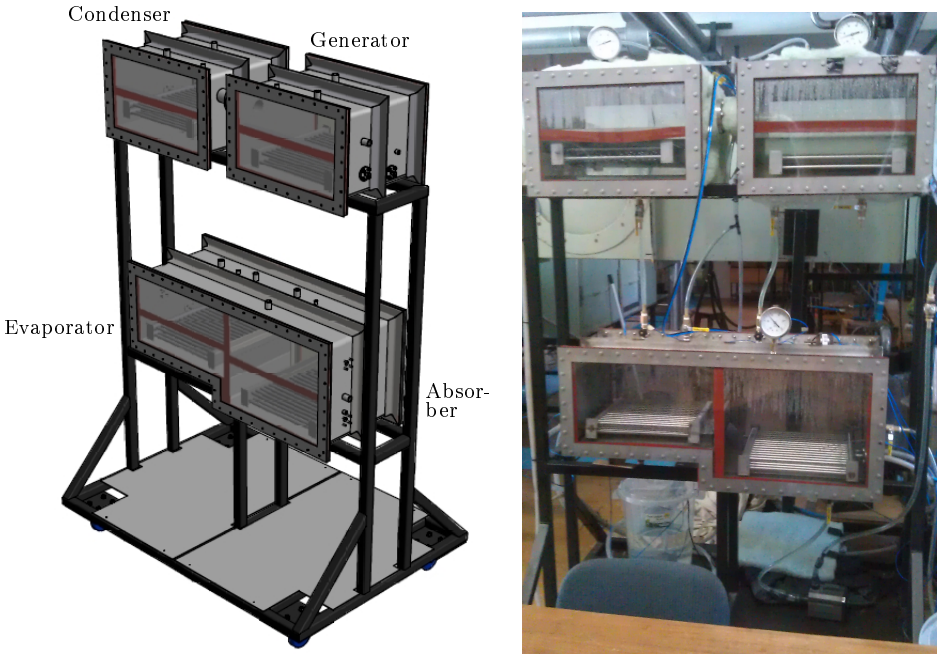

(a) Design of vessels and frame (b) Experimental apparatus

Figure 4.5: Electronic and physical versions of the system

The assembly concerning the external interfaces to the cycle could then commence with the installation of the various valves and fittings that were required to connect the external interfaces like the vacuum pump and the external heat transfer streams. Completion of the flow loop for the heat exchangers was done by fitting the external pipe adaptors to the heat exchanger inlets and outlets. Thereafter the piping for the external load as well as the laboratory heating and cooling and external streams could be connected to the apparatus. The external load was included in the cycle through the inclusion of an additional vessel of water that would be pumped through the evaporator heat exchanger by a small electrical pump.

The process of checking for and eliminating leaks in the apparatus was done at various stages of the assembly. While the apparatus was under vacuum it was filled with water to various levels in order to ascertain whether or not any streams of air were leaking into the apparatus. Corrective measures were taken to eliminate any leaks that were found.

Insulation of the vessels was the last step that was taken in order to prepare the system for operation. Glass wool was secured on the external surfaces of the vessels in order to reduce the influence that the environmental conditions have on the internal behaviour of the system.

4.2 Operating the Experimental Apparatus

A one-time charging of the apparatus took place before the apparatus was tested. This process began with mixing the lithium-bromide salt into a drum of deionized water. Once the mixing of the solution was dealt with the apparatus could be charged with the solution and this was made possible by drawing a vacuum in the apparatus.

The inactive "at rest" state of the apparatus before any testing took place was as follows: The valves that control the flow between vessels are closed, the valves that control the flow of the external heat transfer streams are closed. The apparatus, load and vacuum pumps are off and associated valves are closed. Instrumentation and any associated data capture devices are off.

A generalized approach for starting a test begins with opening the valve between the vacuum pump and the apparatus and subsequently starting the vacuum pump. During the evacuation process the external streams are prepared and the internal valves are set to either isolate sections of the apparatus or manipulate the flow between vessels. This will be determined by which components are being tested. Once a vacuum is established and the external streams are at the desired conditions the instrumentation and logging is activated. Apparatus pumps internal and external to the cycle are then turned on followed by the external laboratory supply streams. The behaviour of the apparatus is then monitored until steady state conditions are reached.

Shutting down of the apparatus starts with turning off the external heating stream. Thereafter the remaining external streams can be turned off followed by the apparatus pumps. All of the valves are then closed and the logging is stopped.

The planned activities for testing of the experimental apparatus was to operate and test the combination of generator and condenser followed by the evaporator and absorber pair. Once these separate tests were complete the entire system would be tested. This plan was not realised as during the testing of the evaporator and absorber it became apparent that the evaporator-absorber component required alterations to the mounting and sealing of the polycarbonate windows. These alterations were necessary to reduce the deflection found in the windows under vacuum conditions and improve on the separation of the evaporator and absorber liquid pools.

An excerpt of the results obtained from the generator and condenser test can be seen in Figure 4.6. This figure illustrates the manner in which the component pair of generator and condenser reached steady state conditions in under an hour of operation with an external generator heating stream of 70 ℃ and a condenser cooling stream of 18.5 ℃.

An important observation that can be made from these results is that the initial assumption that was made with regard to the temperature of the vapour in generator-condenser vessel was incorrect. It can be seen that the generator-condenser vapour temperature T_{GCv} is lower than the generator liquid temper-

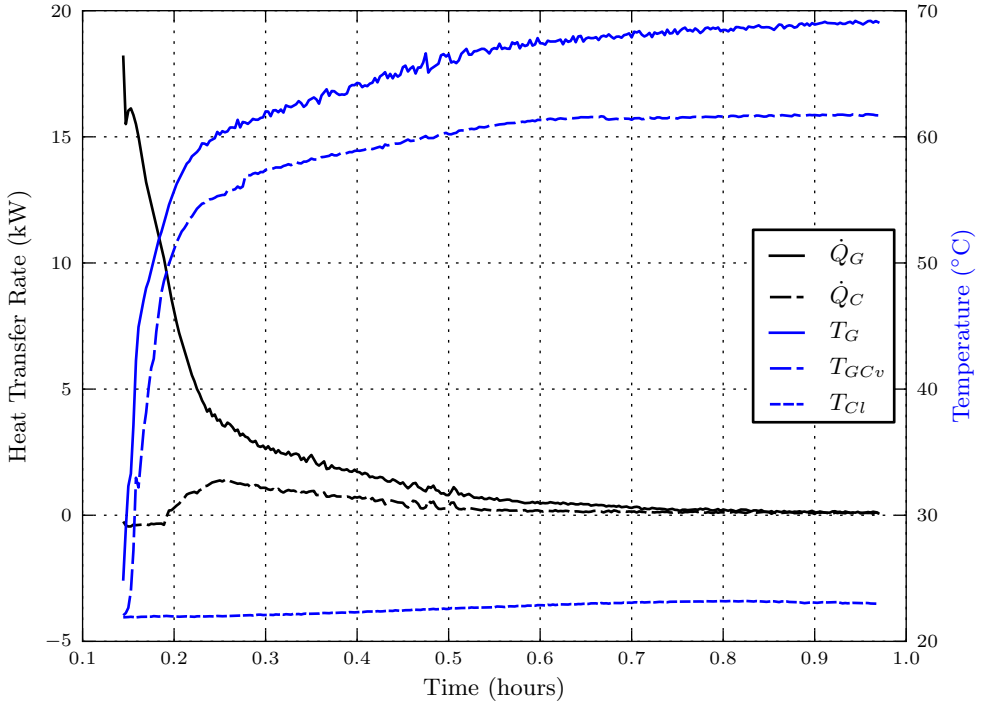

Figure 4.6: Temperature and heat transfer rates obtained from experimental apparatus for the generator and condenser section

ature T_G. This phenomenon would have to be taken into consideration when attempting to simulate the behaviour of the experimental apparatus. With regard to the heat transfer rates to the generator $\dot{Q}_G$ and the condenser $\dot{Q}_C$, it can be seen that the condenser is removing significantly less energy than the generator. This can be attributed to environmental heat losses, an insufficient condensation surface area, the sensible heat requirements for the large mass of solution or the heat of mixing in the generator solution that requires additional energy beyond that of the heat of vapourization in order to separate refrigerant from the solution (Herold *et al.*, 1996).

A more detailed discussion surrounding the results of a test run obtained from the apparatus will be covered in the comparison between the theoretical simulation and experimental apparatus in the next chapter.

5 Experimental and Theoretical Results

This section of the report will discuss the comparison made between the results obtained from the theoretical simulation and the experimental apparatus for the purpose of validation of the theoretical results. Before the specifics of a comparison are discussed there are two topics that must be covered briefly. The first of these topics is the adjustments that were made to the simulation based on the preliminary results obtained from the experimental apparatus. In addition to this, the process that was followed to determine the concentration of the solution in the apparatus is also discussed.

5.1 Simulation Alterations

Observations from the behaviour of the experimental apparatus lead to three alterations being made to the simulation of the generator and condenser. These three changes covered heat loss, the vapour temperature and an alternate method of handling the condenser heat transfer rate calculation.

Energy loss from the generator to the environment was included through a heat loss term in the energy balance equation for the generator and condenser (Equation 3.4.4). The following equation describes the heat loss mathematically:

$$\dot{Q}_{Gloss} = UA_{loss}(T_G - T_{atm}) \tag{5.1.1}$$

where the value for UA_{loss} was calculated from the experimental data by examining the rate at which energy was lost to the environment.

The second change that was made to the simulation was an adjustment to the assumption that was made with regard to the vapour temperature in the generator-condenser vessel. It was initially assumed that the vapour temperature would be the same as the solution temperature, but the experimental results indicated that the actual vapour temperature was about midway between the solution temperature and the vapour saturation temperature. To take this into account the following equation was used to describe the vapour temperature in the simulation:

$$T_{GCv} = T_{GCsat} + c(T_G - T_{GCsat}) \tag{5.1.2}$$

where the user can now alter the vapour temperature by adjusting the value of c between 0 to 1.

The third and last change that was made to the simulation was the implementation of an alternate calculation method for the condenser process that was compatible with the use of a *UA*-value for the condenser heat exchanger.

5.2 Measurement of Solution Concentration

A number of methods are feasible for measuring concentration in an aqueous solution. Four methods of varying complexity will be discussed in this section.

Herold *et al.* (1996) discusses the use of titration as a means through which the concentration of a solution can be determined. This method requires the manipulation of a sample of solution in a laboratory environment. Accurate measurements can be obtained through titration, but at the cost of a time consuming process.

Measuring the electrical conductivity of a solution is a method in which the concentration of a solution can be ascertained in an indirect manner. The combination of solution temperature and electrical conductivity makes it possible to determine the concentration from property equations (Fried and Segal, 1983; Shahata *et al.*, 2012).

In a similar manner, measuring the density of a solution is a means through which the concentration of a solution can be determined. This can be achieved through the use of a Coriolis flow-meter, where this type of flow measurement instrument can measure the flow rate and density of the fluid passing through it. Utilizing a known temperature and density makes it possible to determine the concentration of the solution from property equations.

The concentration of a solution can also be determined in a situation where the volume and temperature of the solution is known in addition to the mass of salt that is present in the solution. These three pieces of information are sufficient to calculate the concentration of the solution through an iterative calculation. This last method for concentration calculation was the method that was used for determining the solution condition in the experimental apparatus.

5.3 Comparison of Results

This section will discuss the comparison of the results obtained from the experimental apparatus and the theoretical simulation when operated under similar conditions. The test run that was chosen for comparison is a set of data in which the inlet temperature of the generator heating stream was varied during the course of the test.

During this test the inlet heating stream was set at 70 ℃ for the initial portion of the test. After equilibrium was reached, the heating stream was then closed while the geyser temperature was increased to 80 ℃. Once the geyser was at the new temperature the heating stream was circulated until

Table 5.1: Initial internal conditions of apparatus test run in combination with external stream characteristics

Control Volume	Variable	Value	Control Volume	Variable	Value
Generator Solution	T_G	22 ℃	Generator	$\dot{m}_{Ghw}$	0.45 kg/s
	m_G	20.8 kg	Heating Stream	T_{Ghwi}	70.3 ℃[1]
	C_G	0.384		T_{Ghwi}	80.4 ℃[2]
Condensate Pool	T_{Cl}	22 ℃		UA_G	249.4 W/K
	m_{Cl}	9.17 kg	Condenser	$\dot{m}_{Ghw}$	0.26 kg/s
Vessel	V_T	0.11 m^3	Cooling Stream	T_{Ccwi}	18.2 ℃
	UA_{loss}	1.44 W/℃		UA_C	11.9 W/K

1: between minute 8 and 58, 2: between minute 98 and 142

equilibrium was reached. Table 5.1 shows the initial internal conditions of the apparatus as well as the external streams for this specific test. Furthermore, the decision was made to use a value of 0.6 for the constant "p" used in Equation 5.1.2. The simulation made use of a time step of 0.1 seconds and simulated a time period of 2.5 hours in a computation time of 184 seconds.

Figure 5.1 shows a comparison between the theoretical and experimental temperatures plotted for the duration of this test run. It can be seen that while the theoretical temperatures do not match the experimental results exactly, the overall tendency is captured remarkably well. In comparing the three data sets it was determined that the largest average difference and maximum difference in theoretical and experimental values is 3.50% for T_{GCv} and 23.0% for T_G. The difference in gradient that is seen in the rise from the initial conditions to the steady state conditions can be attributed to the sudden release of vapour from the generator's solution.

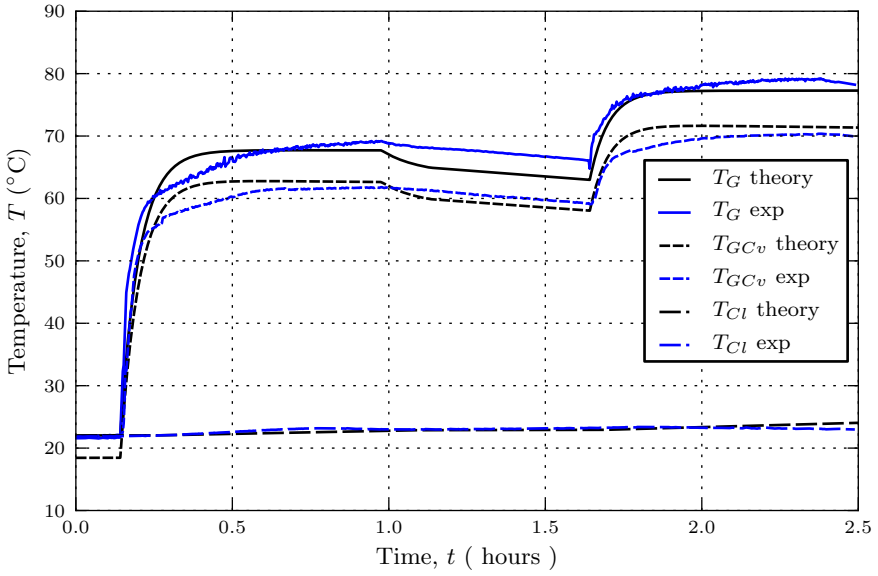

Figure 5.1: Comparison of temperatures obtained from theoretical and experimental work for different conditions as reflected in Table 5.1

6 Discussions, Conclusions and Recommendations

This closing chapter will discuss the results of this project and the possible implications thereof with respect to future work. A number of observations with regards to how well or poorly the goals of the project were satisfied will start the discussions.

The primary goal of this project was the development of a transient simulation of a vapour absorption cycle. Through the application of the basic principles for the conservation of mass and energy a transient simulation was developed for a single effect water/lithium-bromide vapour absorption refrigeration cycle. This developed simulation can be used to simulate the start-up process as well as the dynamic response to alterations in operating conditions. Furthermore, the simulation is robust with respect to the ways in which the user can alter the specifications of the simulated cycle.

With regard to the simulation results, comparison to similar literature was not performed as an appropriate source of literature that documented a similar simulation could not be sourced. The extent to which the simulation models the behaviour of an actual vapour absorption cycle was not completely assessed as only preliminary results could be obtained from the experimental apparatus. What could be compared gave an indication of promising results in that the behaviour of the experimental apparatus was emulated to a reasonable degree, with the largest average difference in temperature for any set of experimental and theoretical values being 3.50% and the largest difference in temperature in any data set of 23.0%.

Additional features and improvements that can be added to the theoretical simulation are a graphical user interface that will give a more user friendly method of using the simulation as well as more flexible methods of varying the external stream conditions that interact with the simulation. In addition to this, further improvements can be made to the combined heat and mass transfer found in the vapour-liquid interaction in the absorber as there are many theoretical and semi-empirical approaches that can be used for the determination of the vapour-liquid interaction.

With regard to the experimental apparatus, the design and construction of the experimental apparatus yielded insights into the practical and physical aspects of a vapour absorption cycle. The portion of the experimental apparatus that was operational and tested can still be improved by increasing the performance of the condenser. Additional work and refinement is needed in order to realise a fully functional vapour absorption system. Furthermore, the

inclusion of more extensive instrumentation, for the measurement and logging of pressure, mass flow rate, density, liquid levels and concentration conditions, will make it possible to examine the behaviour of the apparatus in greater detail. This will also be relevant to the investigation of the vapour absorption coefficient that describes the vapour-liquid interaction in the absorber.

Taking a step back from the details of the vapour absorption technology itself gives the possibility for additional studies that can assess aspects of the technology and their application to a South African environment. Studies towards waste heat recovery, incorporation into larger plants and the feasibility from an economical standpoint are some of the directions in which research projects can venture.

With regards to possible future research using the experimental vapour absorption apparatus, emphasis has to be placed on two different avenues of research. Firstly, in a situation where the desired goal of a project is the investigation and manipulation of the internal workings and mechanisms of a vapour absorption installation, then the use of the experimental apparatus can be beneficial. This is due to the manner in which a custom built apparatus will provide the opportunity to realise custom or innovative design elements in addition to the inclusion of extensive instrumentation for comprehensive measurement capabilities. Secondly, in a scenario where the purpose of a research project is the investigation of a larger hybrid installation that includes a vapour absorption system, such as a combined heat and power plant or a micro/smart-grid, then the experimental apparatus will need improvements to the absorber in addition to the inclusion of a control system so that the system can produce a required refrigeration output using the available external streams.

Appendices

A Fluid Properties

This appendix provides some supplementary information with regards to the properties of the working fluids that are relevant to the absorption process.

A.1 Fluid Property Graphs

The equilibrium chart that describes the relationship between the temperature, concentration and saturation pressure of the working pair lithium-bromide/water is shown below in Figure A.1. Figure A.2 on the following page shows the relationship between the concentration, temperature and enthalpy for lithium-bromide/water.

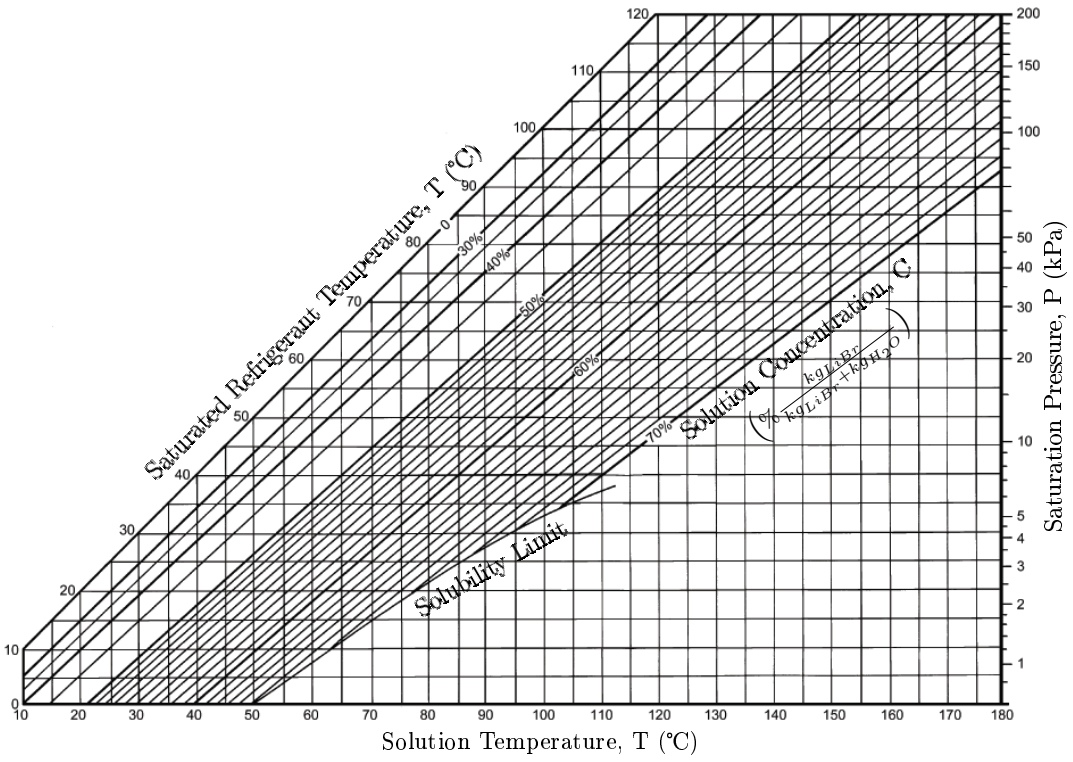

Figure A.1: Saturation pressure and temperature of water/lithium-bromide as a function of solution temperature at various concentrations (Owen, 2009)

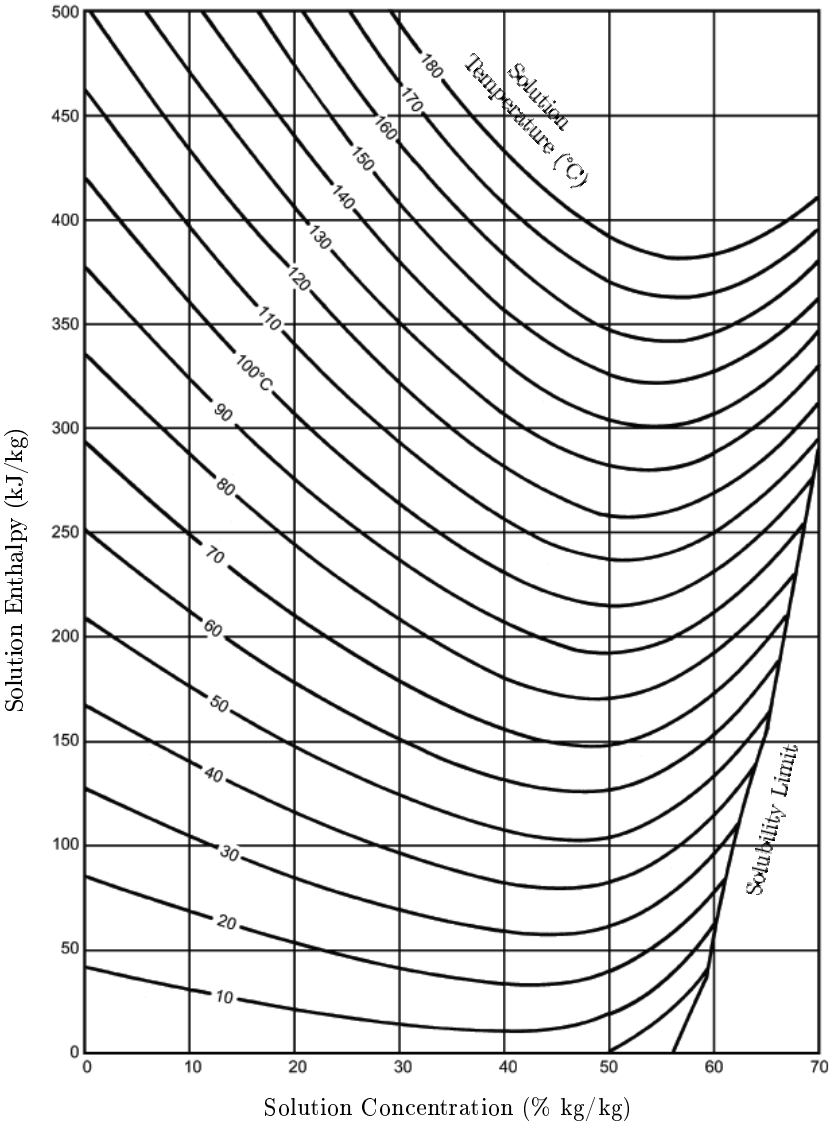

Figure A.2: Enthalpy of water/lithium-bromide as a function of concentration at various solution temperatures (Owen, 2009)

The decision was made to exclude any property graphs for water, ammonia as well as the combination of ammonia/water. Part of this decision was due to the manner in which graphs for the properties of water are readily available. As for the graphs of ammonia and ammonia/water, these substances were not used or investigated extensively in this project and the inclusion of any graphs was deemed unnecessary.

A.2 Property Equations

This section will discuss the property equations and the equations of state that were incorporated into the simulation. In a number of these equations very slight modifications were included in the coded versions in order to ensure that all of the equation input and output units were compatible. This ensured that in the calling and subsequent returning of values to and from the property equations would always be in the appropriate units. These primary units are shown below in Table A.1:

Table A.1: Primary units for the theoretical simulation

Variable	Unit
Mass	kg
Time	s

Variable	Unit
Temperature	℃
Energy	J

Variable	Unit
Pressure	Pa
Distance	m

Table A.2 shows the temperature, pressure and enthalpy equations that were included in the simulation for the liquid and vapour phases of water. The majority of these property equations were incorporated from "The IAPWS Industrial Formulation 1997 for the Thermodynamic Properties of Water and Stream", Wagner *et al.* (2000).

Table A.2: Property equations that were implemented for water

Description	Format	Source
Saturation Pressure	$P_{sat}\{T\}$	IAPWS-IF97, Eq. 28
Saturation Temperature	$T_{sat}\{P\}$	IAPWS-IF97, Eq. 55
Liquid Enthalpy	$h_f\{T,P\}$	IAPWS-IF97, Eq. 15
Liquid Temperature	$T_f\{h,P\}$	IAPWS-IF97, Eq. 37
Liquid Enthalpy	$h_{fsat}\{T\}$	IAPWS-IF97, Eq. 15 & 28
Vapour Enthalpy	$h_g\{T,P\}$	IAPWS-IF97, Eq. 19
Vapour Temperature	$T_g\{h,P\}$	IAPWS-IF97, Eq. 37
Enthalpy of Vapourization	$h_{fg}\{T\}$	IAPWS-IF97, Eq. 15,19,28
Density of Vapour	$\rho_g\{T,P\}$	IAPWS-IF97, Eq. 19
Density of Liquid	$\rho_f\{T\}$	Çengel (2003), Table A-9

The heat transfer and transport properties of water were incorporated from Table A-9 of Çengel (2003). These properties are listed below in Table A.3:

Table A.3: Heat transfer property equation for saturated water

Description	Input(s)	Format
Specific Heat of Liquid	Temperature	$c_{pf}\{T\}$
Specific Heat of Vapour	Temperature	$c_{pg}\{T\}$
Thermal Conductivity	Temperature	$k_f\{T\}$
Prandtl Number	Temperature	$Pr\{T\}$
Dynamic Viscosity	Temperature	$\mu\{T\}$

Table A.4: Property equations for water/lithium-bromide

Description	Input(s)	Format	Source
Enthalpy	Temperature & Concentration	$h_{sol}\{T, C\}$	ASHRAE (2009), F30.70
Temperature	Enthalpy & Concentration	$T_{sol}\{h, C\}$	ASHRAE (2009), F30.70
Temperature	Pressure & Concentration	$T_{sol}\{P, C\}$	ASHRAE (2009), F30.71
Pressure	Temperature & Concentration	$P_{sol}\{T, C\}$	ASHRAE (2009), F30.70
Thermal Conductivity	Temperature & Concentration	$k_{sol}\{T, C\}$	Teja *et al.* (1991), Chapter 2
Specific Heat	Temperature & Concentration	$c_{sol}\{T, C\}$	Teja *et al.* (1991), Chapter 5
Density	Temperature & Concentration	$\rho_{sol}\{T, C\}$	Khairulin *et al.* (2006), Eq 2

Table A.4 shows the property functions that were included for the lithium-bromide/water solution. The source equation for the enthalpy of the solution is shown in Equation A.2.1, where the concentration is supplied to the equation as a percentage value. Coefficients for this equation are shown in Table A.5.

$$h = \sum_{n=0}^{4} A_n X^n + t \sum_{n=0}^{4} B_n X^n + t^2 \sum_{n=0}^{4} C_n X^n \tag{A.2.1}$$

The solution enthalpy is defined as a function of temperature and concentration, but if one were to look only at the relationship between the enthalpy and temperature, at a known concentration, it can be seen that the equation is in the form of a quadratic equation. This makes it feasible to rewrite the solution enthalpy equation in a manner that will make it possible to determine an unknown solution temperature from a known enthalpy and concentration.

Equation A.2.2 from Owen (2009) specifies the manner in which the temperature of a lithium-bromide/water solution can be determined as a function of refrigerant temperature and concentration. The coefficients for this equation can be found in Table A.5. It is also possible to rewrite this equation in order to make the refrigerant temperature a function of the solution temperature and concentration.

$$t = \sum_{n=0}^{3} E_n X^n + t' \sum_{n=0}^{3} D_n X^n \tag{A.2.2}$$

Equations A.2.1 and A.2.2 both have limitations in that they are only defined over a specific range with respect to concentration and temperature. These concentration ranges through which the two equations are valid is 40 to 75% and 45 to 70% respectively. The concentration limits were taken into

Table A.5: Coefficients for the enthalpy and equilibrium chart of water/lithium-bromide (Owen, 2009)

n	A_n	B_n	C_n	D_n	E_n
0	-2.02433×10^{3}	1.82829×10^{1}	-3.7008214×10^{-2}	-2.00755×10^{0}	1.24937×10^{2}
1	1.63309×10^{2}	-1.169175×10^{0}	2.8877666×10^{-3}	1.6976×10^{-1}	-7.71649×10^{0}
2	-4.88161×10^{0}	3.248041×10^{-2}	-8.1313015×10^{-5}	-3.13336×10^{-3}	1.52286×10^{-1}
3	6.30294×10^{-2}	-4.034184×10^{-4}	9.9116628×10^{-7}	1.97668×10^{-5}	-7.95090×10^{-4}
4	-2.91370×10^{-4}	1.852056×10^{-6}	-4.4441207×10^{-9}		

account during the development of the simulation and are discussed further in Appendix C.1.

During the analysis of the data obtained from the experimental set-up it was discovered that the concentration in the water/lithium-bromide solution was too low for the equations of state that were implemented in the simulation. This made it necessary to extend the functionality of the simulation by incorporating equations of state that are defined across a larger concentration range. The work presented by Pátek and Klomfar (2006*a*) was chosen due to the type of property functions presented in the article in combination with the composition range of 0 to 223 ℃ and 0 to 75 % mass fraction percentage. Table A.6 shows the property equations that were incorporated from this article:

Table A.6: Extended property equations for water/lithium-bromide

Description	Format	Equations
Saturation Pressure	$P_{sol}\{T, C\}$	A.2.3, A.2.4 & A.2.9
Density	$\rho_{sol}\{T, C\}$	A.2.5, A.2.6 & A.2.9
Enthalpy	$h_{sol}\{T, C\}$	A.2.7, A.2.8 & A.2.9

The property equations for the pressure, density and enthalpy of the solution were included from this article. Each of these properties is calculated through the application of two equations:

$$p(T,x) = p_\sigma(\theta), \quad \theta = T - \sum_{i=1}^{8} a_i x^{m_i} \{0.4 - x)^{n_i} \left(\frac{T}{T_c}\right)^{t_i} \tag{A.2.3}$$

$$p_\sigma(T) = p_c \exp\left[\frac{T_c}{T} \sum_{i=1}^{6} \alpha_i \left(1 - \frac{T}{T_c}\right)^{\beta_i}\right] \tag{A.2.4}$$

$$\varrho(T,x) = (1-x)\varrho'(T) + \varrho_c \sum_{i=1}^{2} a_i x^{m_i} \left(\frac{T}{T_c}\right)^{t_i} \tag{A.2.5}$$

$$\varrho'(T) = \varrho_c \left[1 + \sum_{i=1}^{6} \alpha_i \left(1 - \frac{T}{T_c}\right)^{\beta_i}\right] \tag{A.2.6}$$

$$h(T,x) = (1-x)h'(T) + h_c \sum_{i=1}^{30} a_i x^{m_i} (0.4 - x)^{n_i} \left(\frac{T_c}{T - T_0}\right)^{t_i} \tag{A.2.7}$$

$$h'(T) = h_c \left[1 + \sum_{i=1}^{4} \alpha_i \left(1 - \frac{T}{T_c}\right)^{\beta_i}\right] \tag{A.2.8}$$

and their respective coefficients located in Table A.7, A.8 and A.9. Reference parameters for the properties of water and lithium-bromide are located in Table A.10. A number of conversions to the input and output values were necessary in order to accommodate these equations.

With regard to the input values, the equations need a solution temperature T in Kelvin and solution composition in molar fraction x. The conversion from the simulation unit for temperature (℃) to the equation temperature is straightforward, but the conversion from the simulation unit for solution composition, mass concentration C (kg LiBr/kg Solution), needs to make use of the following relationship:

$$x = \frac{C/M_{\text{LiBr}}}{C/M_{\text{LiBr}} + (1-C)/M_{\text{H2O}}} \tag{A.2.9}$$

where the molar weight of lithium bromide as well as water is specified in Table A.10.

With regard to the output values, the output from the molar density (mol m^{-3}) and the enthalpy (J mol^{-1}) required conversion. This was achieved by calculating the molar mass of the solution using the solution concentration, the molar mass of lithium-bromide and the molar mass of water.

The source material for these equations did not specify any backwards equations for calculating the temperature or concentration from supplied conditions. A simple iterative process was implemented in order to obtain this functionality where the temperature of a solution would be evaluated in the bounds of the equation and solved until a viable answer was found for a given enthalpy and concentration.

Table A.7: Coefficients and exponents for solution pressure of Eq. A.2.3 and A.2.4 (Pátek and Klomfar, 2006*a*)

i	m_i	n_i	t_i	a_i	β_i	α_i
1	3	0	0	-2.41303×10^{2}	1.0	−7.85951783
2	4	5	0	1.91750×10^{7}	1.5	1.84408259
3	4	6	0	-1.75521×10^{8}	3.0	−11.7866497
4	8	3	0	3.25430×10^{7}	3.5	22.6807411
5	1	0	1	3.92571×10^{2}	4.0	−15.9618719
6	1	2	1	-2.12626×10^{3}	7.5	1.80122502
7	4	6	1	1.85127×10^{8}		
8	6	0	1	1.91216×10^{3}		

Table A.8: Coefficients and exponents for solution density of Eq. A.2.5 and A.2.6 (Pátek and Klomfar, 2006*a*)

i	m_i	t_i	a_i	β_i	α_i
1	1	0	1.746	1/3	1.99274064
2	1	6	4.709	2/3	1.099965342
3				5/3	−0.510839303
4				16/3	−1.75493479
5				43/3	−45.5170352
6				110/3	-6.7469445×10^{5}

Table A.9: Coefficients and exponents for solution enthalpy of Eq. A.2.7 and A.2.8 (Pátek and Klomfar, 2006*a*)

i	m_i	n_i	t_i	a_i	i	m_i	n_i	t_i	a_i	i	β_i	γ_i
1	1	0	0	2.27431×10^{0}	16	2	5	3	-4.04479×10^{1}	1	0	0
2	1	1	0	-7.99511×10^{0}	17	2	7	3	1.45342×10^{2}	2	2	2
3	2	6	0	3.85239×10^{2}	18	5	0	3	-2.74873×10^{0}	3	3	3
4	3	6	0	-1.63940×10^{4}	19	6	3	3	-4.49743×10^{2}	4	6	5
5	6	2	0	-4.22562×10^{2}	20	7	1	3	-1.21794×10^{1}	5	34	0
6	1	0	1	1.13314×10^{-1}	21	1	0	4	-5.83739×10^{-3}	i	α_i	
7	3	0	1	-8.33474×10^{0}	22	1	4	4	2.33910×10^{-1}	1	1.38801	
8	5	4	1	-1.73833×10^{4}	23	2	2	4	3.41888×10^{-1}	2	−2.95318	
9	4	0	2	6.49763×10^{0}	24	2	6	4	8.85259×10^{0}	3	3.18721	
10	5	4	2	3.24552×10^{3}	25	2	7	4	-1.78731×10^{1}	4	−0.645473	
11	5	5	2	-1.34643×10^{4}	26	3	0	4	7.35179×10^{-2}	5	9.18946×10^{5}	
12	6	5	2	3.99322×10^{4}	27	1	0	5	-1.79430×10^{-4}			
13	6	6	2	-2.58877×10^{5}	28	1	1	5	1.84261×10^{-3}			
14	1	0	3	-1.93046×10^{-3}	29	1	2	5	6.24282×10^{-3}			
15	2	3	3	2.80616×10^{0}	30	1	3	5	6.84765×10^{-3}			

Table A.10: Properties of water and lithium-bromide for property equations (Pátek and Klomfar, 2006*a*)

T_c	647.096 K	T_t	273.16 K	M_{H2O}	0.018015268 kg mol^{-1}
p_c	22064×10^{6} Pa	p_t	611.657 Pa	M_{LiBr}	0.08685 kg mol^{-1}
ϱ_c	17.873 mol m^{-3}	ϱ'_t	55496.8 mol m^{-3}		

The solubility limit of water/lithium-bromide was also included in the simulation. Pátek and Klomfar (2006*b*) describes the solid-liquid equilibrium of water/lithium-bromide through a series of equations where each equation describes a solid composition. These five compositions are: a) LiBr-5H_2O, b) LiBr-3H_2O, c) LiBr-2H_2O,d) LiBr-H_2O and e) Ice as shown in Figure A.3 with the composition and temperature range through which each region is valid. The relationship between concentration and temperature at which the phase change occurs is described through the following polynomials:

$$T(x) = T_L + \frac{T_R - T_L}{x_R - xL}\{x - x_L) + T_t \sum_{t=1}^{N} a_i (x - x_L)^{m_i} \{x_R - x)^{n_i} \qquad \text{(A.2.10)}$$

$$x(T) = x_L + \frac{x_R - x_L}{T_R - T_L}\{T - T_L) + \sum_{i=1}^{N} b_i \left(\frac{T - T_L}{T_t}\right)^{m_i} \times \left(\frac{T_R - T}{T_t}\right)^{n_i} \qquad \text{(A.2.11)}$$

where each region of solution composition is assigned a unique set of parameters as shown in Tables A.11 and A.12 respectively.

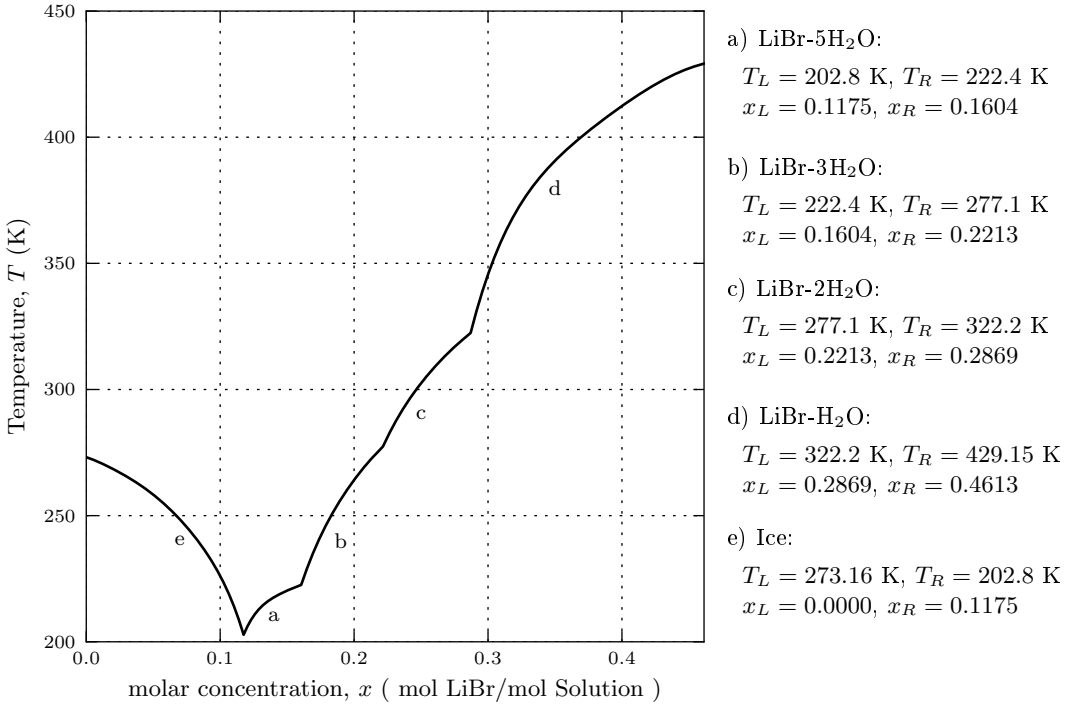

Figure A.3: Phase diagram for water/lithium-bromide solution

Table A.11: Coefficients and exponents of Equation A.2.10 (Pátek and Klomfar, 2006*b*)

	LiBr-5H$_2$O			LiBr-3H$_2$O				Ice		
i	a_i	m_i	n_i	a_i	m_i	n_i	i	a_i	m_i	n_i
1	2.61161×10^{1}	1	1	2.47039×10^{1}	1	1	1	1.33842×10^{1}	1	1
2	2.38994×10^{4}	1	3	4.65459×10^{3}	1	3	2	-4.39293×10^{1}	2	1
	LiBr-2H$_2$O			LiBr-H$_2$O			3	4.02577×10^{3}	3	1
i	a_i	m_i	n_i	a_i	m_i	n_i	4	-5.52364×10^{4}	4	1
1	1.62375×10^{1}	1	1	1.00743×10^{1}	1	1	5	3.28383×10^{5}	5	1
2	2.47098×10^{3}	1	3	3.94593×10^{1}	1	4				

Table A.12: Coefficients and exponents of Equation A.2.11 (Pátek and Klomfar, 2006*b*)

	LiBr-5H$_2$O			LiBr-3H$_2$O				Ice		
i	b_i	m_i	n_i	b_i	m_i	n_i	i	b_i	m_i	n_i
1	-6.17446×10^{0}	1	1	-7.17618×10^{-1}	1	1	1	1.22335×10^{0}	1	1
2	-1.46770×10^{3}	3	1	-1.02551×10^{1}	3	1	2	-1.67781×10^{0}	1	2
	LiBr-2H$_2$O			LiBr-H$_2$O			3	-2.65346×10^{2}	1	4
i	b_i	m_i	n_i	b_i	m_i	n_i	4	-1.93594×10^{3}	1	5
1	-1.06305×10^{0}	1	1	-9.25082×10^{-1}	1	1	5	-5.16209×10^{3}	1	6
2	-1.90921×10^{1}	3	1	-7.22341×10^{0}	3	1				

A.3 Selection of Solution Concentration

This appendix discusses the reasoning behind the manner in which it is a common place practice to make use of a solution of lithium-bromide and water at a concentration in the region of 50% to 55% as the author could not locate any literature that explained the reason why this occurred. The justification for using a solution in this concentration range in the absorber can be approached through the question of finding a balance between the temperature of the evaporator and the temperature of the absorber sections of the vapour absorption cycle.

To elaborate on this, a balance has to be found between the desire to have a low temperature in the evaporator section and the temperature in the absorber section. In the case of the evaporator, the external load that the cycle is to refrigerate will only be cooled if the evaporator section is at a lower temperature than the external load. This makes it a necessity that the temperature in the evaporator is low in order to facilitate a reasonable temperature difference between it and the load. The other portion of this interaction is that the condition of the absorber determines the temperature that can be reached in the evaporator.

The interaction between the absorption of vapour, the solution inlet stream from the generator and the cooling of the absorber solution has to be taken into consideration when evaluating the condition of the absorber solution. Cooling of the absorber solution is done in order to counteract the effect that the absorption of vapour and the solution inlet stream have in disrupting the condition of the solution. It would be quite counterproductive if the stream that was used to cool the absorber would itself require cooling as this would make the cycle redundant. The ideal stream for the cooling of the absorber would originate from a large sink at ambient conditions, for example between 20 and 25 ℃. This is where interaction between the cooling effect from an external stream and the heating effect from vapour absorption and the solution stream will result in determining the condition of the absorber.

The discussion concerning the desired condition in the evaporator and the limitations of the absorber culminate when examining the interaction between these components. In viewing the absorption process as a mass transfer phenomenon that is driven by any difference in pressure, that is caused by a difference in concentration, between the vapour space and the absorber solution implies that in order for absorption to take place the pressure of the vapour space will have to be higher than that of the solution. A set of data showing the conditions at which the saturation pressure of pure water will be equal to the saturation pressure of a solution at various concentrations is shown in Table A.13. Therefore, in order for the absorption process to be continuous, the temperature of a solution has to be kept lower than the indicated solution temperature for its concentration. For example, at a evaporator condition of 5 ℃ and an absorber concentration of 55 % the solution would have to be kept

Table A.13: Comparison of saturation temperatures between pure water and a solution of water/lithium-bromide at various concentrations

		Concentration (kg/kg)			
		0.45	0.50	0.55	0.60
Temperature (℃)	Pressure (Pa)	Saturation Temperature (℃)			
5	872.57	17.97	24.85	33.41	44.28
10	1228.18	22.96	30.06	38.73	50.11
15	1705.74	28.02	35.26	44.04	55.95
20	2339.21	33.08	40.47	49.36	61.79

at a temperature below 33.41 ℃ in order for absorption to take place.

This is illustrated in a more complete manner in Figure A.4 where the data points from Table A.13 are plotted to resemble an excerpt from a Dühring plot. With reference to Figure A.4, consider a scenario where the desired evaporator temperature was between 8 and 12 ℃. Under these specifications there are many possible absorber solution conditions that are compatible with providing this evaporator temperature, but the issue of choosing an appropriate absorber concentration and temperature comes into play.

If the absorber solution was at a concentration of roughly 45 %, the absorber temperature would need to be below 26 ℃ and possibly as low as 20 ℃ in order to achieve the desired evaporator temperature. While it would be possible to achieve this absorber temperature it is deemed undesirable in the sense that it would require an external stream at a relatively low temperature with the possible additional requirement of an increased heat transfer surface area. Furthermore this scenario can also be considered unnecessary as

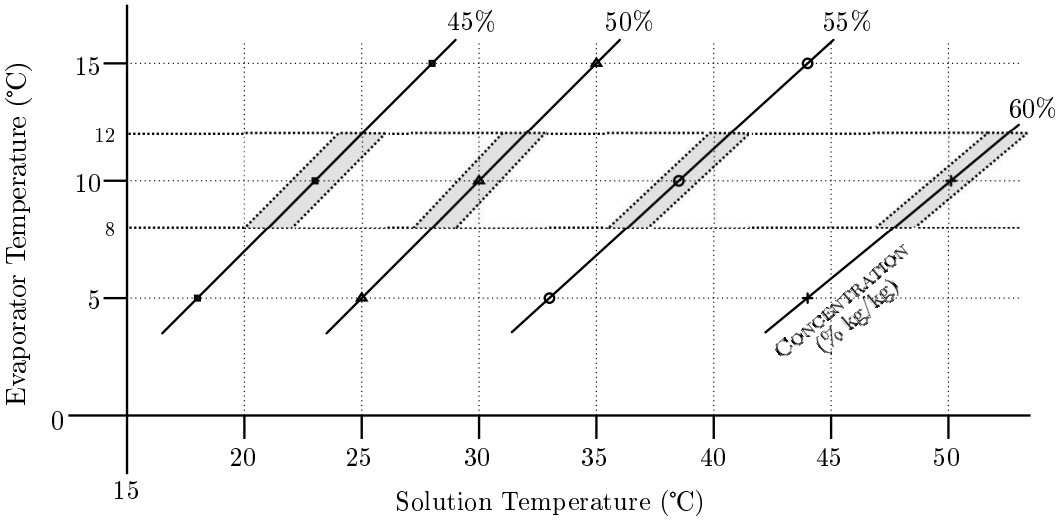

Figure A.4: Comparison of the saturation temperatures of water and water/lithium-bromide at various solution concentrations

the same evaporator temperatures can be realised through an absorber solution at concentration with fewer limitations concerning the temperature of the solution.

In a scenario where the concentration of the solution is roughly 60 % the absorber solution can be at a much higher temperature and still achieve the desired evaporator temperature. While the cooling requirements associated to this scenario are more relaxed the issue concerning the solubility of the solution makes it undesirable. The disconcerting aspect of this scenario is that the concentration as well as the temperature of the solution will increase while passing through the generator and this situation approaches conditions where there is the possibility that the solution will begin to crystallize.

The last scenario that will be discussed is a balance of both of the previous discussed scenarios where the absorber concentration is in the range of 50 to 55 %. The implication of this is that the absorber can be cooled with an ambient stream and the conditions of the solutions can be considered to be healthier than the more concentrated scenario.

Returning to the point that was made earlier concerning the desire to find a balance between the evaporator condition and the absorber condition. It was shown that while there are many factors that play a part in the condition of the evaporator and absorber, a solution in the range of 50 to 55 % gives the possibility to balance the desire to provide for cooling with a reasonable temperature in the absorber.

A.4 Safety Implications Related to Working Fluids

This section extends the discussion that started in Section 2.3 with respect to the safety concerns associated with the current working fluids used in vapour absorption cycles. There are a multitude of regional safety codes that can be referenced with regards to the topic of chemical safety, but this section will only discuss the risks associated with the working fluids in terms of the different types of risk and their resulting effects.

Ammonia/water poses a number of safety concerns with regards to both the ammonia vapour and the aqueous solution of ammonia/water. The operational pressure requirements for this working pair is well above atmospheric conditions and requires pressure vessels. Ammonia can pose a fire hazard if heated when at a sufficiently high concentration. In addition to this ammonia can react in a violent manner when mixed with any number of chemicals. James (1973) discusses the risks associated with exposure to ammonia vapour: at a concentration above 700 ppm causes damage to the eye and can induce loss of sight, at 2000 ppm ammonia will burn and blister a person's skin in a short period of time and when breathing in an environment with an ammonia

concentration of 5000 ppm a person can quickly suffocate. In a similar fashion to exposure to high concentration of ammonia vapour, exposing the dermis to the solution of ammonia/water can lead to the the drying of the skin in such an aggressive manner that the skin "burns" in a manner that bears resemblance to frostbite.

Water/lithium-bromide poses fewer risk than those associated with ammonia/water. It is however important to note that emphasis is placed on the harmful effects linked to the ingestion of lithium-bromide as this can be fatal. While not as hazardous, care should also be taken to avoid or prevent skin contact with lithium-bromide.

This discussion has highlighted the risks attached to the two refrigerant/absorbent combinations. However, a decision had to be made with regard to the working fluid that was to be implemented in an academic environment and the evaluation of the risks led to the project being focused on investigating an absorption cycle that made use of water/lithium-bromide as the risks associated with the use of this working pair could be negated by taking the utmost care to avoid ingestion of any lithium-bromide salt.

B Simulation Flow Diagram

A discussion concerning the operation of the theoretical simulation will be facilitated through the use of a flow digram that illustrates the operations that were performed in the source code of the simulation. The size of the computer simulation made it necessary to break the flow diagram up into a number of units. The first of which covers the initialization of the program and the start of the time loop, as seen in Figure B.1. Standard (sdtio.h, time.h, string.h, math.h) and custom function libraries are then imported into the simulation. The custom function libraries contain the fluid property equations that are discussed in Appendix A.2.

The component configuration that is selected is then specified through the use of "internal_streams", "absorption_pool", "absorption_film" and "solution_hxe_included" which respectively determine the presence and rate of the mass streams that flow between the vessels, the presence of cooling in the absorber solution pool, the presence of a solution film and whether or not it is cooled and the inclusion or exclusion of a solution heat exchanger in between the generator and absorber.

Thereafter, the time related variables of the simulation are specified by a total simulation time in combination with a time step size that is to be used. The initial conditions of the internal control volumes of the simulation are specified followed by the initial conditions of the internal streams. The conditions of the external streams that interface with the simulated cycle are also specified through a temperature, mass flow rate and where applicable an overall heat transfer coefficient. A main output file is always initialized where the simulation parameters are listed and the transient results of the simulation are written at a user specified internal. The option is made available to the user that the state of any of the external streams in

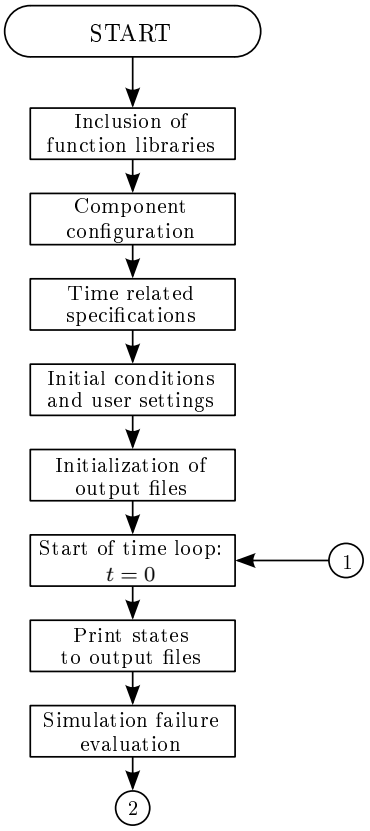

Figure B.1: Initialization of simulation through variable declaration, component specification, output file initialization and the start of the time loop

the heat exchangers can be written to separate output file(s). Once this is complete, the simulation is ready to start the time loop.

The time loop starts with the writing of the current conditions of the simulation to the output file(s). Once this is complete the conditions in the cycle are evaluated in order to ascertain whether the condition of the cycle is at risk through four categories of failure that will lead to the simulation being stopped. The first evaluation is performed to check that the conditions of the solution in the simulation are within the bounds of the property equations. Secondly, the condition of the solution is assessed with respect to the solubility limit. Thirdly, the masses present in the various control volumes have a positive value. Lastly, if the evaporator temperature should decrease below a user specified value the simulation will also be stopped. This last criterion was included to avoid the possible scenario where the pressure in the evaporator-absorber vessel decreased to such an extent that the property equations were no longer valid or the possibility for the formation of ice occurs. All of these failure criteria are discussed further in Appendix C.1.

The second portion of the simulation determines the inter-vessel flow rates in the cycle as well as the conditions at which these streams enter the generator, evaporator and absorber. This is shown in Figure B.2 where it can be seen that the first branch that is encountered checks whether or not the internal streams are active. Should the internal streams be inactive then the mass flow rates for the condenser outlet and the solution pump are set equal to zero.

If the internal streams are active then the condenser and pump mass flow rates are assigned values according to the user specifications at the start of the program. There are currently three possible modes in which the condensate and pump flow rates can be specified. The first of which is where both of

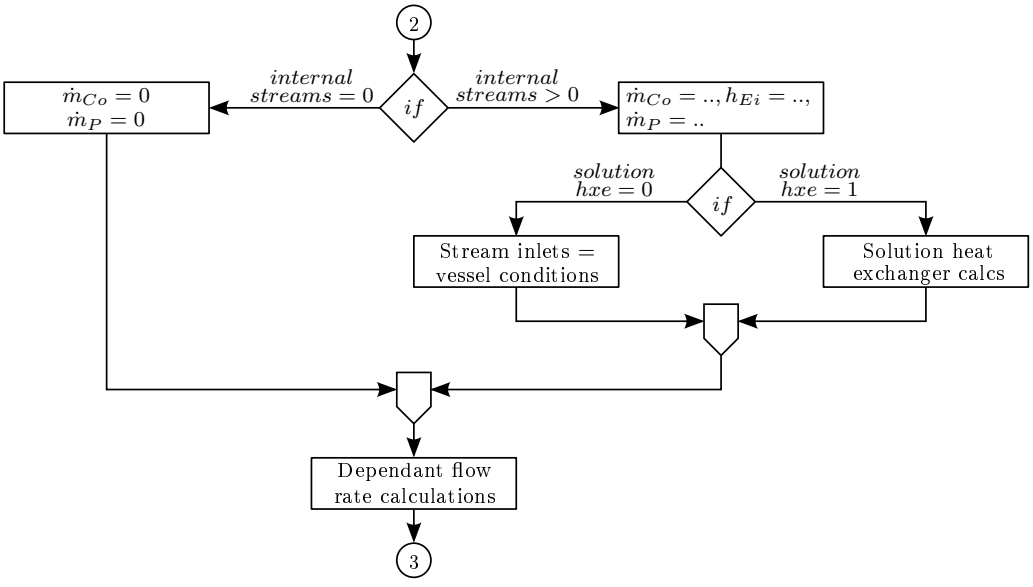

Figure B.2: Inter-vessel stream mass flow rate and temperature calculations

these flow rates are set to fixed mass flow rate values. Secondly, the condenser outlet flow rate is set to a fixed value and the pump mass flow rate is set to a ratio of the condenser outlet mass flow rate. Lastly, the condenser mass flow rate is varied for the purpose of controlling the mass in condensate liquid pool. In this scenario the pump mass flow rate is also specified as a ratio of the condenser mass flow rate. The condition of the stream entering the evaporator is not affected by the presence of the solution heat exchanger which is why the condition is specified before the branch that evaluates the inclusion/exclusion of the solution heat exchanger.

Exclusion of the solution heat exchanger leads to the inter-vessel stream conditions retaining the conditions of the vessel where they originated. In contrast to this, the inclusion of the solution heat exchanger alters the temperatures of the streams that flow between the generator and absorber. The calculation process that was implemented for the solution heat exchanger is discussed in detail in Appendix C.3. Once the branch concerning the inclusion of the internal stream is completed the remaining inter-vessel mass flow rates are defined as functions of the condenser outlet and pump mass flow rates.

Figure B.3 shows the manner in which the condenser calculations were performed. These calculations start with determining the thermal resistance values for the internal fluid flow in the heat exchanger pipes as well as the conduction resistance from the heat exchanger wall. The remainder of the calculations are performed to determine the outer thermal resistance. This is done by evaluating the possibility of condensation occurring through a comparison between the temperature of the fluid in each cell of the condenser heat exchanger with the saturation temperature of the vapour. If this check is successful then an iterative process is followed in an attempt to determine a viable outer wall temperature that will satisfy the criteria discussed in Appendix C.4. If this process does not converge in a specified number of iterations then the calculation is deemed to be unsuccessful with no condensation taking place. Meeting the convergence criteria within the loop limit will increment the total condensation and heat transfer rate for the current time step. During the process of developing the simulation the speed of the iterative condenser calculation was improved through the use of previously converged wall temperatures as the starting point for consequent iterative calculations.

The interfaces that interact with the condensate pool are now all known and can be used to determine the conditions of the condenser liquid pool for the next time step. This portion of the flow diagram concludes with the heat exchanger calculations for the heating stream that interacts with the generator solution pool.

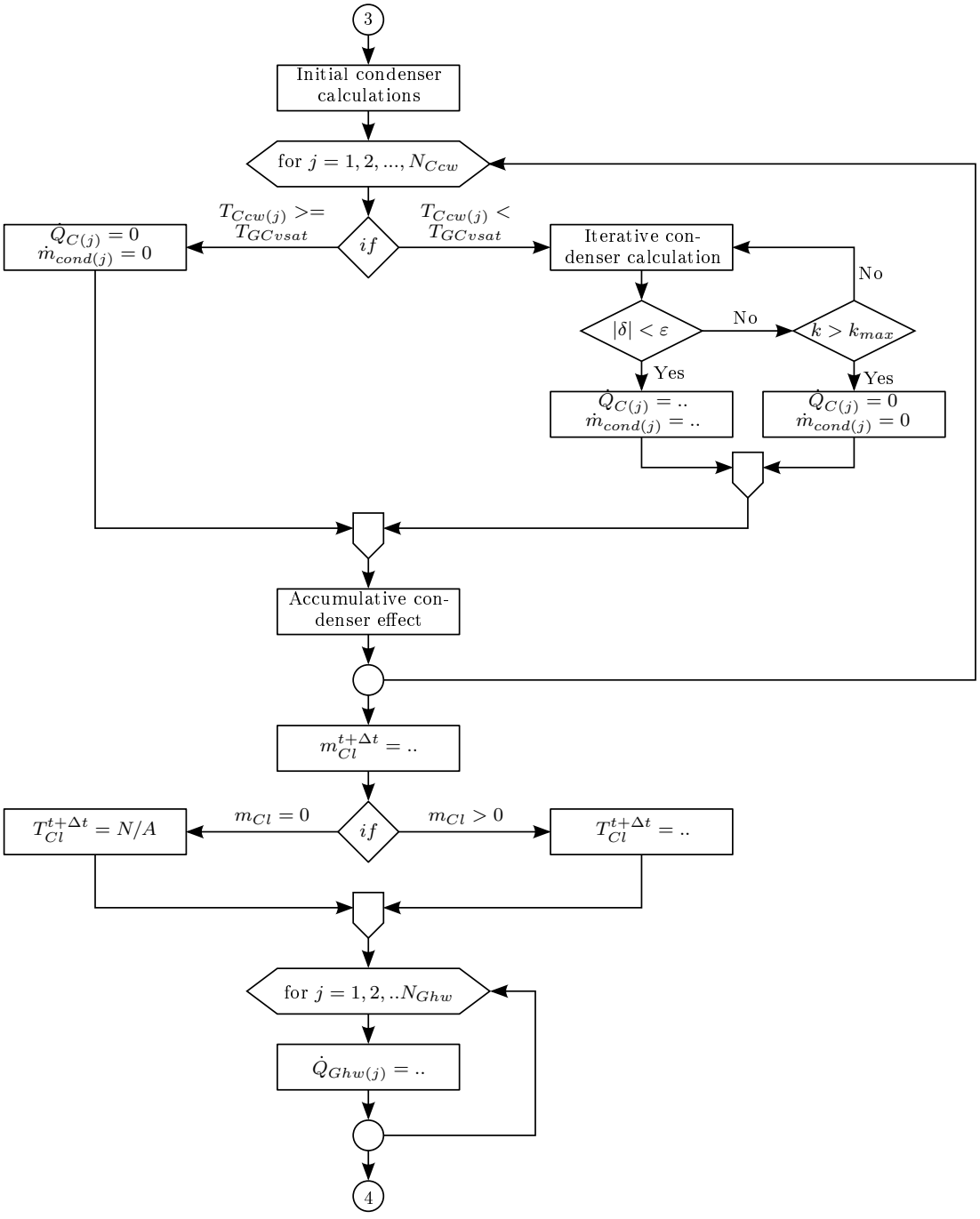

Figure B.3: Condensate film calculations as well as condensate pool

The next portion of the simulation flow diagram shows the manner in which the conditions of the generator and generator-condenser vapour space for the next time step were determined, as seen in Figure B.4. Sections 3.4 and 3.5 discuss the derivation of Equations 3.5.2 and 3.5.3.

Obtaining a solution to these equations was done through an iterative pro-

cess where the desired end result was the values for the mass, concentration and temperature of the generator solution at the next time step. The remainder of the values in the generator control volume could be determined as functions of these variables. Prior to performing the iterative calculation process the volume of the vapour space is updated by subtracting the liquid volumes from the total volume of the vessel.

The iterative calculation begins by assuming that the concentration in the solution is unchanged. Using this concentration value a temperature has to be obtained for the generator solution that will result in the right and left hand side of Equation 3.5.3 being equal. This is done by establishing bounds in which the simulation must search for a valid solution for the temperature. Once a temperature is obtained that satisfies Equation 3.5.3 a check has to be performed in order to confirm that the concentration that was used for the calculation corresponds with the concentration that is obtained from the conservation of mass and energy. If this comparison of these values does not meet the convergence criteria then the iterative calculation must be repeated with the new concentration value as the starting point of the calculation. This entire process is repeated until the concentration check in combination to the mass and energy checks are all satisfied.

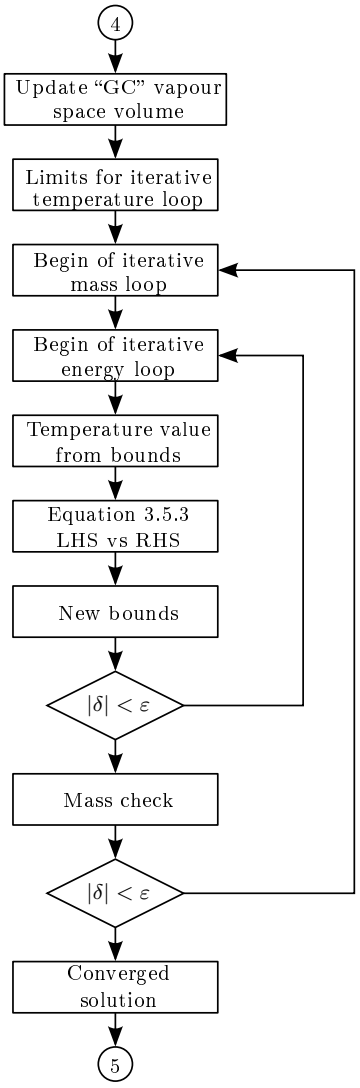

Figure B.4: Generator and common vapour space calculations

In the next section of the flow diagram a few of the internal flow rates are determined (Figure B.5). Starting with an evaluation concerning the possibility for mass to spill over from the evaporator liquid pool to the absorber liquid pool. Any excess mass that is present in the evaporator liquid section, above the user specified limit, flows over into the absorber solution section. The possibility for absorption to the absorber film and absorber solution pool is then evaluated according to the principles discussed in Section 3.6. Should the relevant components be active, through the component variables ("absorption_film"), and the conditions be appropriate then the rate of absorption to the absorber film as well as to the absorber pool are determined by applying Equation 3.6.1 to the respective conditions in the two vapour-

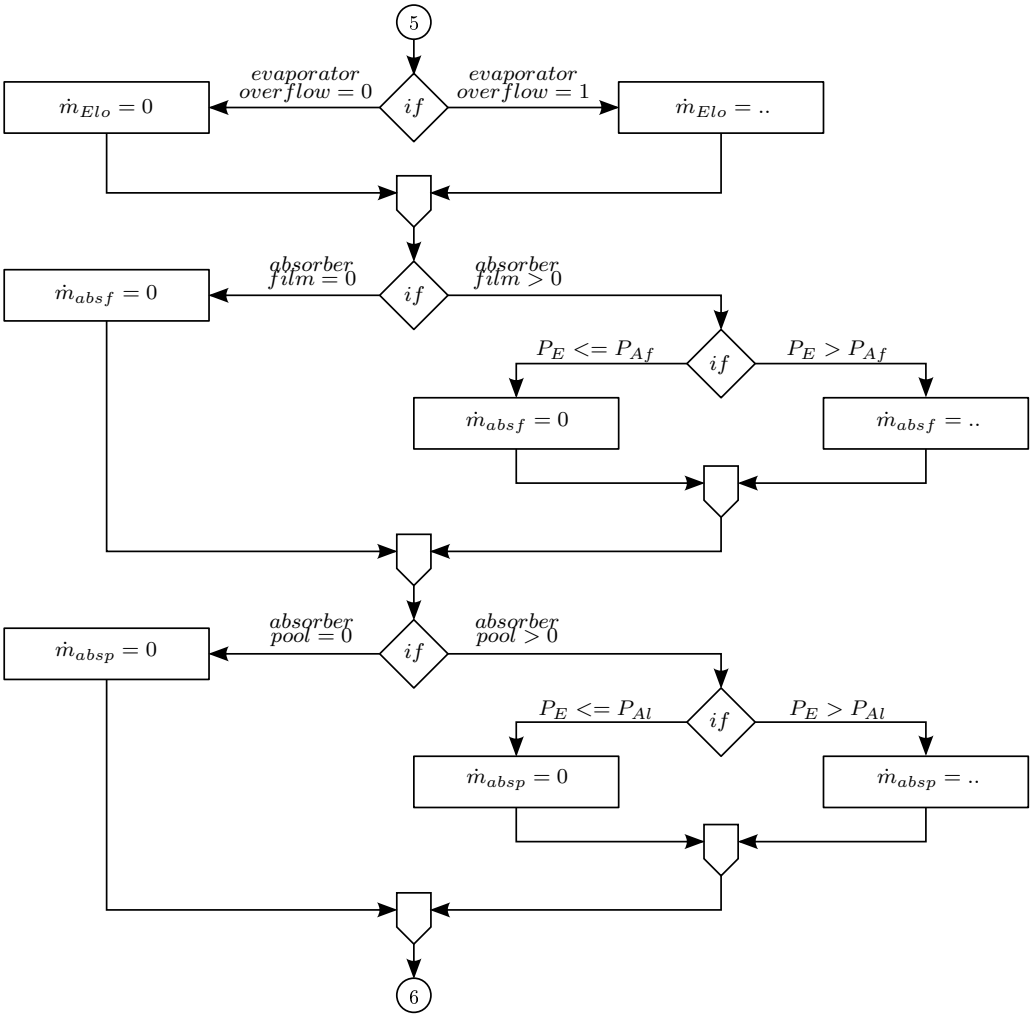

Figure B.5: Mass flow rates in the evaporator-absorber section

liquid interfaces.

Figure B.6 starts with a branch that checks if the absorber film is present in the simulation. If the absorber film is not included in the simulation then the absorber film variables are used as dummy variables through which the absorber inlet conditions are transferred directly to the absorber solution pool. Should the absorber film be included in the simulation then the simulation branches between the cooled and non-cooled scenarios for the absorber film. Thereafter the absorber film conditions for the next time step can be determined.

This portion of the flow diagram continues with the calculations concerning the amount of energy that is transferred to the evaporator liquid pool. Once this is complete the condition of evaporator load for the next time step can be determined.

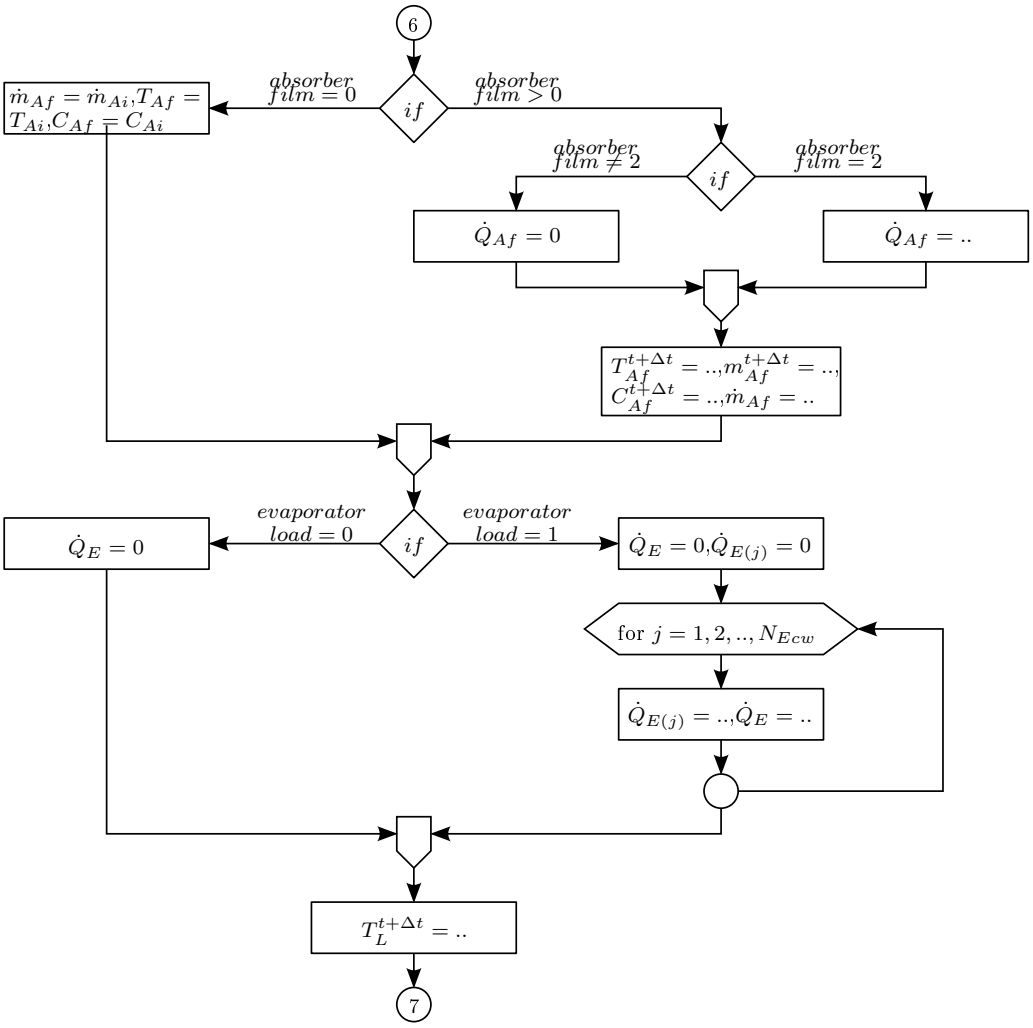

Figure B.6: New absorber film and evaporator load condition

Figure B.7 shows the last of the calculations that are included in the time loop. In preparation for the iterative calculation the volume of the vapour space was updated. The first section makes use of an iterative process to determine the condition of the evaporator for the next time step. This was done by establishing bounds in which the simulation had to search for a viable solution to Equation 3.6.19. Thereafter the possibility for the cooling of the absorber solution pool is evaluated, followed by the calculation of the absorber solution pool conditions for the next time step.

This leaves the simulation in a state where the current conditions have been used to determine the conditions of the simulation at the next time step. The "current" conditions are then assigned the values associated with the next time step. Thereafter, the simulation evaluates whether or not the end time has been reached and will either stop the simulation or return to the start of the time loop.

If any of the failure criteria are triggered in the operation of the simulation

a relevant message is written to the output file stating why the simulation was ended prematurely. Thereafter the runtime of the simulation is written to the output file and the simulation is complete.

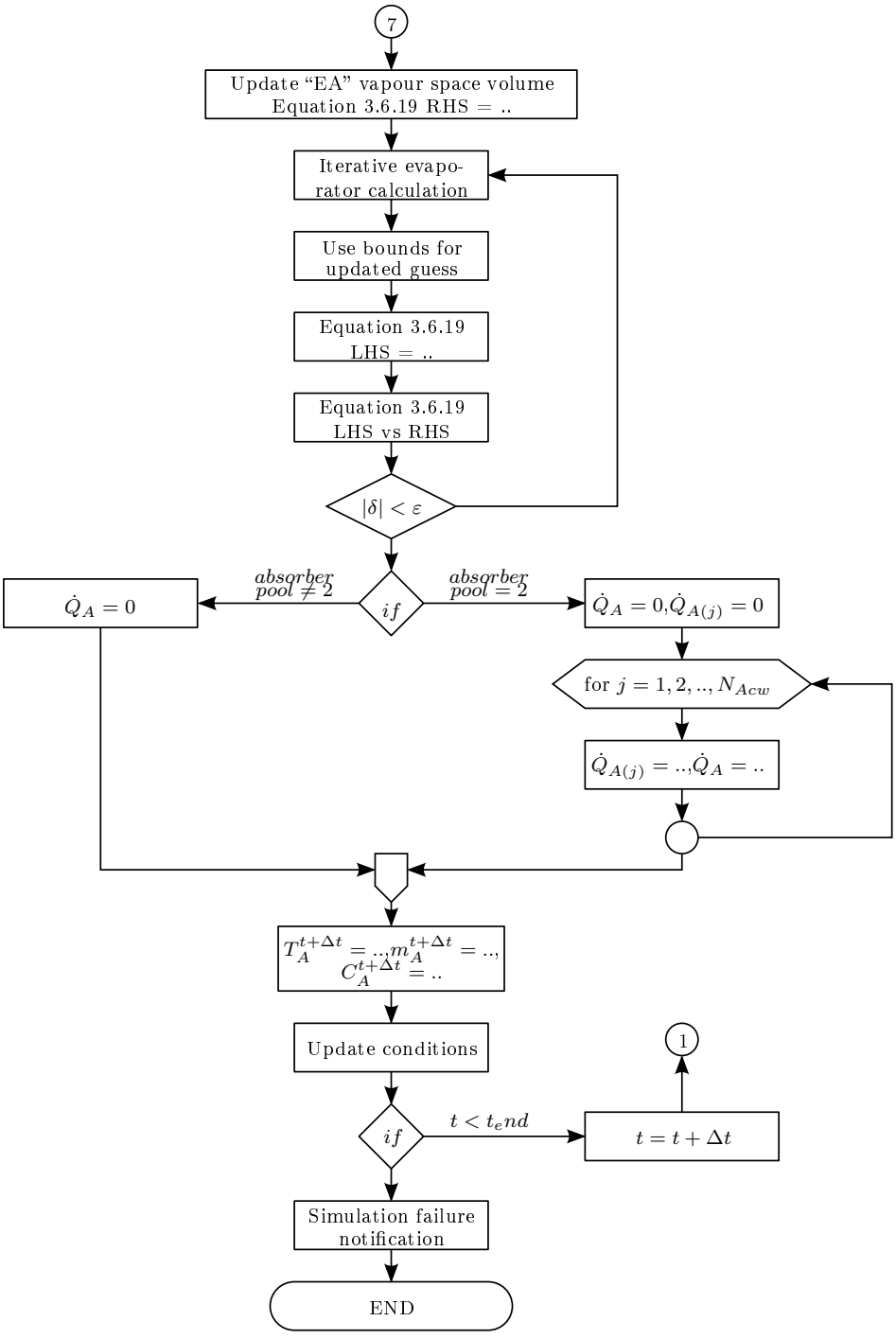

Figure B.7: Evaporator and absorber pool calculations

C Additional Simulation Discussions

This section of the report contains additional information concerning the theoretical model and simulations that were developed for this project. The manner in which the simulation handles the possibility of crystallization in combination with solution variable range is discussed. This is followed by discussions surrounding the method of calculation used for the simulation heat exchangers. Thereafter, the condenser theory is discussed followed by an alternate control volume diagram for the simulation.

C.1 Solution Limits and Simulation Failure Conditions

The property functions in combination with the behaviour of water/lithium-bromide made it necessary to place a number of checks in the simulation in order to ensure that the simulation did not exceed the bounds of the working fluid. These bounds for lithium-bromide/water come in two forms, the first of which is that the property equations for the pressure-temperature-concentration relationship, and to a lesser degree the enthalpy are only defined through a specific temperature and concentration range. The second limitation is that the nature of the salt solution is such that under specific conditions crystallization will occur which will compromise the integrity of the solution.

The limits associated with the property equations were incorporated by checking the condition of each concentration variable to determine if the concentration was approaching an undefined condition. When this feature was added to the simulation there were two evaluations checking the condition of the various solutions in order to warn the user that firstly, the composition was reaching an undefined region and secondly that the composition was undefined and the simulation entirely would be stopped. These conditions were triggered at 69.5% and 45.5% for the warning message and 69.9% and 45.1% for simulation failure. The inclusion of the property equations from Pátek and Klomfar (2006*b*) made these checks unnecessary as the newer equations are defined over a wider composition range (0 to 75%).

With regard to the limitations associated with the crystallization of the water/lithium-bromide solution, the simulation included a check for the condition of the solution that would stop the simulation if the solubility limit was

exceeded. This was initially incorporated via a curve fit of the crystallization line from the equilibrium chart for the solution. At each time step the temperature of the solution was used as the input for the curve fit and if the returned concentration was lower than the actual concentration then the solubility limit of the simulation had been exceeded. This process was kept for the final simulation, but the equation that described the solubility limit was replaced with the work of Pátek and Klomfar (2006*b*).

The manner in which the conservation of mass is implemented in the simulation makes it possible, that under incorrect operating conditions the mass of a control volume can become negative. While mathematically correct, a negative mass is not a realistic physical state. This scenario can be avoided entirely through operating the simulation under appropriate conditions. However, the decision was made to include failure criteria that would halt the operation of the simulation if the mass values in any of the control volumes became negative.

The condition in the evaporator is the focus of the last simulation evaluation into the condition of the system. This evaluation is performed in order to ensure that the pressure in the combined evaporator-absorber vessel does not decrease to such an extent that either of the two following scenarios are encountered. Firstly: the equations of state for the refrigerant are no longer valid. Secondly: the possibility for the formation of ice in the evaporator liquid is not a feature that was included in the simulation and must therefore be avoided.

C.2 Heat Exchanger Calculation Process

The calculation process for the system heat exchangers was first discussed in Section 3.3 with the assistance of Figure 3.2. This section expands on this explanation through the use of a flow diagram that discusses the process through which the heat exchanger calculations were performed in the simulation.

Figure C.1 shows the procedure that was followed for a general heat exchanger "X". Each heat exchanger has a user defined number of parallel pipes and each of these pipes is divided into a number of cells. The assumption is made that the conditions in all of the pipes is identical. This assumption can be seen in the calculations where the heat transfer effect of a single cell is multiplied by the number of pipes when taking into account the total effect of all of the pipes for the active section of the heat exchanger.

The boundary condition for the active heat exchanger cell is then evaluated in order to determine if the inlet is from the source stream or another cell. This is followed by the calculation of the cell conditions for the next time step which can be found in Section 3.3.

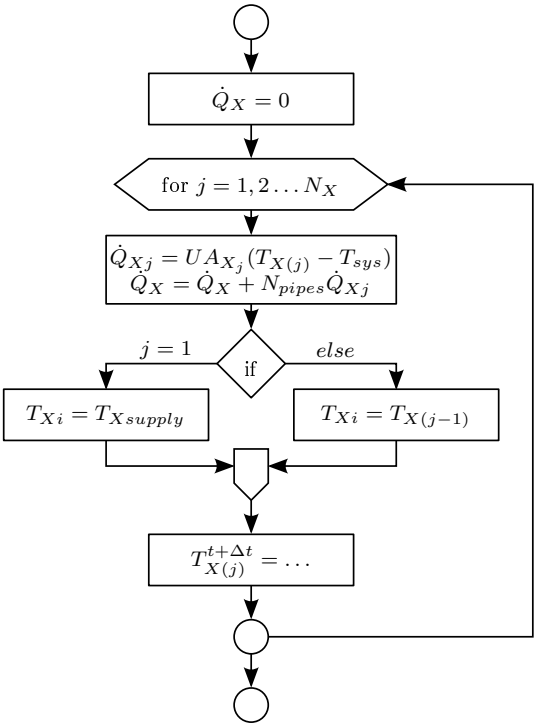

Figure C.1: General heat exchanger calculation process

C.3 Solution Heat Exchanger Calculation Process

This section will discuss the manner in which the solution heat exchanger was incorporated into the simulation of the vapour absorption cycle. The decision was made to simulate the solution heat exchanger with a tube-in-tube heat exchanger. Characterization of the heat exchanger was achieved through the declaration of values for the overall heat transfer coefficient, length, inner pipe dimensions and outer pipe dimensions. Thereafter, the heat exchanger was separated into a number of cells along its length, as seen in Figure C.2. Each heat exchanger cell was assigned temperature, mass and concentration values.

Three generalized equations for mass, concentration and temperature were established in order to determine the conditions in the solution heat exchanger for the next time step (Equations C.3.1 to C.3.3). These three equations were applied to the high and low temperature sides of the SHX. Accommodating the different directions in which the high and low temperature streams flow as well as the inlet conditions from the vessels was achieved by using temporary variables that would be used to feed the appropriate inlet conditions into the three equations. This is shown below in Figure C.3 where it can be seen that if the first cell of the SHX is being assessed the inlet conditions for the high temperature side are taken from the generator conditions. Similarly, if the last

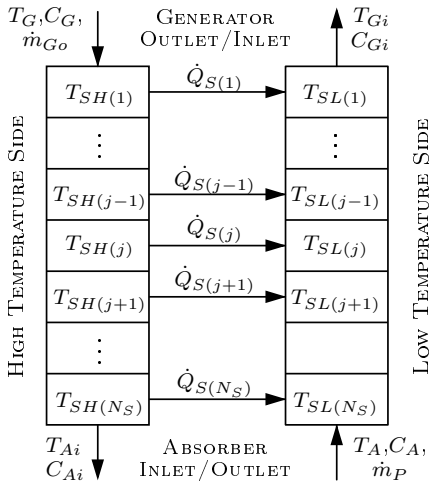

Figure C.2: Heat exchanger with cells

cell is being assessed the inlet conditions for the low temperature side is taken from the absorber conditions. In the default state where one of the inner cells is being assessed the inlet conditions for the high temperature side are taken from one cell backwards $(j-1)$ while the low temperature inlet conditions are obtained from one cell further $(j+1)$. Once the inlet conditions for the cell are established the heat transfer rate between the high and low side is evaluated in addition to the accumulative effect of the SHX for the current time step.

The decision was made to assume that the mass present in each heat exchanger control volume would remain the same throughout the simulation. While this would not be entirely correct, the complexity of incorporating a method to adjust the mass based on any changes in density of the solution was deemed excessive for the application. This assumption to work with a constant mass in each heat exchanger cell simplified the calculations that were required in order to update the conditions of the heat exchanger as no calculations would be necessary to determine the mass in the SHX cells for the next time step. This assumption can be extended by assuming that at each time step the inlet and outlet mass flow rates for each cell is the same.

These assumptions were first applied via the conservation of mass in order to obtain a generalized equation for the concentration in either the high or low temperature side of the SHX at the next time step. This can be seen below in Equation C.3.1 where the "X" notation is a place holder for either SH or SL:

$$C^{t+\Delta t}_{X(j)} = C^{t}_{X(j)} + \Delta t \dot{m}_X (C_{Xi} - C_{X(j)})/m^{t}_{X(j)} \tag{C.3.1}$$

A similar approach was used in order to obtain a generalized equation for the temperature at the next time step. This can be seen below in Equations C.3.2 and C.3.3:

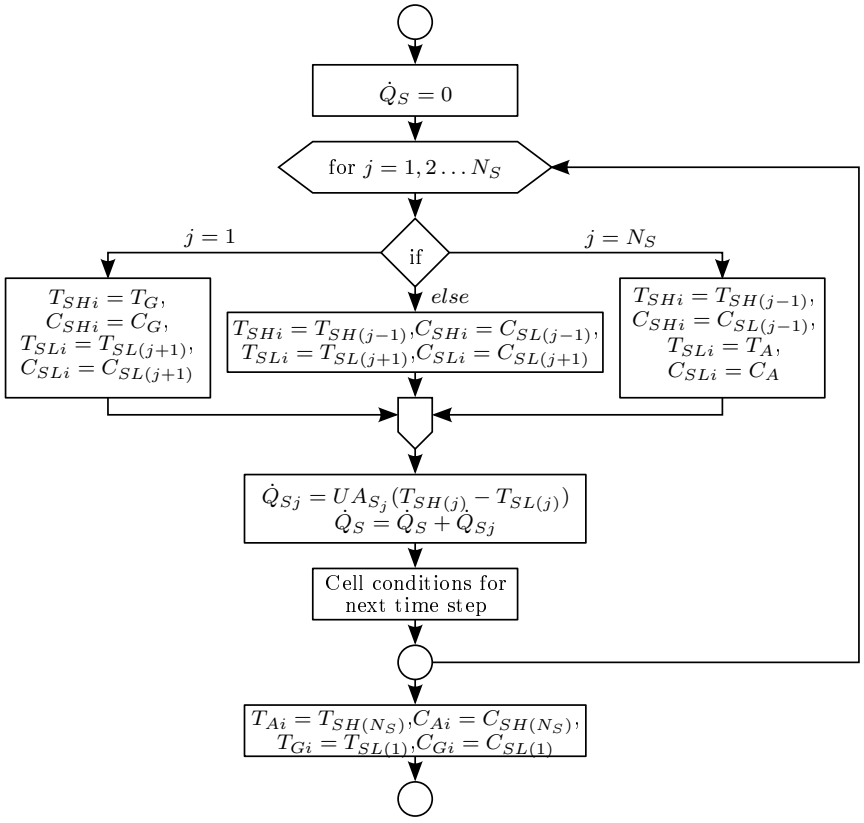

Figure C.3: Solution hat exchanger calculation process with boundary condition evaluation

$$h^{t+\Delta t}_{X(j)} = h^{t}_{X(j)} + \Delta t(\dot{m}_X h_{Xi} \pm \dot{Q}_{Sj} - \dot{m}_X C_{X(j)})/m^{t}_{X(j)} \tag{C.3.2}$$

$$T^{t+\Delta t}_{X(j)} = h_{sol}\{h^{t+\Delta t}_{X(j)}, C^{t+\Delta t}_{X(j)}\} \tag{C.3.3}$$

This concludes the discussion surrounding the simulation of the solution heat exchanger.

C.4 Condenser Theory and Calculation Process

This section will discuss the theory that was used in the condenser calculations that were used to determine the rate of condensation in the generator-condenser section of the simulation. There are a number of manners in which this calculation can be dealt with, but the decision was made to make use of the Nusselt theory for condensation. In addition to this, the wall temperature of the heat exchanger would not be assumed or supplied, but would have to be determined through an iterative approach.

Figure C.4 shows the cross section of a horizontal pipe upon which condensation is taking place. This figure will be used to facilitate an explanation

with regards to the variables that were used and convergence criteria that determined the success or failure of an iteration.

The path through which energy is transferred from the vapour (T_{GCvsat}) to the cooling stream (T_{Ccw}) is described by three thermal resistances that represent the characteristics of the path through which the energy must travel. This can be represented mathematically in the following equation:

$$\dot{Q}_C = \frac{T_{GCgsat} - T_{Ccw}}{R_{Ci} + R_{Cw} + R_{Co}} \tag{C.4.1}$$

where R_{Ci} represents the thermal resistance, due to forced convection in a tube, between the bulk cooling water temperature (T_{Ccw}) and the inner wall temperature (T_{Wi}). R_{Cw} describes the thermal resistance, between T_{Cwi} and T_{Cw}, due to conduction through the tube wall and R_{Co} captures the external convective thermal resistance.

Equation C.4.2 shows the manner in which R_{Ci} is calculated:

$$R_{Ci} = \frac{1}{2\pi L h_i} \tag{C.4.2}$$

The length of the tube being assessed is included through the length term (L). The remaining term h_i refers to the heat transfer coefficient for internal forced convection. This heat transfer coefficient can be described by the thermal conductivity (k) of the fluid in the tube, the internal diameter (D) and the Nusselt number (Nu) in the following manner:

$$h_i = \frac{k}{D} Nu \tag{C.4.3}$$

The behaviour of the fluid that is flowing in the tube can be described by the Reynolds number ($Re = \rho V D/\mu$). This dimensionless number characterises the flow regime that is present in the heat exchanger tube. The manner in which the Nusselt number is calculated is dependant on the value that is

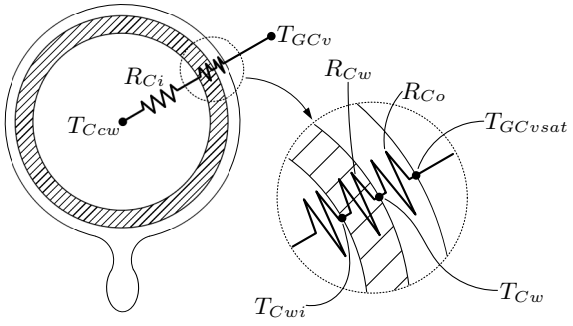

Figure C.4: Condenser film schematic

obtained from the Reynolds number and this is shown below:

$$Nu = \begin{cases} 3.66 & \text{if } Re < 2300, \text{Laminar flow} \\ 0.023 Re^{0.8} Pr^{0.4} & \text{if } Re \geq 2300 \end{cases}$$

The thermal resistance for conduction through the wall of a tube can be described in the following manner:

$$R_{Cw} = \frac{ln(r_o/r_i)}{2\pi L k_{wall}} \tag{C.4.4}$$

where physical characteristics of the tube are included in the calculations through the external (r_o) and internal (r_i) radii as well as the length (L) of tube being assessed. In addition to this, the material properties are included through the thermal conductivity of the tuber material via k_{wall}.

This leaves Equation C.4.1 with one remaining unknown thermal resistance, R_{Co}. Solving for this thermal resistance requires an iterative process as the heat transfer coefficient, that it is dependent on, is a function of the unknown outer wall temperature T_{Cw}.

The process of solving the heat transfer coefficient h_{Co} and subsequently R_{Co} starts by making an assumption for the wall temperature T_{Cw}. This guessed wall temperature is then used to calculate the film temperature in the following manner:

$$T_{film} = (T_{Cw} + T_{GCvsat})/2$$

The fluid properties (ρ_f,ρ_g,h_{fg},k_f,μ_f) of the condensate can then be assessed at the film temperature. A modification to the enthalpy of vaporization is necessary for the Nusselt theory. This modification can be done in two different ways which are dependant on the state of the vapour as shown below:

$$h^*_{fg} = \begin{cases} h_{fg} + 0.68 c_{pf}(T_{GCsat} - T_w) & \text{if vapour is saturated,} \\ h_{fg} + 0.68 c_{pf}(T_{GCsat} - T_w) + c_{pg}(T_{GCv} - T_{GCsat}) & \text{if vapour is superheated} \end{cases}$$

It is now possible to determine the unknown heat transfer coefficient h_{Co} in the following manner:

$$h_{Co} = 0.729 \left[\frac{g\rho_f(\rho_f - \rho_g)h^*_{fg}k_f^3}{\mu_f(T_{GCvsat} - T_{Cw})D} \right]^{1/4}$$

The outer thermal resistance can now be determined in the following manner:

$$R_{Co} = \frac{1}{h_C A_{Co}}$$

A check must now be performed in order to determine if the wall temperature that was used was the correct wall temperature. This check was performed by comparing the result obtained from C.4.1 with the result obtained

from C.4.5 and C.4.6 as seen below:

$$\dot{Q}_C = \frac{T_{Cw} - T_{Ccw}}{R_{Ci} + R_{Cw}} \tag{C.4.5}$$

$$\dot{Q}_C = \frac{T_{GCvsat} - T_{Cw}}{R_{Co}} \tag{C.4.6}$$

If the wall temperature that was used is correct then all three of the equations that described the rate of heat transfer will give the same result. However, if this is not the case then the calculation needs to be repeated with a better guess for the wall temperature. Once a wall temperature has been obtained that satisfies the convergence criteria then the rate of condensation can be determined in the following manner:

$$\dot{m}_{cond} = \dot{Q}_C / h^*_{fg} \tag{C.4.7}$$

In the vapour absorption cycle simulation the condenser heat exchanger is broken up into a number of cells and this condenser calculation is performed on each of these cells in order to determine the accumulative effect of the complete heat exchanger. There are however limitations placed on the calculation in the simulation. Firstly, the iterative condenser calculation is only taken into consideration when the vapour temperature is higher than the condenser cooling stream flowing in the heat exchanger. Secondly, a limit is placed on the number of iterations that can be attempted in order to find a viable wall temperature for each cell. If the simulation cannot find a wall temperature within the iterative limitations then the calculation is considered to be unsuccessful and no energy transfer or condensation will occur for the cell being assessed at the specific time step. This is shown in a flow diagram form in Appendix B, Figure B.3.

C.5 Extensive Control Volume Diagram of a Vapour Absorption System

The control volume diagram shown in Figure C.5 was the starting point of the control volume diagram discussed in Section 3.2. This version of the system control volume diagram includes many terms for internal heat and mass transfer that were removed in an effort to streamline the simulation into a more attainable goal. The formulation of the equations that describe the various components make it possible to work towards the inclusion of any or all of the additional terms that are indicated, if their inclusion is deemed necessary.

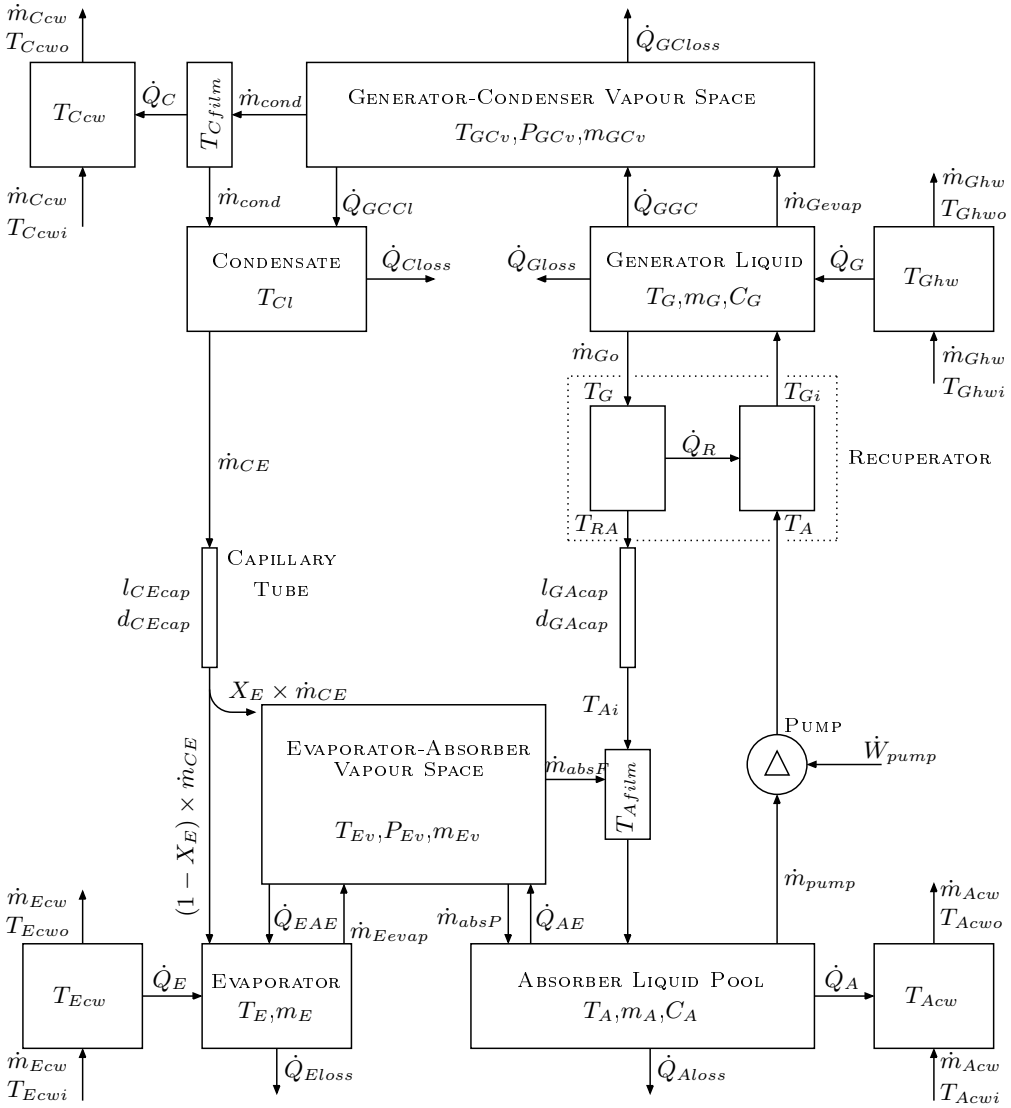

Figure C.5: Extensive model of a lithium-bromide/water vapour absorption system

D Extended Absorber – Evaporator Operating Conditions

It was not feasible to include in the main body of the report a discussion concerning all of the possible operating configurations for the final absorber-evaporator simulation. The absorber-evaporator configuration in question was discussed in Section 3.6.4 and contains variables that configure the state of the absorber solution pool and film. Both of these "parts" can be at three different states, which are: "0" – disabled, "1" – enabled and "2" – enabled with cooling.

There is however a difference between "disabling" the functionality of the absorber pool and the absorber film in the sense that in a physical apparatus it would be possible to remove the surface upon which the absorber film would form. While, in the case of the absorber pool it would not be possible to prevent a pool of solution that is at an appropriate temperature and concentration from absorbing vapour. Therefore, the options where the condition of the pool is set to "0" will not be considered for further discussion. In addition to this, the two configurations that were previously discussed in the main body of the report will not be covered again in this section. These two points are shown in Table D.1, where the possible absorber-evaporator combinations are shown.

The only variation between the six discussed configurations will be the state of the absorber film and pool as well as the simulation time. The external load, external stream, initial conditions and physical characteristics will all remain the same throughout. These general conditions are shown in Table D.1.

Furthermore, functionality was not added to the simulation to accommodate for a scenario where the saturation pressure of a solution is larger than the vapour pressure. Under such conditions the vapour-liquid interfaces are considered to be inactive and will only reactivate if the conditions are conducive to absorption in accordance with Equation 3.6.1.

Figure D.1: Absorber-evaporator configurations

Absorber Pool	Absorber Film	Location of Discussion
0	0	Not viable, no discussion
0	1	Not viable, no discussion
0	2	Not viable, no discussion
1	0	Appendix D.1
1	1	Appendix D.2
1	2	Appendix D.4
2	0	Section 3.6.3
2	1	Appendix D.3
2	2	Section 3.6.4

Table D.1: Initial conditions and constants for all absorber-evaporator states

Absorber Liquid Pool	
T_A	20 °C
C_A	0.5 kg/kg
m_A	5 kg
Absorber Film	
T_{Af}	20 °C
V_{Af}	0.001277 m^3
C_{Af}	0.5 kg/kg
Absorber Cooling	
T_{Acw}	25 °C
$U_A A_A$	300 W/°C
$U_{Af} A_{Af}$	100 W/°C

Common Vapour Space	
T_{AEv}	20 °C
V_{AEt}	1.3 m^3
Vapour-Liquid Interface	
k_{absP}	0.0002
A_{absP}	0.25 m^2
k_{absF}	0.0005
A_{absF}	0.68 m^2
Solution Inlet	
$\dot{m}_{Ai}$	0.012 kg/s
T_{Ai}	50 °C
C_{Ai}	0.54 kg/kg
Solution Outlet	
$\dot{m}_{Ao}$	0.013 kg/s

Evaporator Liquid Pool	
T_{El}	20 °C
m_{El}	5 kg
Evaporator Load	
$U_E A_E$	250 W/°C
$\dot{m}_L$	0.5 kg/s
T_L	20 °C
m_L	100 kg
Refrigeration Inlet	
$\dot{m}_{Ei}$	0.001 kg/s
h_{Ei}	104838 J/kg
Simulation Parameters	
Δt	0.01 second

D.1 Configuration "1-0"

In configuration "1-0" there is no cooling possible in the absorber pool and there are no surfaces upon which the solution inlet can form a film. The purpose of the evaporator-absorber configuration to cool an external load is not met as only a small amount of energy is transferred from the load, see Figure D.2. This can be attributed to the absence of cooling for the absorber as the condition of the absorber liquid is only compatible for absorption from the vapour for a small period of time.

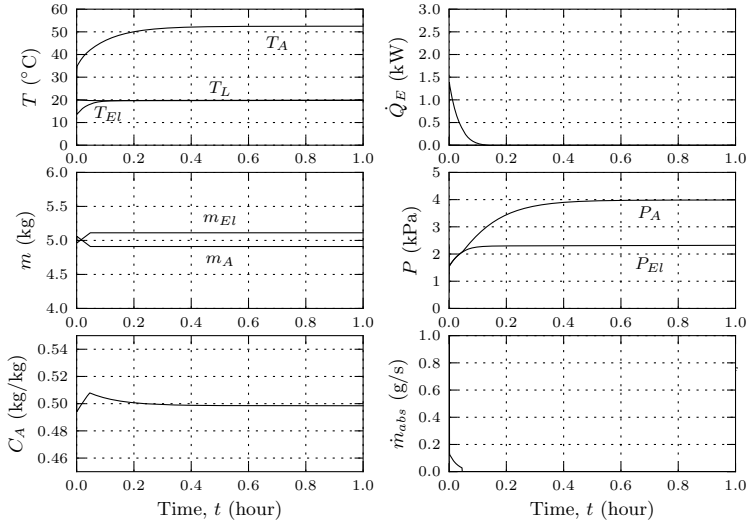

Figure D.2: Absorber-evaporator simulation results when operating in a "1-0" configuration

D.2 Configuration "1-1"

The "1-1" configuration adds a surface upon which a film of solution can form. However, under these conditions no absorption would take place in the film and even if absorption took place it would only occur briefly. This is due to the manner in which the film conditions would quickly reach the inlet stream conditions.

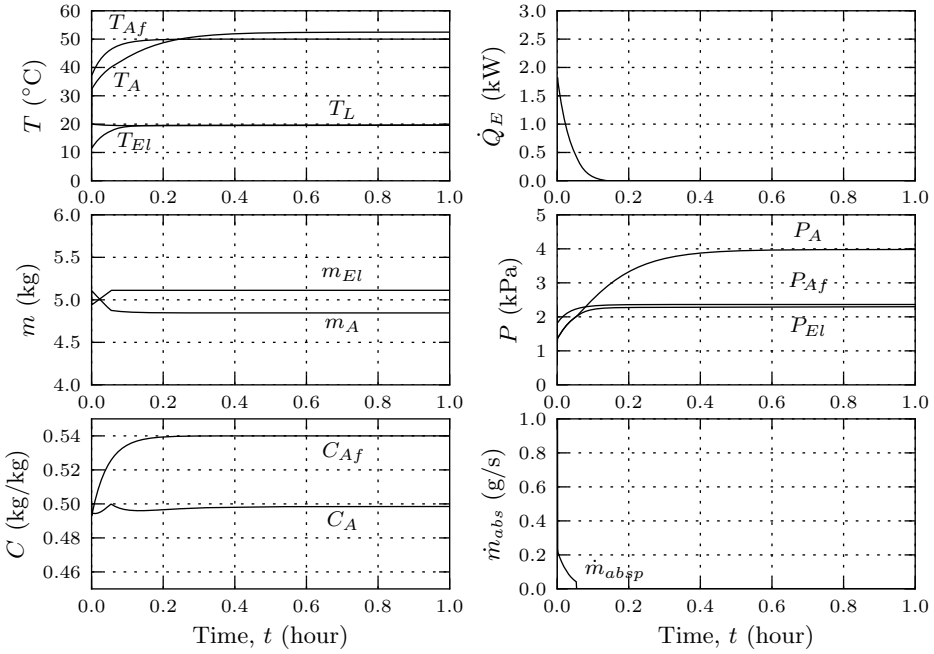

Figure D.3: Absorber-evaporator simulation results when operating in a "1-0" configuration

D.3 Configuration "2-1"

The inclusion of a film without cooling into a configuration that has a cooled liquid absorber pool has no discernible effect on the operation of the configuration beyond slightly delaying the effect that the solution inlet has on the absorber liquid condition. Comparing the result of this configuration, as seen in Figure D.4, with the "2-0" configuration discussed in Section 3.6.3 shows that the inclusion of a film without cooling serves no useful purpose and might as well have been excluded.

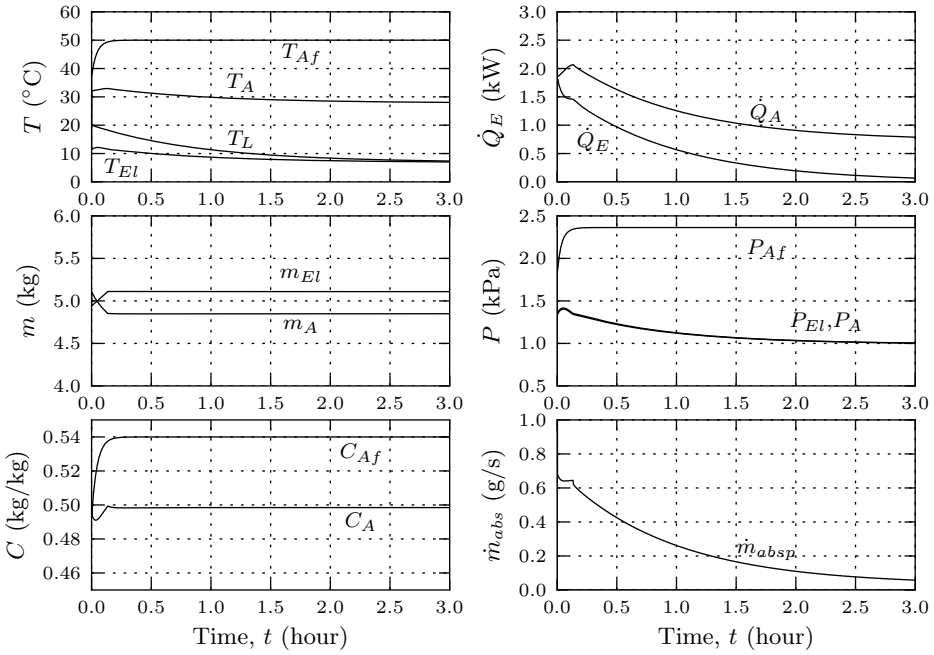

Figure D.4: Absorber-evaporator simulation results when operating in a "2-1" configuration

D.4 Configuration "1-2"

It was discussed in Section 3.6.3 that there were three possible absorber-evaporator configurations that were viable for use in a continuous vapour absorption cycle. Section 3.6.3 discusses the "2-0" configuration where a pool of solution is cooled for the purpose of vapour absorption and Section 3.6.4 discusses the "2-2" configuration where a cooled film is used in conjunction with a cooled pool. The last viable configuration is discussed in this section and

this configuration is the "1-2" configuration where the physical characteristics of an apparatus would have to be conducive to the formation of a film that has access to a source of cooling. In addition to this, a pool of solution would inevitably form at the bottom of the vessel, but would not have access to an external source of cooling.

Without access to cooling the condition of the solution pool will not be conducive to the absorption of vapour and due to this the condition of the solution pool is dependent on the condition of the film and the refrigerant overflow from the evaporator liquid pool.

Figure D.5 shows that the condition of the solution film and the interaction between the film and the vapour facilitates the absorption at a rate and temperature that fulfils the goal of cooling the external load. In this configuration the temperature and concentration of the absorber pool is dependent on the condition of the film and the overflow from the evaporator.

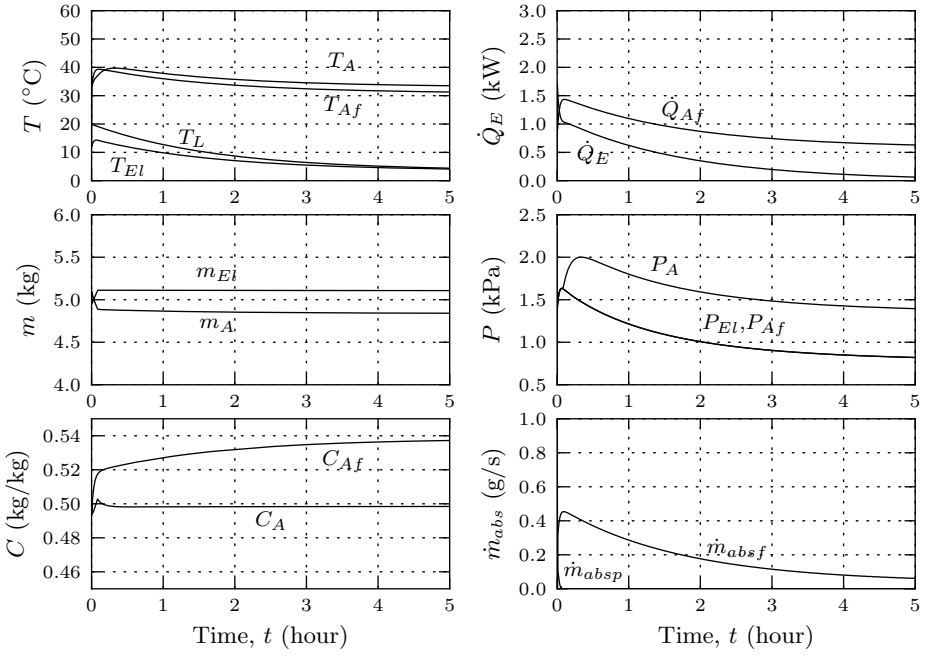

Figure D.5: Absorber-evaporator simulation results when operating in a "1-2" configuration

D.5 No Absorber Cooling

The absorption that takes place in the first absorber-evaporator configuration, that was discussed in Section 3.6.1, comes to a halt very quickly when there is no source of cooling provided for the liquid solution in the absorber section. This is shown in Figure D.6 where equilibrium is reached quickly through a short amount of absorption.

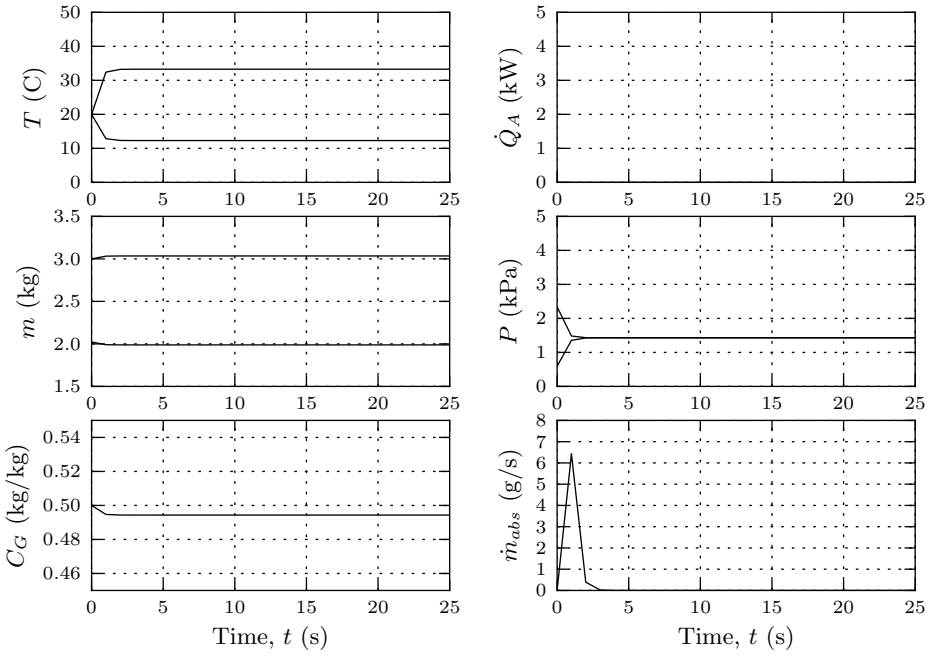

Figure D.6: Behaviour of basic absorber-evaporator configuration without any cooling

D.6 Formation of Ice

The simulation can also cease to function when the saturation pressure of the solution decreases to such an extent that the associated saturation temperature for the refrigerant is nearing freezing conditions. While this scenario can be encountered, it is unlikely to occur when operating the cycle at typical conditions. Conditions were chosen to force an occurrence of this scenario by lowering the temperature of the absorber cooling stream to 20 ℃ and increasing the mass of liquid solution present in the absorber to 10 kg. In doing so, the absorption of refrigerant does not have any significant impact on the concentration and the absorber cooling stream lowered the absorber solution

temperature such that the saturation pressure decreased sufficiently. This can be seen below in Figure D.7:

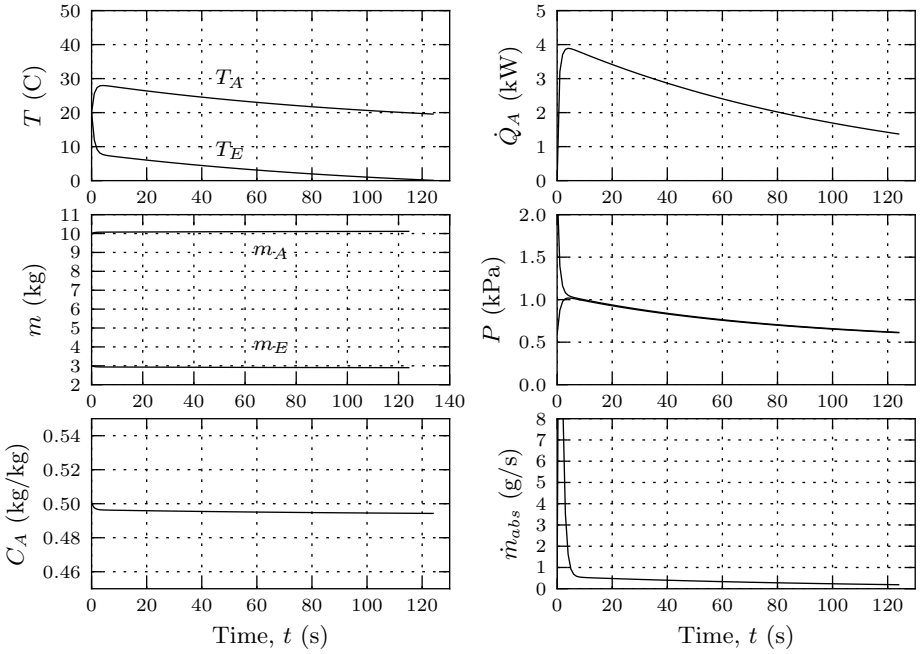

Figure D.7: Behaviour of the absorber-evaporator combination under conditions selected to drastically reduce the pressure

E Vapour Compression vs Vapour Absorption

Introducing the concept of refrigeration through vapour absorption can be approached by examining a basic representation of a generalized refrigeration cycle as shown in Figure E.1. This refrigeration cycle provides for refrigeration through the evaporation of a low temperature liquid refrigerant. The condition of the evaporated refrigerant has to be elevated in pressure and temperature to the high pressure portion of the cycle. Once at a higher pressure it is now possible to condense the refrigerant by exposing it to a temperature that is lower than the high pressure vapour, but higher than the evaporator temperature. The liquid refrigerant can then return to the evaporator through a throttling device and the cycle can repeat itself.

The relevance of this example is that the encompassing principles of the more commonly known vapour compression cycle and the vapour absorption cycle both make use of this generalized component configuration. However, what defines the difference between these two technologies is the manner in which the condition of the refrigerant vapour is raised from the low pressure evaporator section to the high pressure condenser section.

Figure E.2 shows the fundamental components that these two different methods require to facilitate the process that will raise the pressure and temperature of a stream of refrigerant vapour. In the case of the vapour compression process, Figure E.2a, an electrical motor is used to drive a compressor. This compressor mechanically raises the pressure and temperature of the evaporated refrigerant to a higher state where it is suitable for condensation. In contrast to this, the driving energy that powers the vapour absorption components, Figure E.2b, is a source of heat and while this thermal energy can be

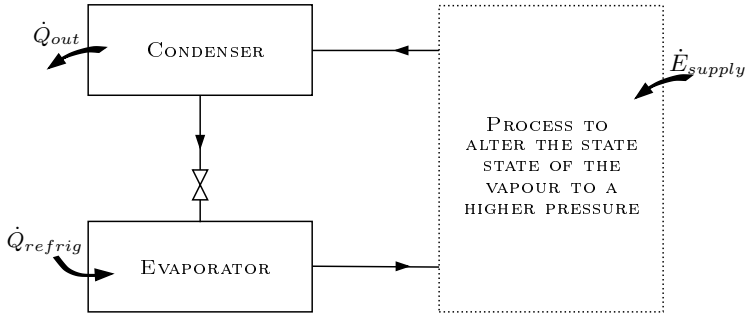

Figure E.1: Generalized refrigeration cycle

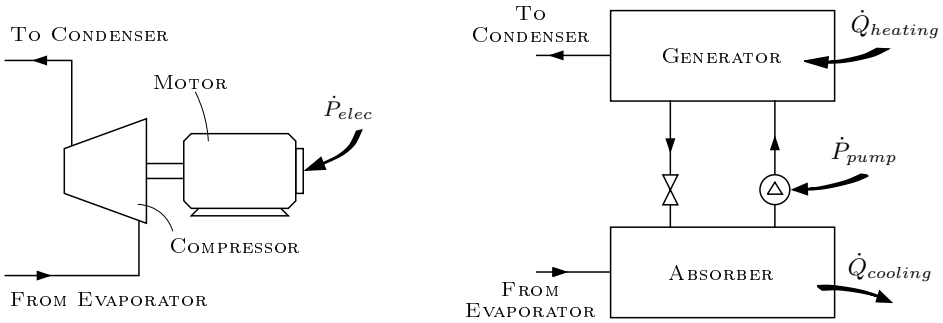

(a) Compression (b) Absorption

Figure E.2: Comparison of components used for the conditioning of refrigerant vapour through a compression and absorption process

supplied through electrical heaters there is a wide variety of possible sources for heat that can used to fuel the vapour absorption components. Emphasis has been placed on the thermal energy used to drive the vapour absorption components, but the vapour absorption components require additional external interfaces in order to operate. These two external interfaces are the cooling required in the absorber component, at a similar temperature to that used in the condenser component, and the electrical energy requirement of a small pump. This pump is referred to as being "small" due to the relative energy requirements of the generator and condenser when compared with the pumping requirements. A more detailed explanation into the operation of a vapour absorption cycle will be discussed in the remainder of this chapter.

F Thermocouple Calibration

An "Agilent Data Acquisition Unit" was used in conjunction with T-type thermocouples for temperature measurement and logging. This section will continue with a discussion concerning the manner in which the accuracy of the various thermocouples was evaluated. The thermocouples were calibrated through the use of the following equipment:

- Fluke 9142 Field Metrology Well
- HP 34401A Multimeter (STB S/N 247446)
- Platinum RTD
- Agilent 34970A Data Acquisition Unit (STB A/N 380114)
- Agilent 34901A 20 Channel Multiplexer(STB A/N 429532)
- Agilent 82357B USB-GPIB Interface (STB A/N 422430)

The conversion from resistance to temperature for the reference platinum RTD was performed through the application of the following supplied equation:

$$T = 0.00111611\Omega^2 + 2.326521202\Omega - 243.7648049 \qquad \text{(F.0.1)}$$

The equipment functions in the following manner: The Fluke controls the temperature of an aluminium bar to a user defined temperature. Thermocouples are inserted into the aluminium bar making it possible to compare the Fluke temperature to the thermocouple temperature measurement on the Agilent. In additional to this, a platinum RTD is inserted into the aluminium bar and the resistance reading from the HP multimeter can be used as a secondary point of reference.

The Agilent temperature measurements as well as the RTD resistance measurements were documented while the Fluke temperature was adjusted from 10 ℃ to 100 ℃ in increments of 15 ℃. The resulting data obtained from this showed that there was a large discrepancy in the data. While the Fluke and the Agilent values were similar, there was a difference of at least 3.5 ℃ between the converted RTD values and the Fluke.

It was decided that the accuracy of the multimeter would be evaluated as a certificate of calibration was included with the RTD. Only after this problem was encountered was it discovered that the Fluke could also be used to measure the RTD resistance values. This lead to a comparison being made between the

Table F.1: Comparison of RTD resistance measurement method

	Heat Source			
	Fluke @ 100 ℃		Kettle	
RTD	Ω	℃	Ω	℃
Fluke	138.437	99.702	138.553	100.007
HP	139.940	103.665	140.130	104.166

RTD resistance values as measured by the multimeter and the Fluke based on two source temperatures. The results from this evaluation can be seen in Table F.1. It can be seen that the converted resistance values show that there is roughly a 4 ℃ difference between the converted RTD readings when taken with the multimeter and those taken with the Fluke. Due to this, the RTD data that was originally captured during the calibration process was discarded.

The decision was made to continue the calibration process without using any RTD measurements as this would have required repeating all of the measurements with the RTD connected to the Fluke. The calibration continued by importing the Agilent and Fluke measurements into a Python script, where the purpose of this script was to calculate the coefficients for each thermocouple such that the coefficients would adjust the raw Agilent values with a gradient and offset in order to makes the readings more accurate.

The results of the thermocouple calibration process can be seen on the following pages where the data for each thermocouple was plotted in a separate sub-figure. Each thermocouple sub-figure contains two sets of measurements, where the error between the raw Agilent data is plotted with circles and crosses and the adjusted measurements retain the respective colour but are plotted with a solid line. It can be seen that the calibration process was successful in the sense that there is an overall improvement between the raw thermocouple data and the corrected values. The coefficients that were calculated for the correction of the raw Agilent temperatures are shown after the graphs.

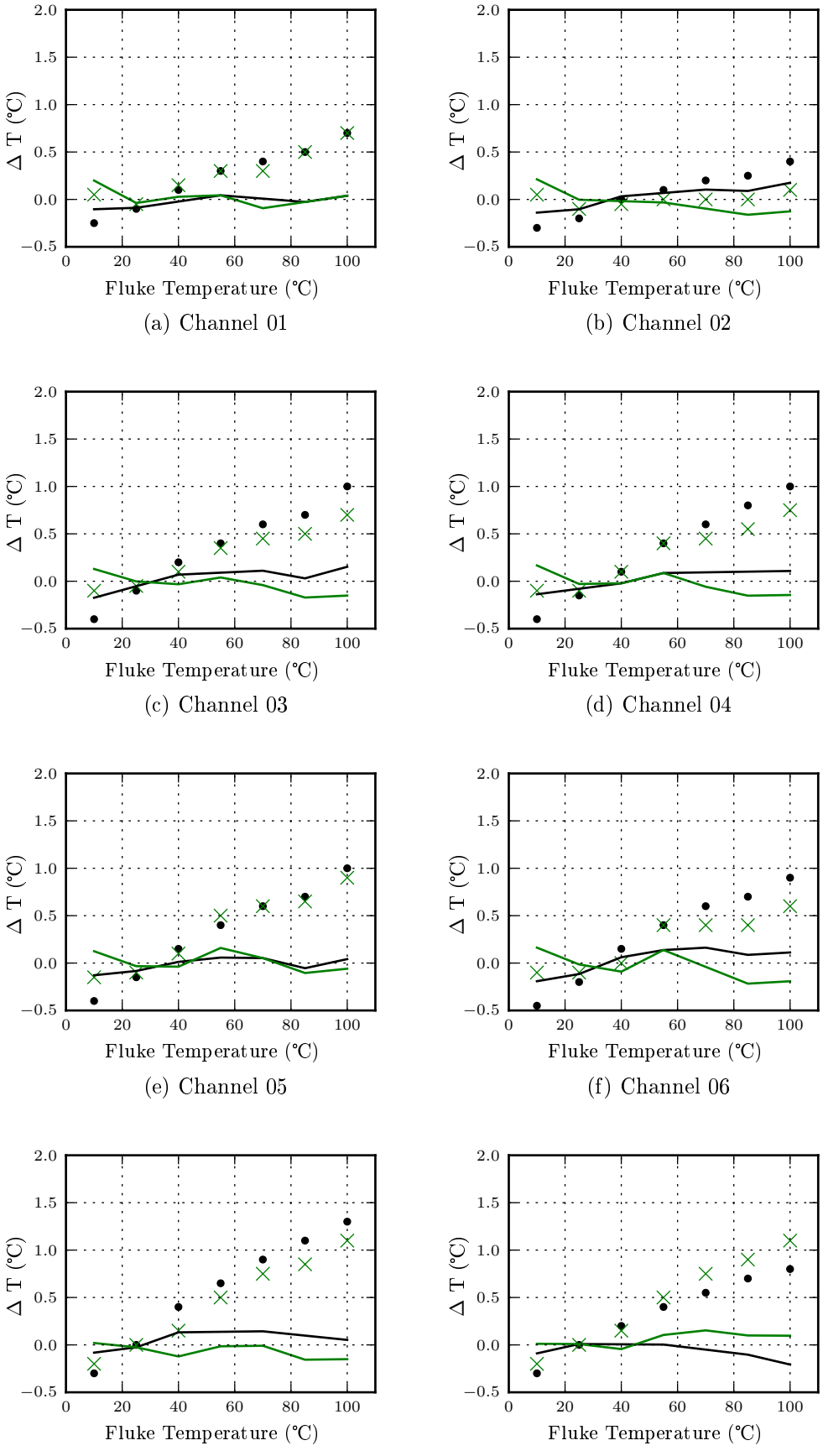

(a) Channel 01 (b) Channel 02

(c) Channel 03 (d) Channel 04

(e) Channel 05 (f) Channel 06

(g) Channel 08 (h) Channel 09

Figure F.1: Temperature difference between Agilent and Fluke plotted vs Fluke temperature with corresponding corrected curve

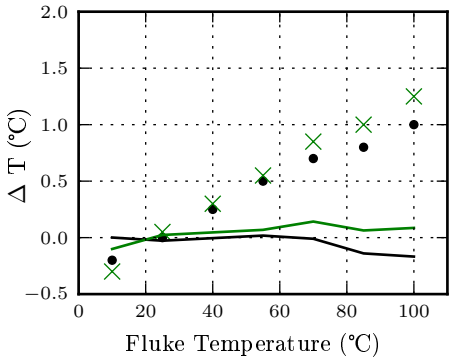

(i) Channel 10

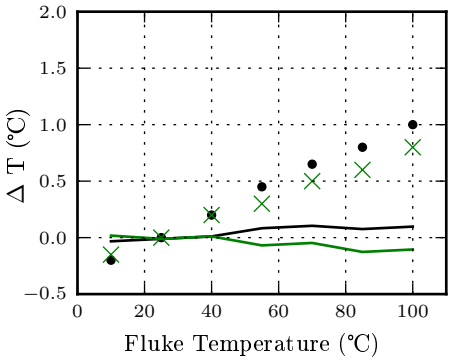

(j) Channel 11

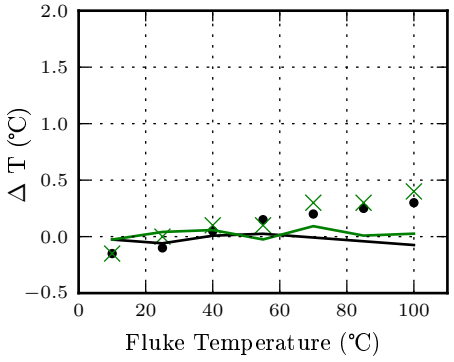

(k) Channel 12

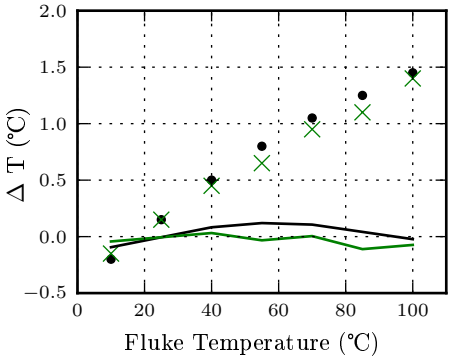

(l) Channel 13

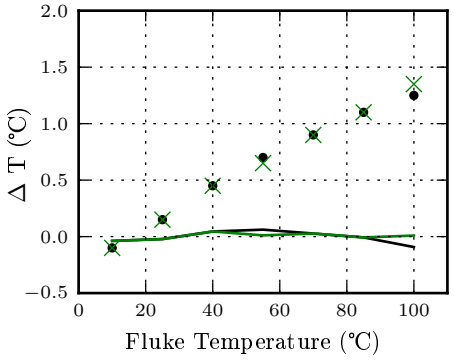

(m) Channel 14

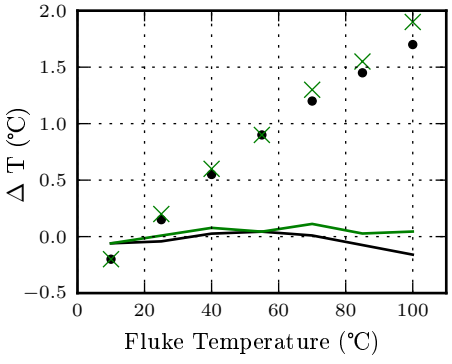

(n) Channel 15

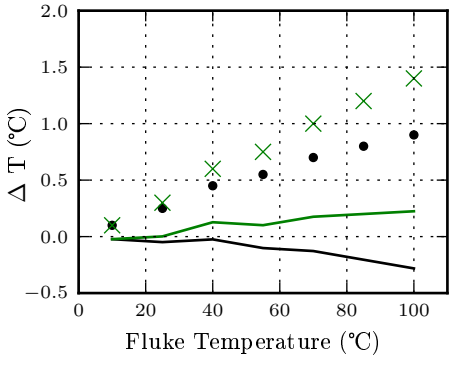

(o) Channel 16

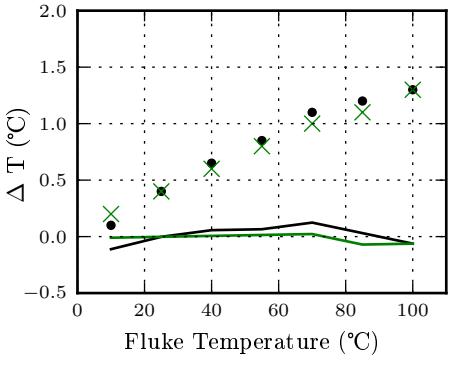

(p) Channel 17

Figure F.1: Temperature difference between Agilent and Fluke plotted vs Fluke temperature with corresponding corrected curve

The adjustment of the Agilent temperature measurements was performed through the use of the following general equation:

$$T_{i_{adjusted}} = M_i \times T_{i_{raw}} + B_i \tag{F.0.2}$$

where it can be seen that the raw temperature reading that is taken by the Agilent is adjusted through the use of a gradient and offset coefficient. The respective coefficients were calculated for each thermocouple based on the data that was obtained from the calibration process. Table F.2 contains the values for the coefficients that were obtained from the Python code and subsequently used in the Agilent:

Table F.2: Thermocouple calibration coefficients

Channel (i)	M_i	B_i
01	1.0090677712	-0.2392827724
02	1.0043132428	-0.2048387632
03	1.0121140459	-0.3517021439
04	1.0130302144	-0.3982180069
05	1.0138773464	-0.4156596433
06	1.0118081582	-0.3819203341
08	1.0165784852	-0.3889021501
09	1.0136961939	-0.3513396510
10	1.0154133531	-0.3580774924
11	1.0120501026	-0.2903921882
12	1.0055651849	-0.1803820092
13	1.0178705688	-0.2885224376
14	1.0158408031	-0.2218303390
15	1.0227043808	-0.3721037999
16	1.0118725323	0.0050552458
17	1.0129606402	0.0830719954

G Data DVD

This appendix contains a disc that collects additional information that is of relevance to this report. The following information has been included on the disc:

- Articles and books
- Theoretical simulation code and results
- Thermocouple calibration code
- Experimental apparatus drawings and results

DISC GOES HERE:

Should the data disc not be included and the reader desires access to the electronic information of this project then please contact Mr R Dobson via rtd@sun.ac.za

List of References

Agrawal, A. and Hindin, B. (1994 August 30). Corrosion inhibition of ammonia-water absorption chillers. US Patent 5,342,578.
Available at: http://www.google.com/patents/US5342578

Agyenim, F., Knight, I. and Rhodes, M. (2010). Design and experimental testing of the performance of an outdoor LiBr-H_2O solar thermal absorption cooling system with a cold store. *Solar Energy*, vol. 84, pp. 735–744.

Asdrubali, F. and Grignaffini, S. (2005). Experimental evaluation of the performances of a H_2O-LiBr absorption refrigerator under different service conditions. *International Journal of Refrigeration*, vol. 28, pp. 489–497.

Bakhtiari, B., Fradette, L., Legros, R. and Paris, J. (2011). A model for analysis and design of h2o-libr absorption heat pumps. *Energy Conversion and Management*, vol. 52, pp. 1439–1448.

BCS Incorporated (2008). Waste heat recovery: Technology and opportunities in u.s. industry.
Available at: http://www1.eere.energy.gov/manufacturing/intensiveprocesses/pdfs/waste_heat_recovery.pdf

Boryta, D.A. (1970). Sobility of lithium bromide in water between -50° and +100°C. (45 to 70% lithium bromide). *Journal of Chemical and Engineering Data*, vol. 15, no. 1, pp. 142–144.

Çengel, Y.A. (2003). *Heat Transfer: A Practical Approach*. 2nd edn. McGraw-Hill.

Charters, W.W.S., Megler, V.R., Chen, W.D. and Wang, Y.F. (1982). Atmospheric and sub-atmospheric boiling of H_2O and LiBr-H_2O solutions. *International Journal of Refrigeration*, vol. 5, no. 2, pp. 107–114.

Chua, H.T., Toh, H.K., Malek, A., Ng, K. and Srinivasan, K. (2000). Improved thermodynamic property fields of LiBr-H_2O solution. *International Journal of Refrigeration*, vol. 23, pp. 412–429.

Einstein, A. and Szilard, L. (1930 November 11). Refrigeration. US Patent 1,781,541.
Available at: http://www.google.com/patents/US1781541

Electrolux (2011). Electrolux history 1920-1929.
Available at: http://group.electrolux.com/en/history-1920-1929-737/

Fernández-Seara, J. and Sieres, J. (2006). The importance of the ammoni purification process in ammonia-water absorption systems. *Energy Conversion and Management*, vol. 47, pp. 1975–1987.

Fried, I. and Segal, M. (1983). Electrical conductivity of concentrated lithium bromide aqueous solutions. *American Chemical Society*, vol. 28, pp. 127–130.

Fujita, I. and Hihara, E. (2005). Heat and mass transfer coefficients of falling-film absorption process. *International Journal of Heat and Mass Transfer*, vol. 48, pp. 2779–2789.

Garland, P.W., DeVault, R.C. and Zaltash, A. (1998). Large commercial absorption chiller development program. Tech. Rep., United states department of energy.

Gosney, W. (1982). *Principles of Refrigeration*. Cambridge.

Grant, T. (ed.) (2003). *International Directory of Company Histories*, vol. 53. St. James Press.

Grossman, G. and Zaltash, A. (2001). ABSIM - modular simulation of advanced absorption systems. *International Journal of Refrigeration*, vol. 24, pp. 531–543.

Herold, K.E., Radermacher, R. and Klein, S.A. (1996). *Absorption Chillers and Heat Pumps*. CRC Press.

James, G.R. (1973). *Ammonia – Part I of IV*. Marcel Dekker.

Jordan, R. and Priester, G. (1949). *Refrigeration and Air Conditioning*. Constable and Company.

Kalogirou, S., Florides, G., Tassou, S. and Wrobel, L. (2001). Design and construction of a lithium bromide water absorption refrigerator. In: *Clima 2000*.

Khairulin, R., Gruzdev, V., Stankus, S. and Verba, O. (2006). Experimental study of the density of aqueous solutions of lithium bromide at temperature of up to 250°C in the range of mass concentrations from 30 to 65 %. *Thermophysics and Aeromechanics*, vol. 13, pp. 575–583.

Killion, J.D. and Garimella, S. (2001). A critical review of models of coupled heat and mass transfer in falling-film absorption. *International Journal of Refrigeration*, vol. 24, pp. 755–797.

Kim, B. and Park, J. (2007). Dynamic simulation of a single-effect ammonia-water absorption chiller. *International Journal of Refrigeration*, vol. 30, pp. 535–545.

King, G. (1971). *Modern Refrigeration Practice*. McGraw-Hill.

Kohlenbach, P. and Ziegler, F. (2008). A dynamic simulation model for transient absorption chiller performance. Part I: The model. *International Journal of Refrigeration*, vol. 31, pp. 217–225.

Kulankara, S. and Herold, K.E. (2000). Theory of heat/mass transfer additives in absorption chillers. *HVAC&R Research*, vol. 6, pp. 369–380.

Labus, J., Bruno, J. and Coronas, A. (2013). Review on absorption technology with emphasis on small capacity absorption machines. *Thermal Science*, vol. 17, no. 3, pp. 739–762.

Mansfeld, F. and Sun, Z. (2003 October 14). Corrosion protection of steel in ammonia/water heat pumps. US Patent 6,632,294.
Available at: `http://www.google.com/patents/US6632294`

Marcriss, R., Gutraj, J. and Zawacki, T. (1988). Absorption fluid data survey: final report on worldwide data. Tech. Rep., Institude of Gas Technology, ORLN/sub/84-47989/3.

Marcriss, R. and Zawacki, T. (1989). Absorption fluids data survey. Tech. Rep., Institue of Gas Technology.

Marsh, R.W. and Olivo, C.T. (1979). *Basics of Refrigeration*. Litton Educational Publishing.

McCarthy, T.S. (2011). The impact of acid mine drainage in south africa. *South African Journal of Science*, vol. 107, no. 5–6, pp. 1–7.

McDaid, L. (2014). The health impact of coal – the responsibility that coal-fired power stations bear for ambient air quality associated health impacts. Tech. Rep., groundWork.
Available at: `http://www.groundwork.org.za/specialreports/groundWork%20The%20Health%20Impact%20of%20Coal%20final%2020%20May%202014.pdf`

Mejbri, K. and Bellagi, A. (2006). Modelling of the thermodynamic properties or the water-ammonia mixture by three different approaches. *International Journal of Refrigeration*, vol. 29, pp. 211–218.

Mills, A. (1999). *Heat Transfer*. 2nd edn. Prentice Hall.

Möller, R. and Knoche, K. (1996). Surfactants with NH_3–H_2O. *International Journal of Refrigeration*, vol. 19, no. 5, pp. 317 – 321.

Owen, M.S. (ed.) (2009). *ASHRAE Handbook – Fundamentals*. ASHRAE.

Pátek, J. and Klomfar, J. (1995). Simple functions for fast calculations of selected thermodynamic properties of the ammonia-water system. *International Journal of Refrigeration*, vol. 18, pp. 228–234.

Pátek, J. and Klomfar, J. (2006*a*). A computationally effective formulation of the thermodynamic properties of LiBr-H_2O solutions from 273 to 500 K over full composition range. *International Journal of Refrigeration*, vol. 29, pp. 566–578.

Pátek, J. and Klomfar, J. (2006*b*). Solid-liquid phase equilibrium in the systems of LiBr-H_2O and LiCl-H_2O. *Fluid Phase Equilibria*, vol. 250, pp. 138–149.

Raybaut, P. (2015). Scientific PYthon Development EnviRonment.
Available at: `https://pythonhosted.org/spyder/`

Red Hat (2015). The Cygwin Project.
Available at: `https://cygwin.com/`

Shahata, A., Elsafty, A. and Abo Elnar, M.M. (2012). Concentration measurement technique for aqueous lithium bromide solution in vapor absorption air conditioning systems. *International Journal of Science and Technology*, vol. 2, pp. 234–237.

Somers, C., Mortazavi, A., Hwang, Y., Radermacher, R., Rodgers, P. and Al-Hashimi, S. (2011). Modeling water/lithium bromide absorption chillers in aspen plus. *Applied Energy*, vol. 88, pp. 4197–4205.

Srikhirin, P., Aphornratana, S. and Chungpaibulpatana, S. (2001). A review of absorption refrigeration technologies. *Renewable & Sustainable Energy Reviews*, vol. 5, pp. 343–372.

Táboas, F., Vallès, M., Bourouis, M. and Coronas, A. (2007). Pool boiling of ammonia/water and its pure components: Comparison of experimental data in the literature with the predictions of standard correlations. *International Journal of Refrigeration*, vol. 7, pp. 778–788.

Teja, A.S., Jeter, S.M., Lee, R.J., Diguilio, R. M. Lenard, J.-L.Y. and Moran, J.P. (1991). Thermophsical property data for lithium bromide/water solutions at elevated temperatures. Tech. Rep., Georgia Institute of Technology School of Chemical Engineering and The George W. Woodruff School of Mechanical Engineering.

Varma, H.K., Mehrotra, R.K., Agrawal, K.N. and Singh, S. (1994). Heat transfer during pool boiling of LiBr-water solutions at subatmospheric pressure. *International Communications in Heat and Mass Transfer*, vol. 21, pp. 539–548.

Wagner, W., Cooper, J.R., Dittmann, A., Kijima, J., Kretzschmar, H.-J., Kruse, A., Mares, R., Oguchi, K., Sato, H. and Stocker, I. (2000). The IAPWS industrial formulation 1997 for the thermodynamic properties of water and steam. *Journal of Engineering for Gas Turbines and Power (ASME)*, vol. 122, pp. 150–182.

Wang, K., Abdelaziz, O., Kisari, P. and Vineyard, E.A. (2011). State-of-the-art review on crystallization control technologies for water/LiBr absorption heat pumps. *International Journal of Refrigeration*, vol. 34, pp. 1325–1337.

Wang, X. and Chua, H.T. (2009). Absorption cooling - a review of lithium bromide-water cooling technologies. *Recent Patents on Mechanical Engineering*, vol. 2, pp. 193–213.

Ziegler, B. and Trepp, C. (1984). Equation of state for ammonia-water mixtures. *International Journal of Refrigeration*, vol. 7, pp. 101–106.

Ziegler, F. (1999). Recent developments and future prospects of sorption heat pump systems. *International Journal of Thermal Sciences*, vol. 38, pp. 191–208.